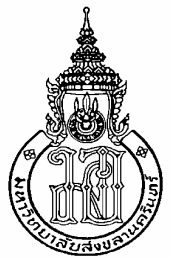

Preliminary Monitoring of the Change of Soil Gas Radon for Earthquake Pre-warning in the Khlong Marui Fault Zone

Pattama Pisapak

A Thesis Submitted in Partial Fulfillment of the Requirements for the Degree of

Master of Science in Geophysics

Prince of Songkla University

2009

Thesis Title	Preliminary Monitoring of the Change of Soil Gas Radon for Earthquake Pre-warning in the Khlong Marui Fault Zone
Author	Miss Pattama Pisapak
Major Program	Geophysics

Major Advisor:

…….....
(Assoc. Prof. Dr. Tripob Bhongsuwan)

Co-advisor:

…….....
(Dr. Helmut Duerrast)

Examining Committee:

……...Chairperson
(Dr. Kamhaeng Wattanasen)

...……..……..
(Assoc. Prof. Dr. Tripob Bhongsuwan)

...……..……..
(Dr. Helmut Duerrast)

...……..……..
(Assoc. Prof. Nares Chankow)

The Graduate School, Prince of Songkla University, has approved this thesis as partial fulfillment of the requirements for the Master of Science Degree in Geophysics

…..……..……..…….
(Assoc. Prof. Dr. Krerkchai Thongnoo)
Dean of Graduate School

ชื่อวิทยานิพนธ์ การเฝ้าติดตามขั้นต้นการเปลี่ยนแปลงแก๊สเรดอนในดินเพื่อการพยากรณ์แผ่นดินไหวในบริเวณรอยเลื่อนคลองมะรุ่ย

ผู้เขียน นางสาวปัทมา พิศภักดิ์

สาขาวิชา ธรณีฟิสิกส์

ปีการศึกษา 2551

บทคัดย่อ

งานวิจัยนี้มีวัตถุประสงค์หลักเพื่อศึกษาความเป็นไปได้ในการประยุกต์ใช้การเปลี่ยนแปลงความเข้มข้นของแก๊สเรดอนในดินเป็นตัวเตือนล่วงหน้าก่อนเกิดเหตุการณ์แผ่นดินไหวท้องถิ่นและในภูมิภาค โดยได้ทำการศึกษาในบริเวณรอยเลื่อนคลองมะรุ่ยทางภาคใต้ของประเทศไทย ซึ่งอยู่ห่างจากแนวรอยมุดตัวซุนดาในทะเลอันดามัน ประมาณ 500 กม.

ในการศึกษาครั้งนี้ได้พัฒนาระบบวัดแก๊สเรดอนในดินด้วยหัววัด SSNTD และติดตั้งที่ 10 สถานีวัด ใน อ.ทับปุด จ.พังงา และติดตั้งเครื่องวัดเรดอน RPM-256 ตรวจวัดความเข้มข้นของแก๊สเรดอนในดินแบบต่อเนื่อง ณ จุดวัดแผ่นดินไหว ที่ อ.ทับปุด จ.พังงา ติดตั้งเครื่องวัดแผ่นดินไหวชนิดคาบสั้น Mark L4-3D เพื่อตรวจวัดสัญญาณแผ่นดินไหวท้องถิ่นและสัญญาณแผ่นดินไหวในภูมิภาค บริเวณแนวรอยเลื่อนคลองมะรุ่ย บันทึกข้อมูลในระหว่างวันที่ 14 มกราคม ถึง 29 เมษายน 2550

จากทั้งหมด 10 สถานี พบว่า ความเข้มข้นแก๊สเรดอนในดินที่สถานี ST10 มีค่าสูงสุด และพบว่าการเปลี่ยนแปลงของค่าเฉลี่ยความเข้มข้นเรดอนในดินรายสัปดาห์มีความสัมพันธ์กับเหตุการณ์แผ่นดินไหว ความเข้มข้นของแก๊สเรดอนในดินตรวจวัดแบบต่อเนื่องพบค่าความผิดปกติ 2 ครั้งคือ ในวันที่ 18 กุมภาพันธ์ 2550 เวลา 15:48:53 (UTC Time) ด้วยอัตรานับ 54 ครั้งต่อ 10 นาที และในวันที่ 1 มีนาคม 2550 เวลา 14:34:35 (UTC Time) ด้วยอัตรานับ 91 ครั้งต่อ 10 นาที โดยค่าภูมิหลังของความเข้มข้นของแก๊สเรดอนในช่วงเวลาดังกล่าวมีค่าเฉลี่ยและค่าเบี่ยงเบนมาตรฐานเท่ากับ 20 ครั้งต่อ 10 นาที และ 7.61 ครั้งต่อ 10 นาที ตามลำดับ ในการวิเคราะห์ข้อมูลเบื้องต้นพบว่าเหตุการณ์แผ่นดินไหวท้องถิ่นและในภูมิภาคมีจำนวนเพิ่มขึ้นภายหลังการตรวจพบความเข้มข้นผิดปกติของแก๊สเรดอนในดินเป็นเวลาหลายวัน ดังนั้นจึงมีความเป็นไปได้ว่าในอนาคตเราสามารถใช้ข้อมูลแก๊สเรดอนเป็นตัวเตือนล่วงหน้าก่อนการเกิดเหตุการณ์แผ่นดินไหวในพื้นที่ศึกษา

Thesis Title	Preliminary Monitoring of the Change of Soil Gas Radon for Earthquake Pre-warning in the Khlong Marui Fault Zone
Author	Miss Pattama Pisapak
Major Program	Geophysics
Academic Year	2008

ABSTRACT

The main objective of this study was to observe a possible variation of radon concentration in soil gas as an earthquake precursor. The Khlong Marui Fault Zone in Southern Thailand 500 km far from the Sunda Subduction Zone to the west in the Andaman Sea was chosen as the study area.

A solid-state nuclear track detector (SSNTD) system was developed for soil-gas radon detection and set up at 10 stations in Phang Nga Province, whereas one automatic continuously radon monitoring system, RPM-256, was setup at the seismic station in Thap Put District. A short-period Mark L4-3D seismometer was installed at the seismic station in Thap Put District, Phang Nga Province along the Khlong Marui Fault Zone in Southern Thailand and recorded for local and regional earthquakes during 14 January and 29 April 2007.

Among the ten stations installed with SSNTD detector the station ST10 showed the highest radon concentration in which its weekly average variation correlated well with earthquake activities. In continuous radon records there were two clear radon anomalies; the first on 18 February 2007 at 15:48:53 UTC with 54 count/10 minute, the second anomaly occurred on 1 March 2007 at 14:34:35 UTC with a count rate 91 count/ 10 minute. The average value is 20 count/ 10 minute, with one standard deviation of 7.61 count/ 10 minute. The preliminary analysis of the earthquake and radon data shows an increase of earthquake activities several days after each radon anomaly. More data and understanding might be possible in the future to use radon gas variations as a possible method for earthquake warning in the study area.

ACKNOWLEDGEMENTS

First of all, I would like to give my deepest gratitude to Assoc. Prof. Dr. Tripob Bhongsuwan, my principal advisor, and special gratitude thanks to Dr. Helmut Duerrast, my co-advisor, for their supervision, suggestions, and efforts for steering me towards the right direction during this research, until this thesis was completed.

My thanks go to the Graduate School, Prince of Songkla University (PSU) and Centennial Education Fund, Shell Company, Thailand, for research grants, Thanks to the Department of Physics, Faculty of Science, PSU, International Program in Physical Science (IPPS) of Uppsala University, Sweden., for supporting to Geophysics Program. Thanks to the Thai Meteorological Department (TMD), for providing the meteorological data.

Special thank to Mr. Mongkon Buathong and his family (Dang and Saw) at Khok Charoen Village, also thanks to the teachers and directors of Ban Khok Chang School, Khok Charoen health center, Ban Thung To Ruea School, Thap Put School, Ban Nai Vang School, Thap Put Wittaya School, Wat Satharam School, Ban Bo Saen School and Ban Bang Toei School in Thap Put and Mueang District, Phang Nga Province, for allowing me to set up a seismic and radon measurement station.

I would never forget all my friends at the Geophysics Group and the other laboratories of the Physics Department, for their help and support, especially from Ms. Phenphak Therdsuwan, who always worked with me in the field. Special thanks to my best friends Ms. Sutharat Thongkleng and Mr. Arthit Mitsuwan for their help and suggestions.

Finally, I am deeply gratitude to my father, my mother, my brother and my sister for their moral support and encouragement during a challenging time.

Pattama Pisapak

CONTENTS

CONTENTS (CONTINUED)

CONTENTS (CONTINUED)

LIST OF TABLES

LIST OF TABLES (CONTINUED)

LIST OF TABLES (CONTINUED)

LIST OF FIGURES

LIST OF FIGURES (CONTINUED)

LIST OF FIGURES (CONTINUED)

LIST OF FIGURES (CONTINUED)

LIST OF FIGURES (CONTINUED)

LIST OF FIGURES (CONTINUED)

LIST OF FIGURES (CONTINUED)

LIST OF FIGURES (CONTINUED)

LIST OF FIGURES (CONTINUED)

CHAPTER 1

INTRODUCTION

The devastating Mw 9.3 Sumatra-Andaman Earthquake occurred on the 26 December 2004 at 00:58:53 UTC (07:58:53 Thai time), off the west coast of Northern Sumatra, Indonesia, at the Sunda Subduction Zone (USGS, 2005). Because of the subsequent uplift of parts of the ocean bottom, a tsunami with devastating effects to Indian Ocean's coastlines was triggered, including Thailand's west coast, with huge losses of life and destruction of near-shore structures (USGS, 2005). The crustal movements related to the 26 December 2004 Earthquake resulted in an increased number of reported sinkholes in Southern Thailand (DMR, 2005; Duerrast et al., 2007).

Changes of the radon concentration in air, groundwater, and soil can be seen as a possible precursor of large tectonic earthquakes (e.g. Ulomov and Mavashev, 1967; Chyi et al., 2001). However, no radon monitoring station was installed in Southern Thailand before the 26 December 2004 Earthquake.

Although the past research has shown that the use of soil gas variation as an earthquake precursor is not always effective, it still can be used as a useful tool to monitor crustal movements (e.g. Einarsson et al., 2008). Over the years, the techniques of radon gas sampling and detection have been improved and still are undergoing further development (e.g. Chyi et al., 2001). Further, the signal to background ratio was improved by placing the detector within a fracture zone of an active fault with upwelling gases. The environmental factors affecting radon variation have been reduced by housing the detector. The radon data recording was then done continuously and retrievable at a remote site, as well as additional meteorological parameters, such as rainfall, air moisture, temperature, and atmospheric pressure were measured (e.g. Chyi et al., 2002).

The variations of soil gas radon with meteorological parameters have been studied by many authors, such as Stranden and coworkers (1984), Wattananikorn and coworkers (1998), and Ghosh and coworkers (2007).

Wattananikorn and coworkers (1998) reviewed that the radon measurements at 100 cm depth less effected by meteorological parameters. Therefore, before using radon measurements as an earthquake precursor, the meteorological effects need to be removed.

However, since the 2004 Sumatra - Andaman Earthquake, there are still concerns among people and governmental agencies for larger earthquakes along the fault zones in Southern Thailand, like the Ml = 2.7 earthquake on 4 May 2008 and on 23 December 2008 with the Ml = 4.1 at the Khlong Marui Fault Zone (TMD, 2008).

This study is based on field measurements of radon emission and local earthquakes and shows that the correlation of radon anomalies with earthquakes can provide an important insight e.g. stress changes in an active fault zone. The results of this study confirm earlier work of Dangmuan (2008) that the faults zones in Southern Thailand are reactivated and presently active, but with lower magnitude seismicity.

1.1. Review of Literature

1.1.1 Radon

Radon is an important terrestrial gas whose presence and concentration is easy to detect. Radon concentration levels are strongly affected by geological and geophysical conditions, as well as atmospheric influences, such as rainfall and barometric pressure rather than by chemical processes, as it is an inert gas. Formed as a result of radioactive decay of the element uranium and thorium radon gas is naturally present in rocks and soils. Rock types, such as black shales and some igneous rocks, can have a higher content of uranium and thorium than the average values of the earth's crust. It is the only naturally radioactive gas and is the heaviest of all of the elements that occur a gas at room temperature and pressure conditions. Radon is one of a number of intermediate radioactive elements formed during the radioactive decay of uranium-238, uranium-235 and thorium-232 isotopes to form stable, non-radioactive isotopes of lead (Figure 1.1). Radon-222 is the radon isotope

of most concern to public health because of its longer half-life, 3.8 days, than other radon isotopes, like radon-219, 4 seconds, or radon-220, 55.3 seconds (CGS, 2008).

Solid-state radionuclides remain where created by decay processes unless they are redistributed by dissolving in groundwater or by becoming airborne. Given the chemically inert nature of radon, there are no known compounds that include this element. Thus isotopes of radon may diffuse away from their place of origin and usually end up dissolved in groundwater or mixed with air above the soil and rocks that bear their solid precursors.

Source of radiation exposure

Radiation comes from both natural and human sources. Many elements exist in one or more radioactive forms. The most common of these is an isotope known as potassium-40. Isotopes are forms of an element that differ from each other in the structure of their nuclei. Other radioactive isotopes found in nature include hydrogen-3, carbon-14, chlorine-39, lead-212, radium-226, and uranium-235 and 238. Humans and other organisms cannot escape exposure to radiation from these radioactive sources. They constitute a normal radiation, called background radiation that is simply part of existing on earth. Although some harmful effects can be produced by exposure to natural background radiation, those effects are relatively minor and, in most cases, not even measurable. Human activities have added to normal background radiation over the past half century. When nuclear weapons are exploded, for example, they release radioactive isotopes into the atmosphere. As these radioactive isotopes are spread around the world by prevailing winds, they come into contact with humans and other organisms (HPS, 2008). Figure 1.2 shows the source of ionizing radiation exposure of the population of the United States. The main source for radiation exposure, with 55 %, comes from radon sources (NCRP, 1987).

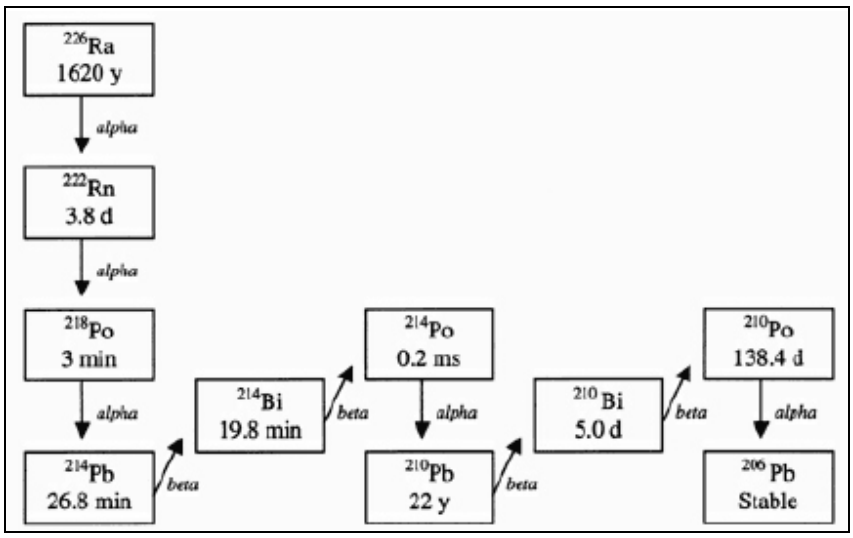

Figure 1.1 Products of radioactive decay of radon (CGS, 2008).

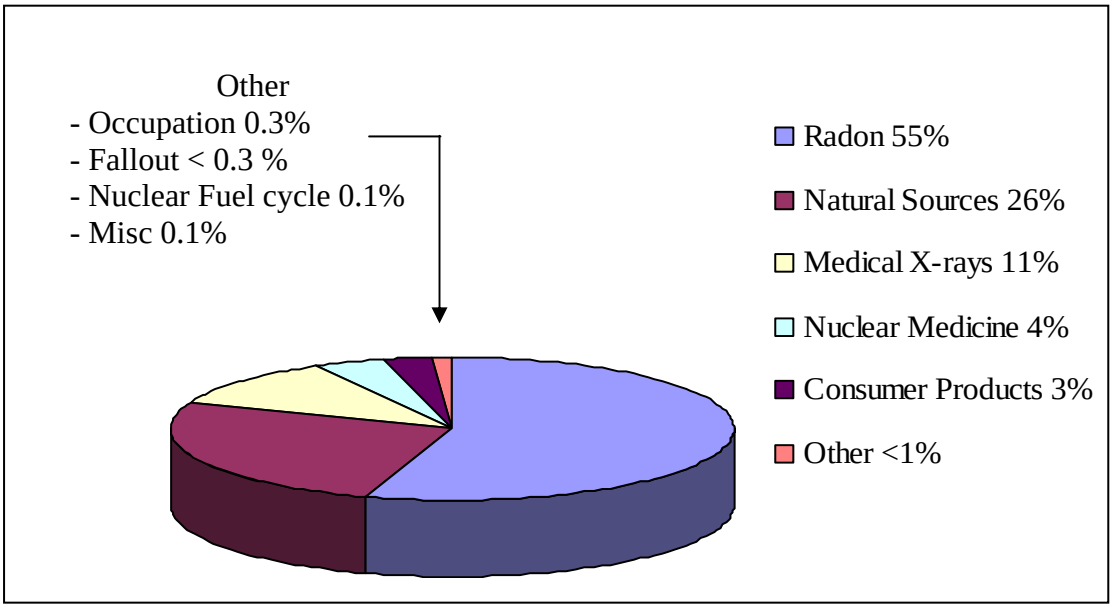

Figure 1.2 Source of radiation exposure in the United States (from NCRP, 1987).

From Figure 1.1 it can be seen that the primary, very long lived U-238 decays to U-234, and then, U-234 decays to thorium-230 (Th-230), which decays to radium-226 (Ra-226). Ra-226 with a half life of 1,620 years decays to Rn-222 with a half life of 3.8 days. Thus, Ra-226 is the immediate parent of Rn-222, whereas U-238 is the ultimate parent. Rn-222 decays through intermediate steps until the longer lived lead-210 (Pb-210) is reached. The important feature is that the decay products, mainly alpha particles, down to Pb-210 pose a hazard to human health.

Therefore, in order to have radon gas in groundwater, it is necessary not only for the U-238 decay series to operate, but for there to be a process whereby Ra-226 is in contact with the water. Furthermore, because of the short half life of Rn-222, the radium must be fairly close by. That is, Rn-222 can not move very far in groundwater in the 20 days required for nearly complete decay. In fact, most of the radon decays in five to six days. The process leading to radon gas seems fairly straightforward, but chemical and rock properties combined create a rather complicate situation in the field (Makofske et al., 1988).

Sources of global atmospheric radon

The major source of radon-222 in the atmosphere (at least 80%) is from emanations from soil from rock formations close to the ground surface from the decay of U-238 through Ra-226 to Rn-222 (Table 1.1) (NCRP, 1984). Radon dissolved in groundwater is the second most important potential source of atmospheric radon. Nonetheless, in most locations it is a minor source of human exposure in view of the small absorbed dose following oral ingestion. In some locations where water from highly radioactive deep wells is used, it can be a significant contributor. For example, in Maine, New Hampshire, U.S.A., some regions of the Appalachian Mountains, and Florida, concentrations found in some private wells exceed 10,000 pCi/liter. When water use is high in the home, air levels are found to be elevated due to outgassing from the water (Pritchard and Gesell, 1981).

Measurement techniques of radon

There are three classes of measurement techniques that are used today: (1) grab sampling, (2) continuous and active sampling, and (3) integrative sampling. The choice between these classes will depend on the costs involved, the time over, which an instrument can be devoted to measurements at a single location, the kind of information required, and the desired accuracy with which measurements can be related to an estimate of risk (Bodansky et al., 1987; Brill, 1994).

Table 1.1: The major source of radon-222 in the atmosphere (NCRP, 1984).

Source	(million Ci per year)
Emanation from soil	2000
Ground water (potential)	500
Emanation from oceans	30
Phosphate residues	3
Uranium mill tailings	2
Coal residues	0.02
Natural gas	0.01
Coal combustion	0.0009
Human Exhalation	0.00001

Grab sampling

Grab samples consist of essentially instantaneous measurements of the radon or radon progeny concentration in air over time intervals that are short (on the order of minutes) compared to the time scale of fluctuations in concentration. The air is collected in a container and brought back to the laboratory for analysis. Typical containers include plastic bags, metal cans, and glass containers. The volumes of the containers are usually between 5 and 20 liters.

Continuous sampling

Continuous sampling involves the automatic taking of measurements at closely spaced time intervals over a long period of time. The result is a series of measurements, which can give information on the pattern with which the concentration varied throughout the measurement interval.

Integrating sampling

Integrating devices collect information on the total number of radiation events, which occur throughout some fairly long period of time, usually on the order of several days to months. The result from integrating devices is an estimate of the approximate average concentration through the environment interval (Cothern and Smith, 1987).

1.1.2 Earthquakes

Earthquakes in Thailand

Thailand is situated close to an active seismic region, the Sunda Subduction Zone, which is about 500 km east of Thailand in the Andaman Sea. The earthquake epicenters are mainly located along the north-south trending Burma-Andaman Sumatra subduction and fault zone along Thailand's westernmost frontier. Over 450 historical earthquakes have been recorded in Thailand (Nutalaya and Sodsir, 1984). Further earthquakes epicenters have been located mainly in western and northern regions of Thailand. In 1963 the Meteorological Department set up the first seismic station in Chiang Mai. Since then the monitoring of earthquakes in Thailand has become more systematic. Seismic events recorded on February 17, 1975 at Tak Provinces (M=5.6) and on April 22, 1983 at Kanchanaburi Provinces (M=5.9) (Poobrasert, 1987). Frequently strong and very strong earthquakes occur, sometimes very big ones, like the Mw 9.3 on 26 December 2004. However, these earthquakes have only less direct rather than more an indirect impact on Thailand, like shaking of high-rise building (USGS, 2005).

Shortly after the devastating Mw 9.3 Sumatra-Andaman Earthquake on 26 December 2004, the Geophysics Group in the Department of Physics at the Faculty of Science, Prince of Songkla University established in collaboration with the Department of Mineral Resources a seismic network in Southern Thailand in order to monitor possible local earthquakes along the Ranong and Khlong Marui Fault Zone (Dangmuan, 2008).

Seismic sources

Seismic sources are divided in to two types: natural events, which are basically earthquakes, and man-made events (Figure 1.3). Earthquakes are caused by the movement of tectonic plates over the asthenosphere. Sandwiched between the earth's crust and the molten outer core, the vast mantle accounts for 83 % of the planet's volume. It is filled with solid rock but, heated by the core and by its own radioactive decay. That circulation is the driving force behind the surface motion of tectonic plates, which builds mountains and causes earthquakes. Tectonic earthquakes

occur from a sudden break-up of the lithosphere due to deformation and stress loading. These earthquakes can be separate by focal depth, with shallow 0 and 70 km, intermediate 71 and 300 km, and deep earthquakes between 300 and about 700 km. Earthquakes in the last category only occur at subduction zone (Bormann et al., 2002).

Man-made event are seismic events, which are generated by people, such as controlled sources, reservoir induced earthquakes, and mining induced rock bursts or collapses and cultural noise. Man-made events often have focal depths near the surface, about one or a few kilometer. Therefore, they produce higher amplitude surface wave, or Rayleigh wave (Rg wave), which can be identified in seismograms (Bormann et al., 2002).

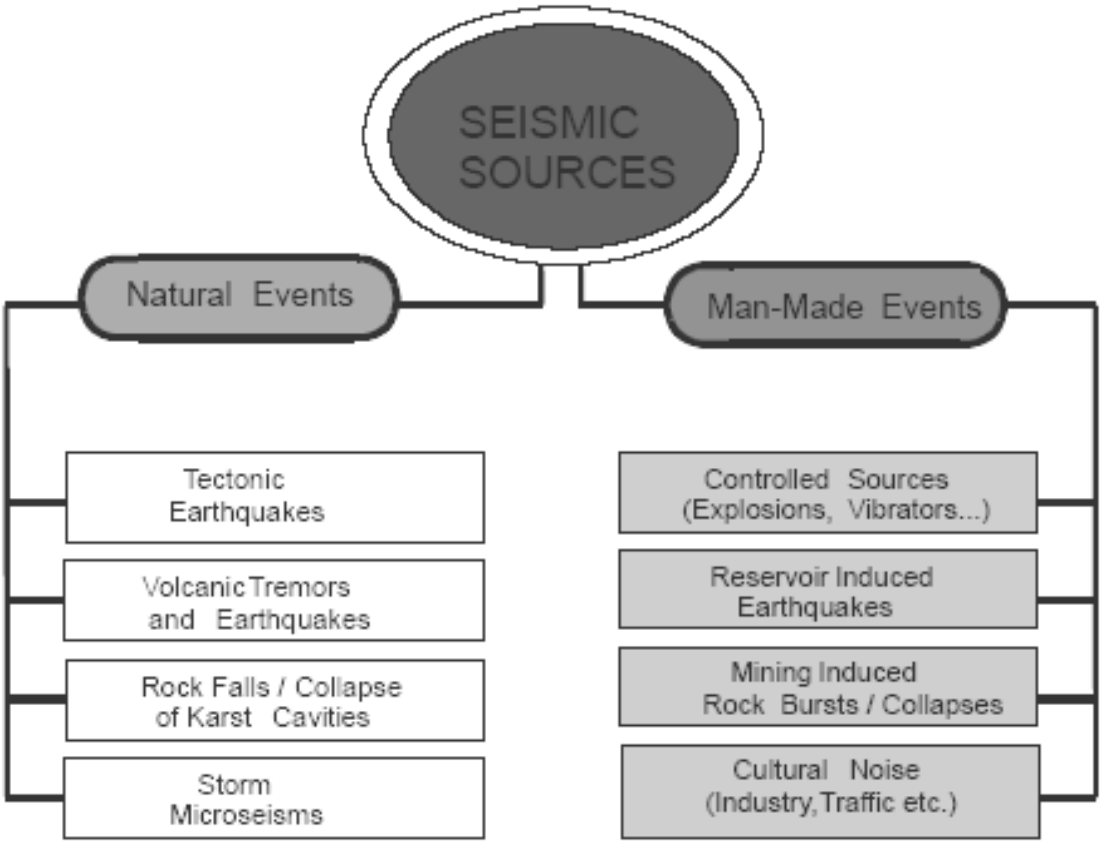

Figure 1.3 Seismic sources from two causes: natural events and man-made events (Bormann et al., 2002).

Geology and tectonics of Andaman Sea and Peninsular Thailand

Thailand presents the special case of a section of a geosynclinal complex, lying between well marked conventional orogenic belts, in which a somehow atypical orogen has developed, and in which rather moderately folded sediments have been heavily invaded by granites. The orogen described here is a section of the Triassic-Jurassic Yunnan-Malayan orogen. The description is based on Peninsular Thailand only, but data from hydrocarbon exploration indicate that this apply equally to the Gulf of Thailand to the east. The orogen has a length, measured N-S along strike, of 1080 km. Both the western and eastern parts of the orogen are largely beneath the sea. On the east, the Yunnan-Malayan orogen must abut against the Cambodian Shield ('Indosinia'). East of the latter lies the Annamitic cordillera, another former geosynclinal tract, which probably connected with the Yunnan-Malayan geosyncline in the Indochina-China border area. On the west, the Yunnan-Malayan orogen is overlain by the younger strata of the Andaman Sea, bordered by the 'stretched' orogen of the Andaman-Nicobar Islands. The west margin of the orogenic belt is unknown and the width of the orogenic belt cannot be measured; it might be ca. 700 km, of which only 150 km lies above the sea level (Burton, 1974).

Seismicity associated with Andaman-Sumatra Arc

The Andaman-Nicobar Arc in the northeastern Indian Ocean defines a nearly 1,100 km long active plate margin, where the Pacific Arc system through its continuation into the Sunda arc gradually transits northward along the strike to young fold belts of Burma (Figure 1.4). The Andaman-Nicobar Arc is part of the Sunda Arc of nearly 6,000 km that extends from the eastern Himalayan syntaxis in the north through the western Burma, the western Andaman sea, Sumatra and Java and continues into the Banda arc of eastern Indonesia (Curray, 1989). It is a typical example of a convergent or subduction margin where the Indian-Australian plate (or plates) subducts beneath the Eurasian or southeast Asian plate. Active subduction beneath the arc might have started following the breakup of Gondwanaland in Cretaceous (130 Ma). The Andaman-Nicobar ridge and the Indo-Burman ranges were uplifted as a sedimentary arc during Oligocene to Eocene (45-28 Ma) simultaneously with the uplift of the non-volcanic ridge to the southeast along the Sunda arc. Active

andesite volcanism occurs all along this arc and seismicity associated with this convergent margin shows a distinct Benioff zone, with variable focal depth of the order of 150-700 km. Deep focus earthquakes originate at a depth of nearly 700 km in the Java part of the trench, whereas the focal depth reduces towards north. Active subduction of the Indian Ocean Lithosphere below the Andaman Arc is primarily documented by (1) an east-dipping Benioff zone down to 200 km, (2) anomalous heat flow, (3) an active volcanic arc, (4) large amplitude gravity anomalies, and (5) a correlation of arc-trench bathymetry to morpho-tectonic elements and their underlying seismic zone. Major variations occur around the length of 6,000 km arcuate shaped segment of the Sunda Arc. These variations are mainly due to the direction and spread of convergence across the subduction zone, the thickness of the accreted sediments, the age of the lithosphere all along the trench axis, etc. (Curray, 1989). The Andaman back arc basin behind the Andaman-Nicobar trench is the effect of the oblique convergence of Indian-Australian plates at the Sunda Arc.

The Andaman Sea might have started opening approximately in an E-W direction as a typical back arc extensional basin during Oligocene (34-23 Ma) and resulted in the formation of the Mergui Basin, a northerly continuation of the North Sumatra Basin (Figure 1.4). According to Curray and coworkers (1982), the entire Central Andaman Basin might have opened in slightly more than 10.8 Ma. However, in a recent study, Kamesh and coworkers (2004) suggested on the basis of swath bathymetry and single channel seismic and magnetic data that the time of initiation of spreading in the back arc basin is not more than 4 Ma. A two phase opening of Andaman Sea has been described by Khan and Chakraborty (2005) based on seismotectonic evidence.

The volcanoes and volcanic rocks of the Andaman Sea have been studied by several workers (e.g. Dasgupta, 1992). Most conspicuous volcanic features in the central Andaman basin are the Barren and Narcondam Islands and the Alcock and Sewell seamounts (Figure 1.4). Recent Barren Island volcanism was initiated in March 1991 and completed by October 1991. Volcanic activity is also reported from the Barren Islands within few months of the 2004 Sumatra earthquake. The Andaman-Nicobar Sumatra Trench, which is part of the Sunda arc, is the only convergent margin in the Indian Ocean.

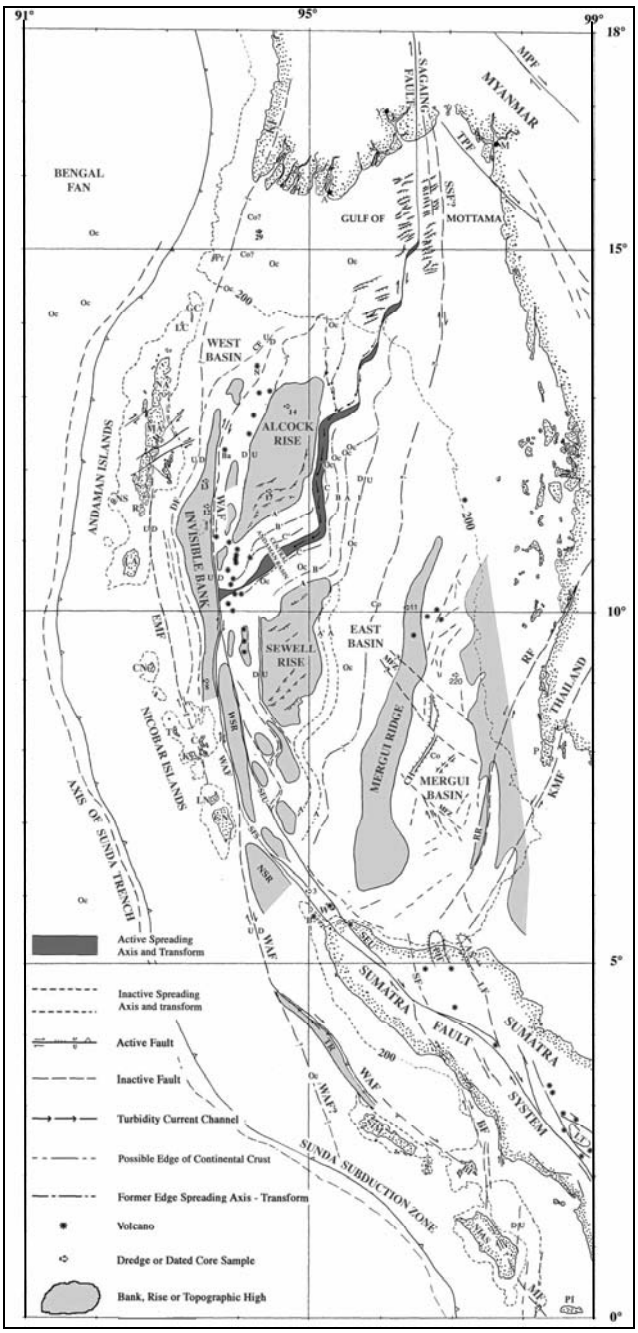

Figure 1.4 Tectonic map of the Andaman Sea and adjacent southern Myanmar and northern Sumatra. Ba is Barren Island, CN is Car Nicobar Island, Co is continental crust, GN is Great Nicobar Island, KMF is Khlong Marui Fault, LA is Little Andaman Island, MF is Mentawei Fault, MFZ is Mergui Fault, N is Narcondam Island, NA is North Andaman Island, NSR is North Sumatra Ridge, Oc is oceanic crust, P is Phuket Island, RF is Ranong Fault, SFS is Sumatra Fault System, WAF is West Andaman Fault, Y is Yangon (Rangoon); from Curray (2005).

Though the seismicity associated with this arc is moderate and does not raise any concern so far, the scenario has significantly changed after the 26th December, 2004, Sumatra Andaman Earthquake with a magnitude of Mw 9.3. The rupture of this earthquake propagated northwards towards the Nicobar-Andaman Island arc, and to this date as many as few thousand aftershocks were reported after the main event. Apart from the main shock of 26th December, the aftershocks of 28th March 2005 (Mw 8.4) and 24th July 2005 (Mw 7.3) were felt along the coastal area of Andhra Pradesh and Tamilnadu margin, India. The frequency and amplitude of earthquakes in the Andaman and Nicobar belt show significant rise since December, 2004 and thus pose a new seismic hazard for the coastal region of India, Myanmar, Thailand and Indonesia, though fortunately none of these aftershocks were associated with a Tsunami.

The great Sumatra Andaman Earthquake of December 26, 2004 initiated at a depth of about 30 km beneath the Sunda Trench off the west coast of Sumatra, Indonesia (3.244^{o}N; 95.825^{o}E) at 00:59 UTC time (Stein and Okal, 2005). The rupture propagated upwards on a shallow-dipping (8^{o}) fault plane and northward along the Nicobar and Andaman islands that delineate the boundary between the Indian- Australian plate and the southern edge of the Eurasian plate (Bilham, 2005, Ni et al., 2005, Figure 1.5 and 1.6). Up to 15 meters of thrust displacement was accommodated at the plate interface within a few minutes, offshore from Banda Ache, Sumatra where the strongest excitation of the tsunami occurred (Figure 1.6, Lay et al., 2005). Farther north, the rupture slowed considerably and for the last five of its eleven minutes duration, no further tsunami waves were produced. During the following hour, however, this northern section of the rupture accumulated many meters of slip, which contributed perhaps a third of the total energy released. This slow slip accounted for a three-fold upward revision of magnitude from 9.0 to 9.3 (Bilham, 2005).

Later analysis of continuous-recording GPS stations revealed that co-seismic horizontal displacements had occurred over a vast region. From decimeter-scale shifts at the nearest stations (e.g. 270 mm at Phuket, Thailand, to the west) to several millimeters measured at points in southern China, the Philippines and India (Vigny et al., 2005). The total length of the rupture is comparable to the distribution

of aftershocks, which is more than 1,200 km for the December 26 event. This increases to more than 1,600 km when the contiguous Nias earthquake (moment magnitude Mw 8.7) of March 28, 2005 is included (Figure 1.6). The March 28 earthquake indicated further rupture of the plate interface to the southeast and raised concern about the altered state of stress and possibly heightened tsunami hazard on adjoining sections of the plate boundary.

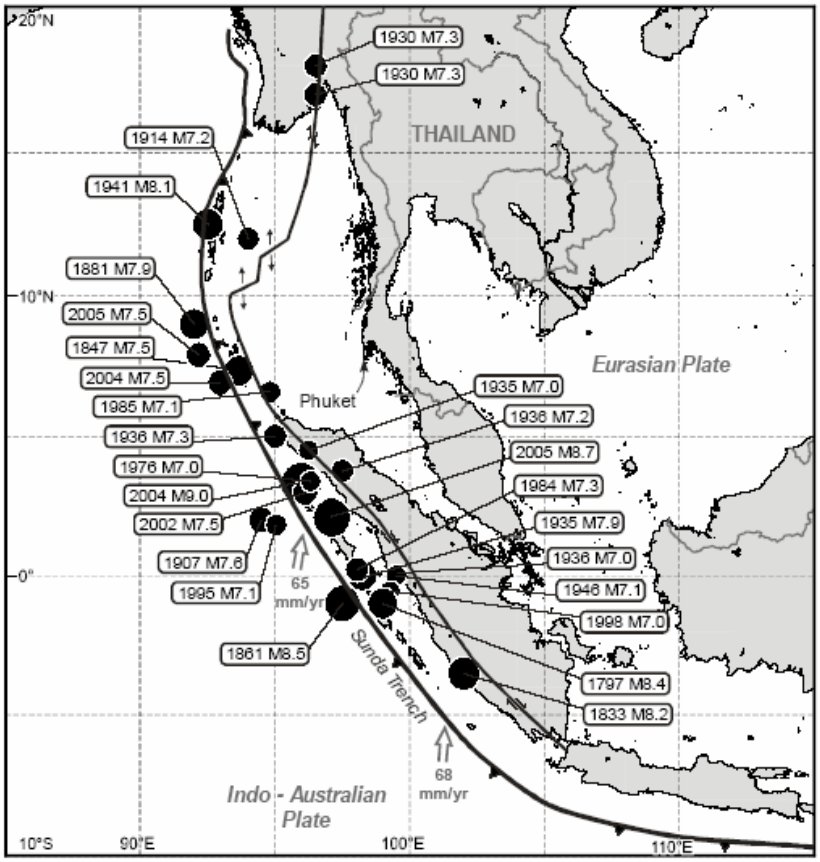

Figure 1.5 Historical large and great earthquakes of the Andaman plate boundary and region adjacent to the December 26, 2004 and March 28, 2005 earthquakes. Event of magnitude ≥ 7.0, depth < 100 km. (Bell et al., 2005).

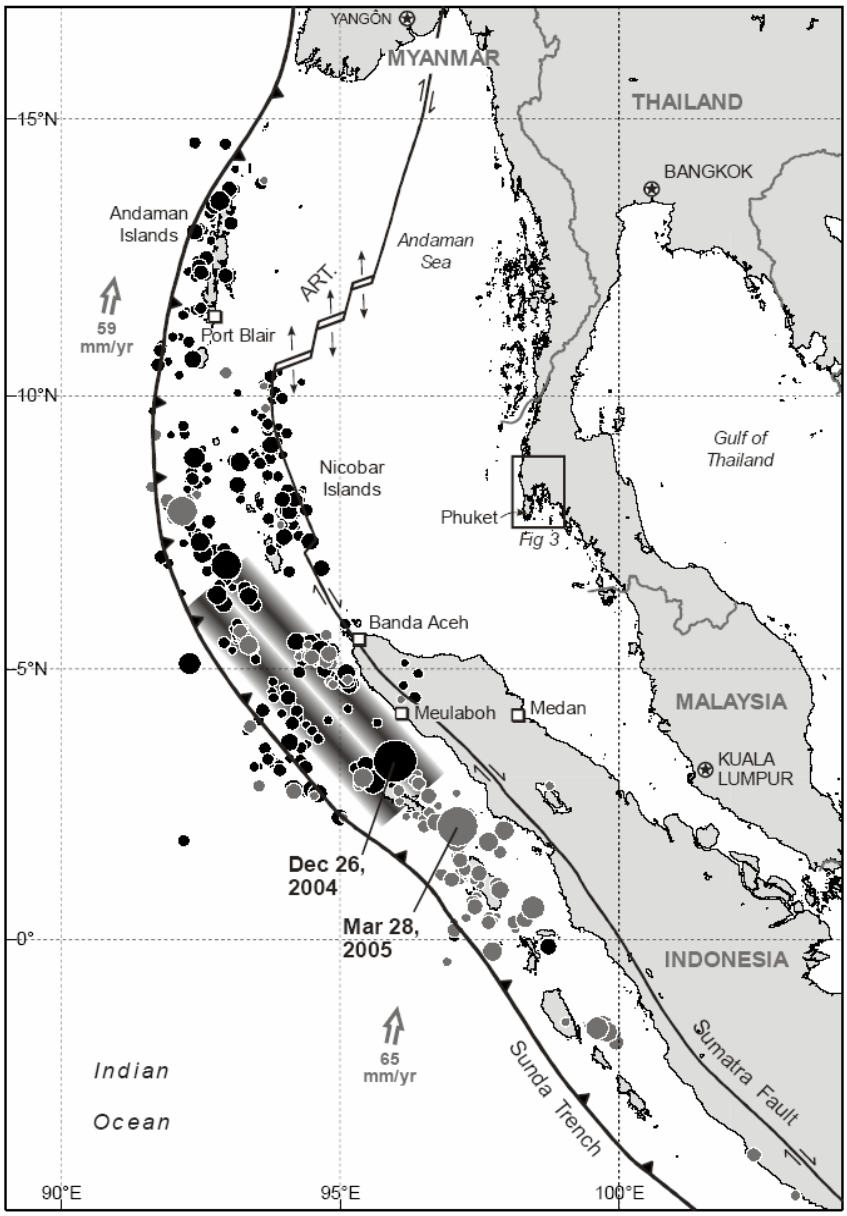

Figure 1.6 Major Structural elements of the Indian-Australian and Eurasian plate boundary, with the mainshock Mw 9.3 and aftershocks for the December 26, 2004. Great Sumatra-Andaman earthquake (black circles), and the contiguous Nias earthquake of March 28, 2005 and combined aftershocks earthquake (Mw 8.6) of thereafter (gray circles). The earthquake sequence encompasses a rupture zone 1,600 km long and 200 km wide (Lay et al., 2005).

Large earthquakes are known to have ruptured the Andaman section of the over-thrust plate boundary in 1847 (Mw 7.5), 1881 (Mw 7.9), 1941 (Mw 7.7), and in the northern Andaman Sea, a section of the Andaman Ridge-transform boundary near the coast of Myanmar, in 1930 (Mw 7.3) (Nutalaya et al., 1985; Ortiz and Bilham, 2003; Bilham et al., 2005, Figure 1.5). Those historical events produced tsunami that, while locally destructive in the islands, had limited regional impact, probably due to their involving slip on deeper parts on the plate interface than occurred on Dec. 26, 2004. The earthquakes of 1930, centered in the far north of the Andaman Sea on a section of the plate boundary characterized by right-lateral strike-slip faulting, destroyed the ancient seaport of Pegu. Tsunami associated with those events caused severe flooding and fatalities in Myanmar (Nutalaya et al., 1985).

Farther south, offshore from Sumatra, the potential for great earthquakes has long been recognized from historical events with estimated magnitudes even larger than those mentioned above (Newcomb and McCann, 1987). Earthquakes there, in 1797 (Mw 8.4), 1833 (Mw 9) and 1861 (Mw 8.5) generated large tsunami. The waves of the 1833 event probably made landfall nearby with heights in the range 5-10 m (Cummins and Leonard, 2004). A smaller event (Mw 7.8) in 1907 just south of the December 26 rupture zone also produced a locally destructive tsunami in northern Sumatra (Newcomb and McCann, 1987). The inferred rupture area of that and the adjoining 1861 event were broken again by the recent (March 28, 2005) Nias earthquake.

Fault zones in Southern Thailand

Thailand is part of a geological entity extending from the Chinese province of Yunnan and Shan of Myanmar to the Malay Peninsula in the south. A number of faults are apparent in southern Thailand (Bunopas, 1981). There are two major faults in southern Thailand; they are N-NE-trending strike-slip faults, which dissect peninsular Thailand. They have been assumed to be conjugate to the NW-trending Three Pagodas Fault (TPF) and Mae Ping Fault (MPF) in Northern Thailand (Figure 1.7), the Ranong Fault (RF) and Klong Marui Fault (KMF) Zones. Both are presumably converge in the Gulf of Thailand under thick load of late Tertiary

sediments within a structural trough to form a single fault, which displaces the Rayong gneissic granites to the Hua Hin area (Garson and Mitchell, 1970).

The Ranong Fault Zone (RFZ) is a strike-slip fault, constituted by a series of faults parallel along NE-SW from the Andaman Sea in Ranong Province to the northeast Gulf of Thailand in Prachuap Khiri Khan and Chumphon Province. The fault lies in the channel of Kra-Buri River, about 270 km in length. The Carboniferous–Permian rocks in the area (Kang–Kra-Chan Group) have been affected by these faults (Garson and Mitchell, 1970). The fault moved 20 km eastward over the period of 113 $\pm$ 8 million years. During the period of Tertiary, the fault zone moved right lateral (Bunopas, 1981; Tapponnier et al., 1986). The Khlong Marui Fault Zone (KMFZ) is of strike-slip nature, aligned parallel to Ranong Fault Zone. It initially moved 150 km sinistral, and then moved right lateral at the transition of Jurassic and Cretaceous. In the middle of Tertiary, the fault is similar to the Ranong Fault Zone (Tapponnier et al., 1986; see Figure 1.7).

The development of the South China Sea and the Cenozoic basins of offshore Vietnam, Cambodia and in Northern Thailand, have also been attributed to movements on the NW-trending strike-slip faults (Tapponnier et al., 1986; Polachan et al., 1991; Briais et al., 1993), and offshore extensions of the KMF and RF have been linked to extension in the Andaman Sea and the Gulf of Thailand (e.g. Polachan, 1988; Packham, 1993; Pigott and Sattayarak, 1993). However, the timing and extent of deformation on the NW-trending structures is still under debate (e.g. England and Houseman, 1986; Rangin et al., 1995; Hall and Morley, 2004; Searle, 2006), and recent workers have favored processes such as subduction rollback (Morley, 2001), lower crustal flow (Morley and Westaway, 2006), and changing intraplate stresses as a result of edge forces (Hall and Morley, 2004), as principal controls on extension in the basins, reducing the importance of large strike-slip faults in the evolution of Southeast Asia. The KMF and RF have undoubtedly played a part in this evolution. Early work on the KMF identified a phase of brittle sinistral strike-slip deformation, based on the apparent offset of granites across the fault (Garson and Mitchell, 1970). Detailed field-based studies of fault kinematics have been notably lacking, until Intawong (2006) recognized an additional, older, ductile phase.

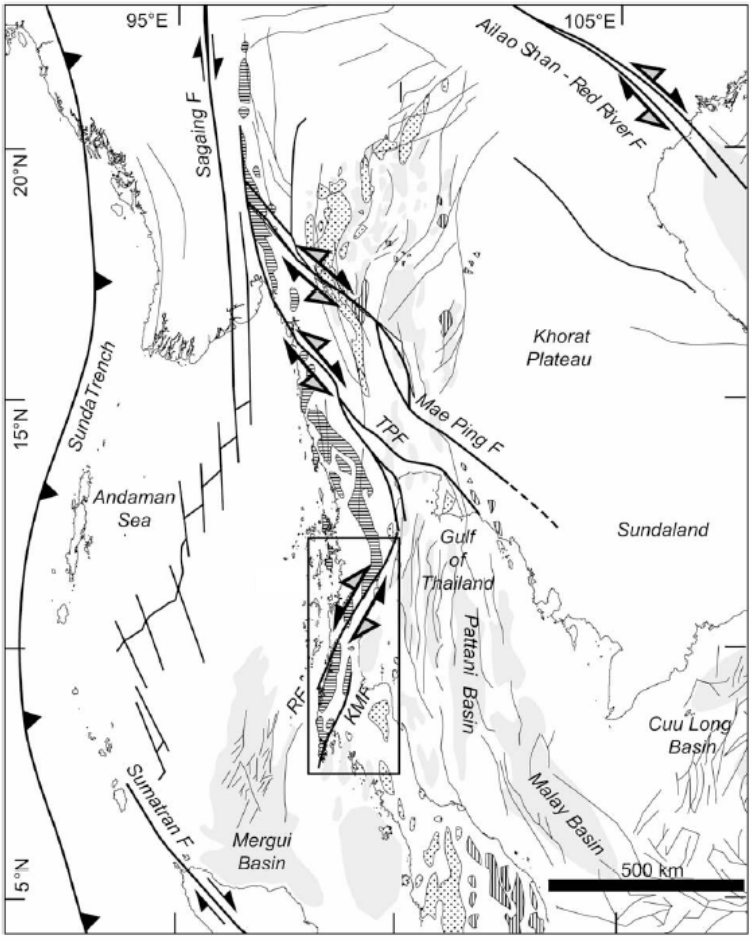

Figure 1.7 Regional tectonic elements of mainland Southeast Asia. Horizontal line ornament - Western Province granites; dotted ornament - Main Range granites; vertical line ornament - Eastern Province granites; pale grey - Cenozoic basins, black lines - brittle faults, grey half arrows - ductile shear sense, black half arrows - brittle shear sense. From Watkinson et al. (2008), after Cobbing et al. (1986), Polachan (1988), and Morley (2002).

Geological setting of the Thai Peninsula

The structural geology of the N–S trending Thai Peninsula is dominated by the KMF and RF, both broadly linear NNE-trending strike-slip fault zones centered around elongate slivers of ductile fault rocks (Figure 1.8). These are bounded and overprinted by brittle strands, which are part of a population of parallel and branching sinistral faults, which are localized into the two similar but discrete

fault zones. The smaller KMF passes from Ko Phuket in the south towards Surat Thani in the north, while strands of the RF can be traced from Takua Pa in the south to Pran Buri in the north, crossing the peninsula entirely. A relatively undeformed block with a strike-normal width of no more than 50 km lies between the two faults (Watkinson et al., 2008).

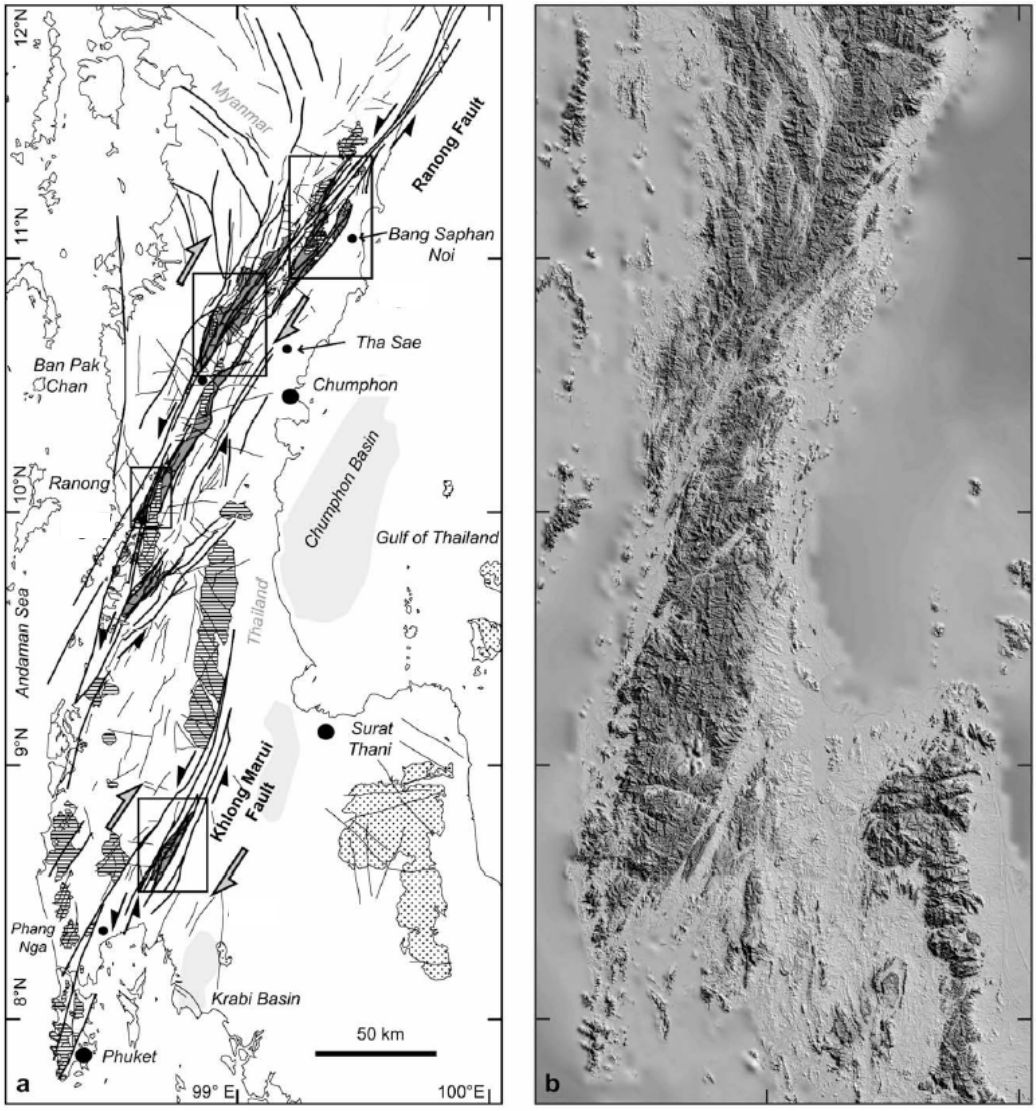

Figure1.8 The Thai Peninsula showing the Ranong and Khlong Marui fault zones. (a) Fault map. (b) SRTM (Shuttle Radar Topography Mission) digital elevation model of the same area (from Watkinson et al., 2008).

Rocks in and around the fault zones are dominantly Late Palaeozoic marine sediments deposited at mid-southern latitudes (Metcalfe, 2002, 2006). Most prominent are siliciclastic deposits of the Permo-Carboniferous Kaeng Krachan or Phuket Group, the oldest exposed rocks in the fault zone, which occupy a broad area of the central Thai Peninsula (DMR, 1982).

They comprise grey mudstone, siliceous shale, sandstone, and conglomeratic sequences between 2 and 3 km thick. Distinctive pebbly mudstones, interpreted as diamictites (Bunopas et al., 1991), are ubiquitous to the north of the KMF, and can be recognized even where they have been strongly deformed in the ductile shear zones. However, they rarely occur in the Permo-Carboniferous succession south of the fault zone. Permian Ratburi Group carbonates overlie the Kaeng Krachan Group with either a locally conformable or unconformable contact (Garson et al., 1975a; Bunopas et al., 1991). They are exposed as tropical tower karsts (Baird and Bosence, 1993), the long axes of which typically parallel the NNE–SSW structural trend on the peninsula. Sandstones and shales of the Jurassic to Cretaceous Thung Yai Group crop out on the eastern side of the RF, and all lithologies are progressively overlain by Quaternary deposits as topographic relief decreases towards the Gulf of Thailand (DMR, 1982, 2006).

Earthquakes at fault zone

Earthquakes are natural phenomena that occur as a result of plate movement (Stein and Wysession, 2003). Plates normally move with friction at their boundaries, causing stress and energy trapped inside. At a level where energy becomes excessive, it will be released in the form of an earthquake.

The plate movements create faults, which are fractures or deep cracks in the earth crust along which displacement occurs. Fault zones are parallel to each other and form a braided pattern it may vary in width ranging from a few meters to several kilometers. Faults are expanded through a series of minor movements due to stress in the crust and sudden release of energy. The displacement of faults ranges from a few centimeters to hundreds of kilometers. Faults rarely occur in a single rupture (Hamblin and Christiansen, 2001).

Thus, the major cause of earthquake is the stress originating in tectonic plate and faults that culminate in an earthquake. An earthquake virtually occurs on faults and if occurs on land close to the surface, it often leaves apparent ground breaking along the fault, for example, the earthquake that occurred on April 18, 1906, a 7.8 magnitude earthquake struck San Francisco, California, collapsing buildings and causing out of control fires to ravage the city for four days. The earthquake ruptured the ground along 270 miles (Figure 1.9) of the San Andreas Fault, severely damaging much of the Bay Area and the Northern coast of California as well.

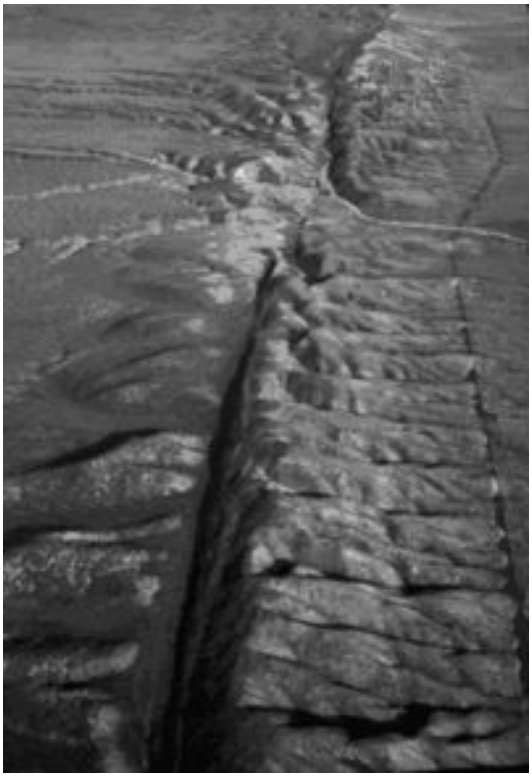

Figure 1.9 A branch of the San Andreas Fault zone in Southern California, U.S.A. (Britt, 2005).

1.1.3 Relationship between radon and earthquake

The identification techniques of proposed earthquake related signals of radon anomalies has been difficult because of several other influences, like the earth's tides, barometric pressure, temperature, rainfall, tectonic processes. The effect of tectonic activities on the permeability of aquifers or crack patterns of the earth's crust

are difficult to correct or to estimate and therefore it is also difficult to find significance in the temporal variation of earthquake related signals in radon anomalies. However, many researcher interested in relation between concentration of radon and earthquakes.

The relationship between radon and earthquakes has been studied in South Iceland since 1977, when the first equipment for this purpose was installed. The instruments were operated until 1993. The radon monitoring network consisted of up to 9 stations. Samples of geothermal water were collected from drill holes every few weeks and sent to the laboratory for radon analysis. The resulting time series varied in length from 3 to 16 years. Many earthquake-related radon anomalies were identified (Jo´nsson and Einarsson, 1996).

Environmental research, the mapping of fault zones, the prediction of earthquakes, and geological trace analysis has been developed mainly using uranium. There have been various researches dealing with the measurements of radon concentration in soil, gas emanating from the ground along active faults, which may provide useful signals before seismic events. Radon tends to migrate from its source mainly upwards. This rate of migration is affected by many factors, such as distribution of uranium (especially 226-Ra in the same series) in the soil and bedrock, soil porosity and humidity, micro-cracks of bedrock, rainfall, air temperature, barometric pressure, surface winds (Planini´c et al., 2001). Durrani and Ili´c (1997) discussed the subject of the radon emanation from fractures and fault zones in the bedrock. They have also discussed the radon concentration changes with earthquakes in fault zones and the radon transportation by diffusion or groundwater movement in fracture zones. Radon activities are clearly high in some areas such as geological fault systems, geothermal sources, uranium deposit and volcano areas (Al-Tamimi and Abumurad, 2001).

1.2 Objectives

The main objective of this study was the observation of possible variations of radon concentration in soil gas and to investigate changes in radon gas as possible earthquake precursor for the fault zones in Southern Thailand and adjacent

areas. Before the radon observation could start a radon detection system needed to be developed, calibrated, and tested in the field. Before the main field investigations and radon monitoring program field profiles needed to be measures in order to identify the locations of possible active faults and from there identify monitoring site. Parallel to the radon field measurements earthquakes needed to be monitored, especially the local earthquakes in Southern Thailand, as they are not in the records of national and international seismic networks. Finally, the results if the study will be used to test the current hypothesis that radon gas variations can be used as a possible method for earthquake warning in the study area.

CHAPTER 2

RESEARCH METHODOLOGY

The methods applied in this study aimed to measure the soil radon gas release at selected locations, and to determine the location and magnitude of local earthquakes in southern Thailand. For the radon measurements two systems were used, a solid-state nuclear track detector (SSNTD) with CR-39 cumulative track over several weeks and an automatic continuously recording device, the RPM-256. For the earthquake measurements, a short-period seismometer was installed in Thap Put District, Phang Nga Province.

2.1. Radon measurements

2.1.1. Nuclear track-etched detector

The principle of radon detection by solid-state nuclear track detectors (SSNTDs) is based on the production of alpha particle tracks in solid-state materials, such as cellulose nitrate films LR-115, type II, non-strippable (Kodak Pathe´ Co, F-93270 Sevran, France) and allyl diglycol carbonate plastic films, like CR-39, which was used as detectors during the radon measurement in this study (Pershore Mouldings Ltd, Worcestershire WR10 2DH, UK) (Alter and Fleischer, 1981).

Before applying the SSNTD system in the field, testing in the laboratory has been carried out. The temperature and time for the etchants was varied so that later the improved etchants was used for producing tracks as earlier shown by Sirijarukul (2000). The procedure has following steps:

Steps of the nuclear track-etched detector:

1. Prepare the NaOH solution with a concentration of 6.25 N, 1,000 cm^3
2. Take a beaker with NaOH solution in the water-bath (Grant-W14), etching can be accelerated by increasing the temperature to 85^oC and keep it constant (Figure 2.1).

3. Put the CR-39 plastic film for etching treatment 100 minutes in the NaOH solution at 85^{o}C, by this enlarging the etched tracks to sizes which can be viewed with an ordinary optical microscope.
4. After 100 minutes take out the CR-39 plastic film and wash it thoroughly.
5. Waiting for the CR-39 plastic film to be dry and put it on a microscope slide.
6. The tracks were counted using an optical microscope (OLYMPUS-BHC) (x 100 magnifications).
7. Adjust the focus of the optical microscope (OLYMPUS-BHC) at a magnifications 10x10 (x100) with the tracks appeared in a raster frame box (100 windows per 1 frame), as shown in Figure 2.2.

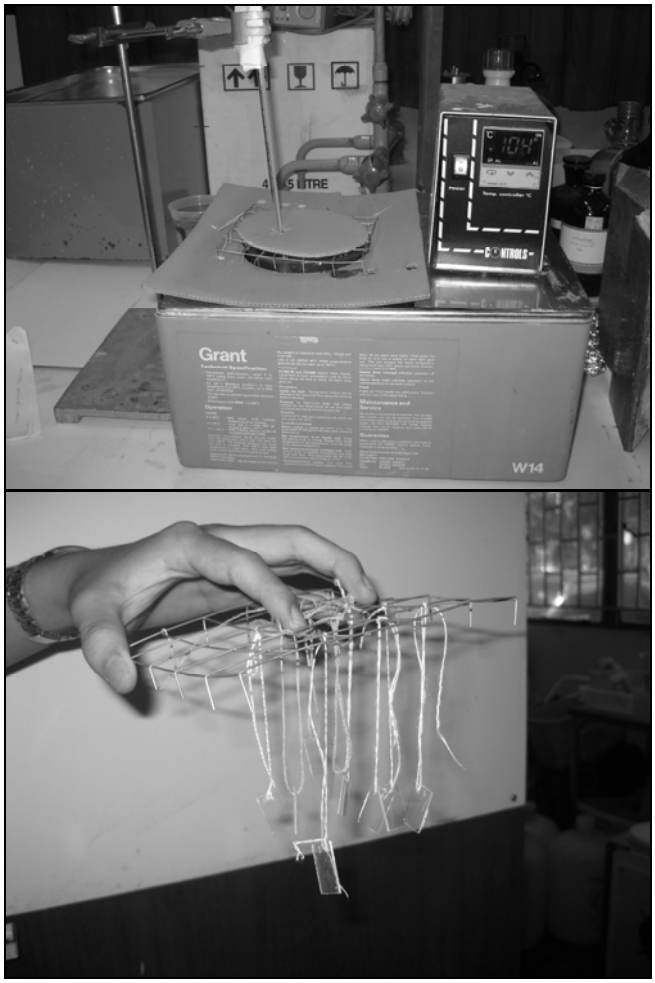

Figure 2.1 Water bath (Grant- W14) setup of the nuclear track-etched detector.

8. Counting the tracks on the CR-39 plastic film within 25 frames (1 frame = 1 mm^2) with a total area of 25 mm^2 or 0.25 cm^2. The track density is measured on the CR-39 plastic film in tracks/mm^2.
9. Changing from tracks/mm^2 in tracks/cm^2 as 25 mm^2 x 4 = 1cm^2

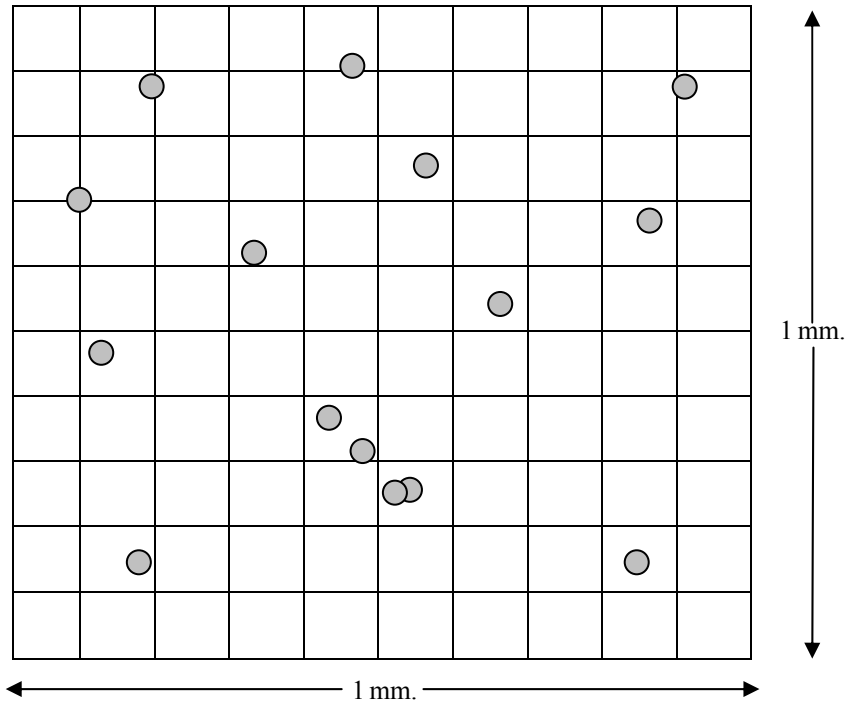

Figure 2.2 Schematic sketch of a frame of 1 mm^2 with a 10x10 raster for counting apparent density of the tracks using an optical microscope.

Figure 2.3 Counting tracks by using an optical microscope (OLYMPUS-BHC) at magnifications 10x10 (x100).

On the CR-39 plastic film a large number of tracks appear as shown in Figure 2.4. The number to be counted can be decreased by using the frame with the counting track and randomly cover the CR-39 plastic film and then using statistical analysis of the data for determination of the track density.

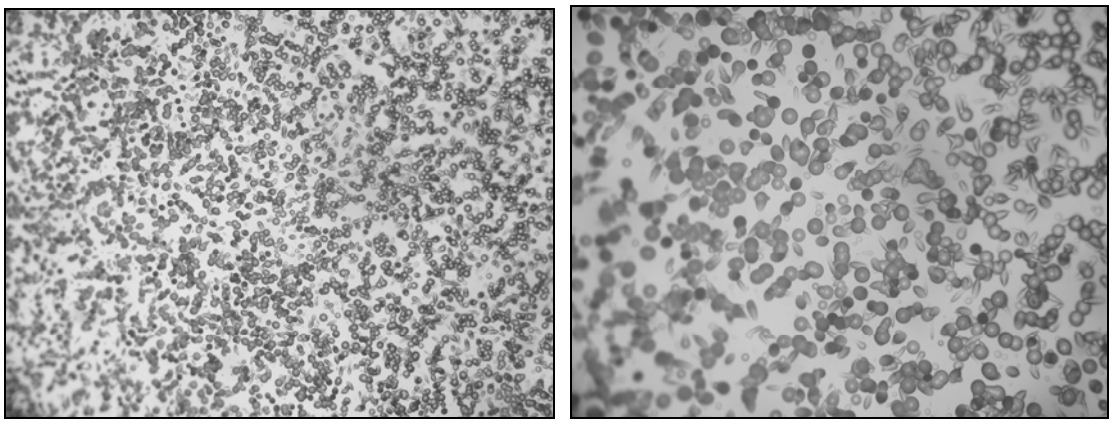

(a) (b)

Figure 2.4 After chemical etching particle tracks can be viewed under an optical microscope at (a) x100 magnification and (b) x200 magnification.

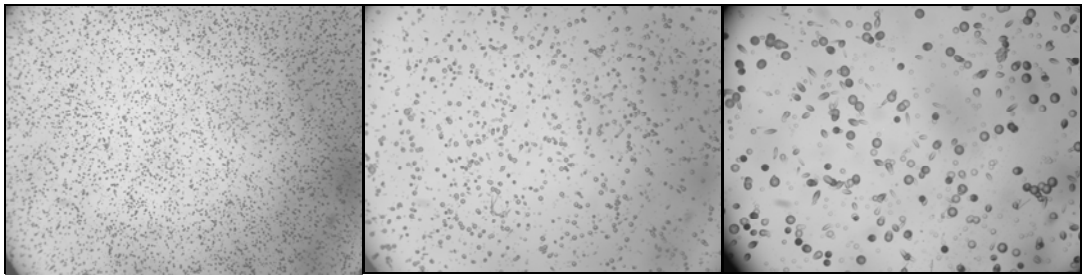

(a) (b) (c)

Figure 2.5 Alpha-tracks an apparent track density on the CR-39 plastic film. Optical microscope images (OLYMPUS-BHC) at different magnifications: (a) at x50 magnifications, (b) at x100 magnifications and (c) at x200 magnifications.

2.1.2 Track Measurement Method

The track measurement method is using a plastic detector usually placed inside a cylindrical tube of 2 inch diameter, and 1 m in length, and then put in a hole of 1 m depth. The detectors are on the top of the tube and sealed airtight against the outside environment by a standard electrical tape. The changes of radon concentrations in the soil gas were determined by using solid-state track detectors in monitoring profiles. The CR-39 plastic film, 2 cm x 2 cm, was mounted inside at the top of the cylindrical plastic lid can of each tube. Before the cans were put on the top of the tube, the opening of the tube was covered with thin polyethylene film to filter ^{220}Rn (Thoron) emission and humidity coming through the bottom opening of the tube as shown in Figure 2.6 and 2.7.

The detectors were put into holes of 1 m depth that were dug at ten different sites in Thap Put District, Phang Nga Province. The tubes were placed 1 to 5 km apart from each other. The detectors at the top of each tube were changed every week (see in Figure 2.8).

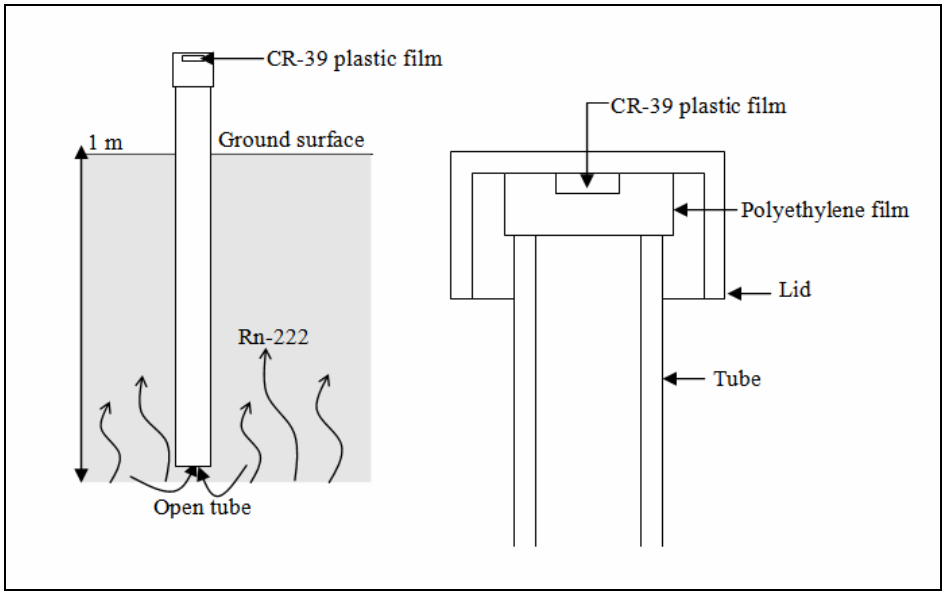

Figure 2.6 Schematic sketch of a track measurement method using a plastic pipe of about 1 m length put into the soil and a CR-39 plastic film as the detector. The polyethylene film filters ^{220}Rn (Thoron) emission and humidity coming through the bottom opening of the tube.

Figure 2.7 The measurement method of track detector for radon in soil gas: (a) a hole of 1 m depth, (b) a plastic tube put into the hole, (c) the tube was covered with thin polyethylene film and sealed airtight by a standard electrical tape, (d) the CR-39 film in a lid, (e) cover tube lid down and sealed airtight by a standard electrical tape, and (f) CR-39 film was changed every week.

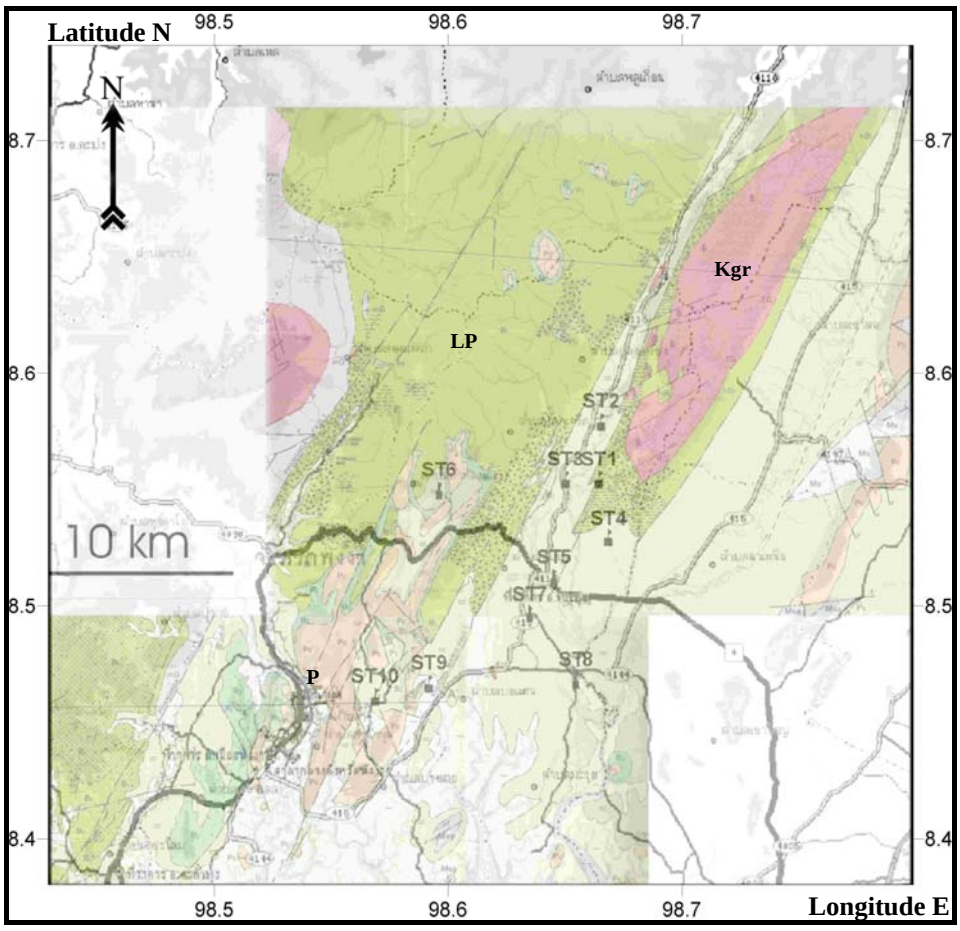

Figure 2.8 The locations of the ten track detectors (ST1 to ST10) for radon in soil gas in Thap Put District, Phang Nga Province with geological base map (from Garson et al., 1975b); P = Permian limestone, LP = Lower Permian and Kgr = Cretaceous granite.

Standard calibration

The calibration procedure aims at finding the relationship between the alpha track density on the SSNTD CR-39 plastic after etching and the standard radon concentration of known activity. The track detector system has to be calibrated using a known activity radium solution. The detector geometry and environment must be similar when performing the calibration and in the field measurement. Further the calibration procedure was performed for 100 cm tube length track detectors. The length where the atmospheric influence on the radon emission was minimal. (see also Wattananikorn et al., 1998).

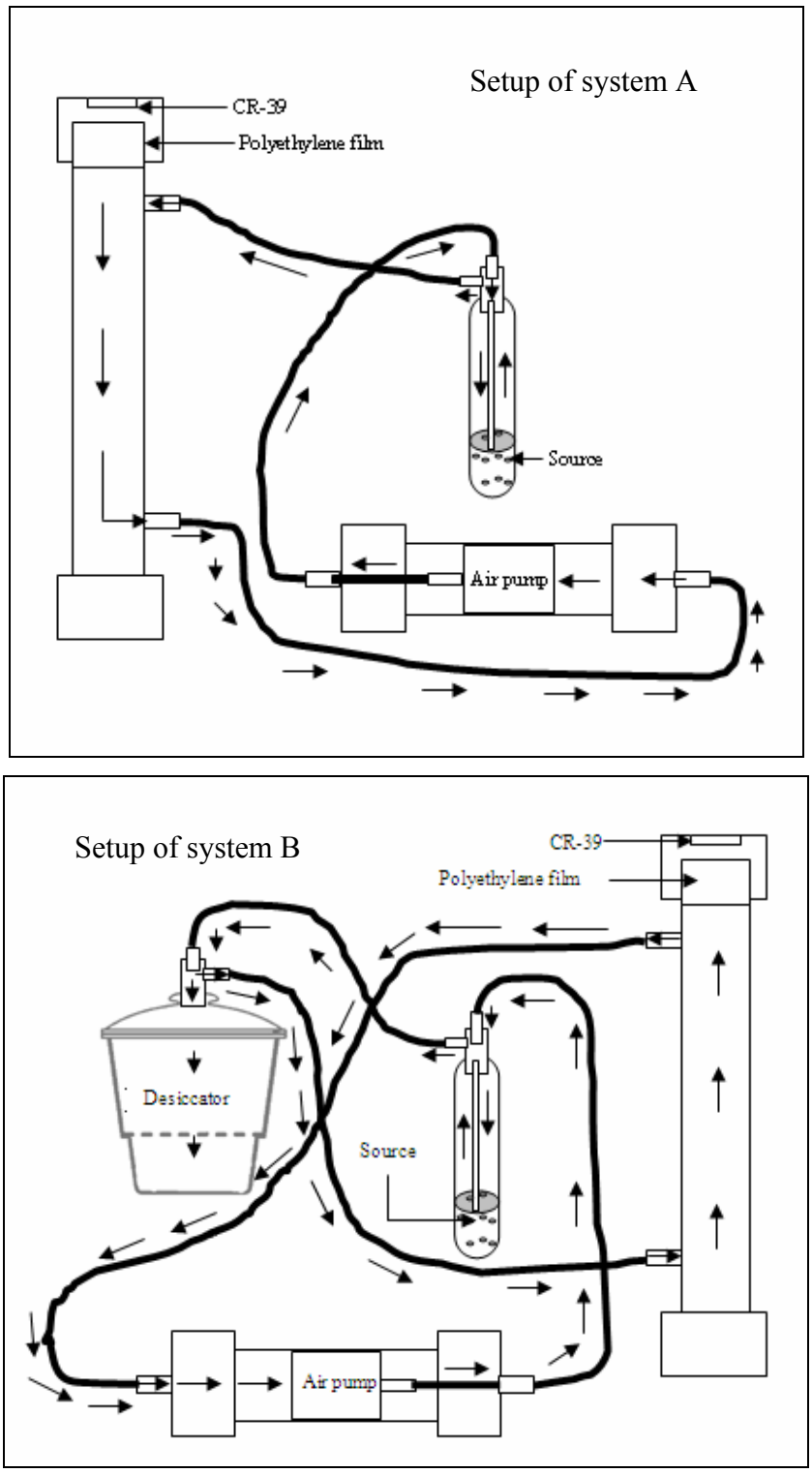

Figure 2.9 Schematic sketch of track detector system calibration using a known radium source for field measurements with two setups; system A has a smaller air volume than B; the plastic tube length is 100 cm.

A diagram of the calibration set up is shown in Figure 2.9. Setup A with a smaller air volume is used to perform a calibration for radon concentration of 1,700 Bq/m^3 standard, whereas setup B with a larger air volume is for 564 Bq/m^3 standard. SSNTD CR-39 plastic films are placed inside the radon detector and then exposed to the standard radon concentrations for 7 and 14 days each in setup A and B. These standard setups are considered to be similar to the track detector exposed to soil-gas radon in the field measurement. After exposure to radon the CR-39 plastic films then underwent track etching and counting following the steps explained earlier.

The standard calibration curve

The standard radon concentrations of 564 and 1,700 Bq/m^3 are calibrated with the track density counted as a function of exposure time. The calibration equation obtained is as follows:

$$\text{Rn Conc.}\,(\text{Bq/m}^3) = \frac{106.524 \times \text{Corr.TD}\,(\text{T/cm}^2)}{\text{Exposure Time}\,(\text{day})}\ , \qquad (2.1)$$

where *Rn Conc* (Radon concentration) is the concentration of radon in soil gas in Bq/m^3 unit, *Corr.TD* (corrected track density) is the alpha track density that corrected in Track/cm^2 unit, *Exposure Time* is the value of days of radon exposure to the SSNTDs detector, which in this case is 7 and 14 days and *106.524* is the constant of the standard calibration curve for a close system at a pipe length of 1 meter.

2.1.3 Radon Progeny Monitor (RPM-256)

The Geofyzika Brno RPM-256 Radon Progeny Monitor is a compact portable instrument powered either from batteries or external power supply, designed for measurement and/or monitoring of volume activities of daughter products of transformation of radon (RDP), in the indoor air (Figure 2.10). It is based on 256 channel real time alpha spectrometer to which is connected a probe with an air pump that sucks inspected air through a filter placed in front of the detector of alpha

radiation. Air is flowing with a stabilized flow rate of 1 liter per minute. The sensor is a semiconductor barrier silicon 250 mm^2 detector of alpha radiation with a charge-sensitive pre-amplifier. The RPM-256 has a memory of 1000 data blocks and can measure from 1-999 minutes interval.

(a) (b) (c)

Figure 2.10 The Radon Progeny Monitor (RPM-256) instrument for continues measurement set up at the station in Thap Put District, Phang Nga Province. a) Setup inside a shelter with a power backup, b) front display, and c) shelter housing the instrument with the plastic tube 1 m in the ground in front of it.

The radon concentrations in soil gas were automatically measured with the RPM-256 detector every 3 hours for 10 minute counting time. The detector is connected to a 1.5 m long and 2 inch in diameter PVC tube (Figure 2.10), which was put 1 m inside the ground. The tube is opened at its bottom end and airtight at the surface. These tube is covered with thin polyethylene film to filter ^{220}Rn (thoron) emission and humidity at the bottom, similar as described above.

Measurement steps using the RPM-256 detector

The measurement can be carried out as following:

1. The monitor is placed in the room to be measured.
2. The filter is changed.
3. The place and approximate time of the start of measurement are recorded.
4. The monitoring is started by holding the button **START**.

5. The end of measurement is indicated by an audio signal and by dashes on the display.

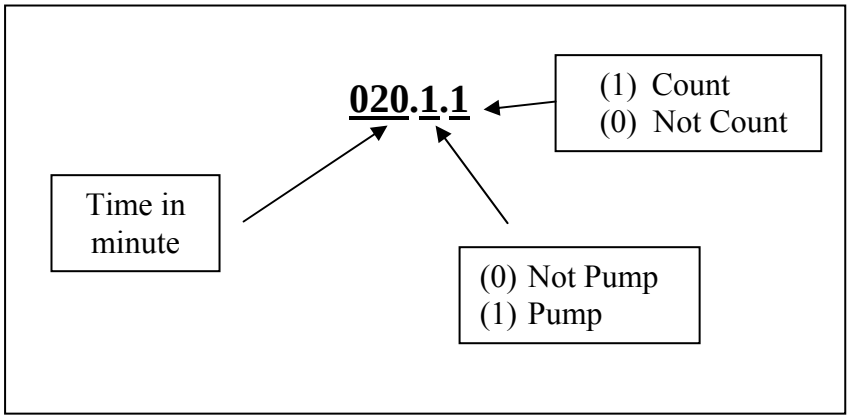

Figure 2.11 Example of time mode setting in 20-minute pumping interval is keyed in using the button of menu show in Figure 2.10b.

Air sampling is performed in soil gas with the sampling interval every three hours for ten minutes. This time mode is set by means of functions **PUMP1** steps:

1. By pressing the buttons **(SHIFT) PUMP1** the programming of timing instructions is called. The buttons Up and Down are used for scanning of the previously set sequence of instructions. If these functions cannot be easily modified to the measurement mode, they are erased by pressing the button **CLEAR** twice and confirmed by pressing the button **STORE**.
2. The 10-minutes pumping interval is keyed in using :

   01v 010.1.1 (see Figure 2.11)
3. The 170-minutes waiting interval is input.

   02v 170.0.0 (see Figure 2.11)
4. On pressing the buttons STORE.
5. The RPM starts recording when pressing the button START by preprogrammed switch-on times setting before.

Standard selection of channel windows

In the 256-channel spectrum four areas-ROI (Regions of Interest) can be delimited. Calculated in these regions is the sum of recoded impulse used to establish the volume activities of Radon Daughter Products (RDP) (Figure 2.12). Selection of channel windows is given by total gain of the shape of peaks RaA and RaC'. The maximum of RaC' peak should be on the 178th channel. To achieve a correct result, the following limits of energy windows must be retained. In the data processing of RDP the list of values should appear on the display of the window designation (1-4), designation of the lower (L) or upper (H) limit of energy window. In this study the RDP is presented in the first window; it holds for the summation of concentration of radon anomaly that was pumped in unit of counts.

Window	L	H	Energy window
1	100	220	summation channel window for check
2	100	142	channel window for RaA activity
3	152	185	channel window for RaC' activity
4	194	220	channel window for ThC' activity

Figure 2.12 Selection of channel windows for the RPM-256 detector.

In the field work, the sampling was carried out as spot checks with RPM-256 measurement every 1 km on the road for detect the fault position and monitoring site in the KMF zone covering three districts, Phanom, Kiriratnikom and Phunphin District in Surat Thani Province, with 108 sampling points along 116 km road. The RPM-256 automatic measuring detector determined the radon concentration in soil gas every 5 minutes, along a line from 470849 E 978097 N to 529150 E 1001505 N as shown in Figure 2.13.

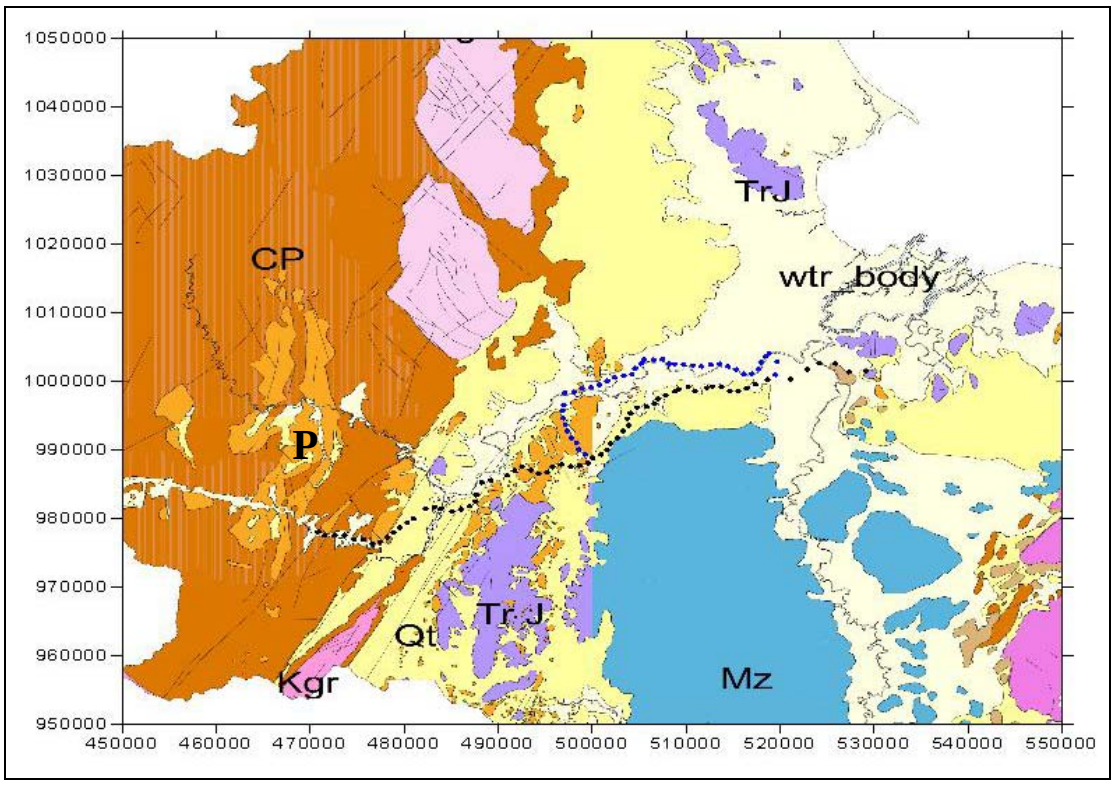

Figures 2.13 The locations of the spot check measurements of soil gas radon on the road cover 470849 E 978097 N and 529150 E 1001505 N in Surat Thani Province with geological base map; CP = Carboniferous, P = Permian, Qt = Quaternary, Kgr = Cretaceous granite, Tr J = Triassic- Jurassic and Mz = Mesozoic.

2.2. Seismic Measurements

The seismic recording system consists of following main parts: a seismometer, which is recording the ground motion, a seismograph, which is digitizing and filtering the analog data before storing them on a hard drive, a global positioning antenna, which is receiving the time information, and a power supply system.

2.2.1 Equipment

Seismometer

For this study, a Mark L-4-3D seismometer from Sercel (2002) with a frequency of 1 Hz was used. The waterproof cylinder, 20.32 cm in diameter, 18.19 cm in height, 9.1 kg weight, contains three geophones in three perpendicular directions: north-south (N-component), east-west (E-component), and vertical (Z-component). Figure 2.14 shows the seismometer form the outside and inside.

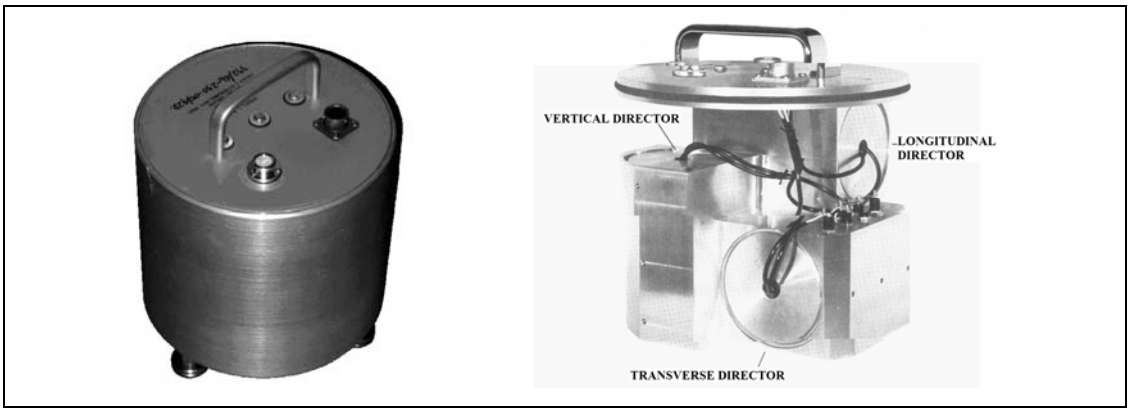

Figure 2.14 Exterior view of the Mark L-4-3D seismometer (left) and after removing the cover the three measuring components in the perpendicular arrangement are visible (right, from Sercel, 2002).

The seismometer has a pendulum or mass mounted on a spring attached to a fixed base. During ground velocity measurements, the base moves but the mass not. The movements of the base result in the generation of electrical voltage, which is recorded in a digital file. The voltage is proportional to the motion of the seismometers mass in relation to the ground, and can be mathematically converted to absolute motion of the ground.

Seismograph

The seismometer was connected via a data cable to an Orion short-period seismograph, manufactured by Nanometrics, Canada. This seismograph, with the appearance of a yellow hard plastic suitcase, is a portable seismic data logger of 47 cm in length, 37 cm width, 19 cm depth, and 10.9 kg weight with 24-bit digitizer and 100 sampling rate. A global positioning (GPS) antenna (coaxial) for time

rectification is directly connected to the seismograph. The device can either be operated with 6V-12A internal batteries or with a household power supply (Figure 2.15).

Data cartridge

Inside the Orion data cartridge is a recording hard disk of 22 cm in length, 6 cm height, 14 cm width and 0.5 kg weight. It contains a hard-disk drive of altogether 1.99 GB memory space, for each component 697 MB (Figure 2.15). In the continuous recording mode of the seismograph during this study the memory space lasts for about two to three weeks. Therefore, during this study the seismic station was visited every two weeks. The data on the Orion data cartridge were transferred via an SCSI-cable to a personal computer. A data set from one station consist of three 697 Mb files, one for each component. Additional files contain the State-of-the-Health (SOH) of the seismic recording system, and a file with all seismic events listed.

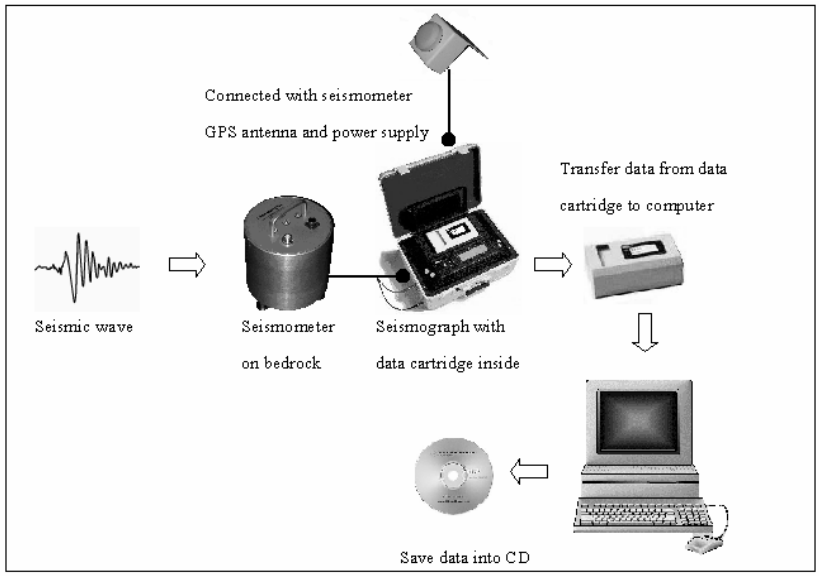

Figure 2.15 Schematic diagram of the data flow: Seismic waves travel through the solid earth recorded by the seismometer. These analog data were transferred to the seismograph via cable. Additionally time information came from a GPS antenna connected to the seismograph. All data were digitized and stored on the data cartridge. The data were regularly moved to a personal computer and additionally saved on CD.

2.2.2 Station

The location of earthquake monitoring site was situated within the Khlong Marui Fault Zone at 8°33'N and 98°39'E, in Khok Charoen Village, Thap Put District, about 20 km ESE from the Phang Nga Province, in the South of Thailand. The elevation is 55 m above sea level. The geology of the site is Lower Permian-Ordovician sandstone (bedrock outcrop). A concrete tube and small concrete cover were built to protect seismometer and seismograph from environmental perturbations. The location was remote from human settlements and close to a stream. Power was provided by a community nearby, about 20 m away. Local residents were responsible for the equipment safety (Figures 2.16 and 2.17).

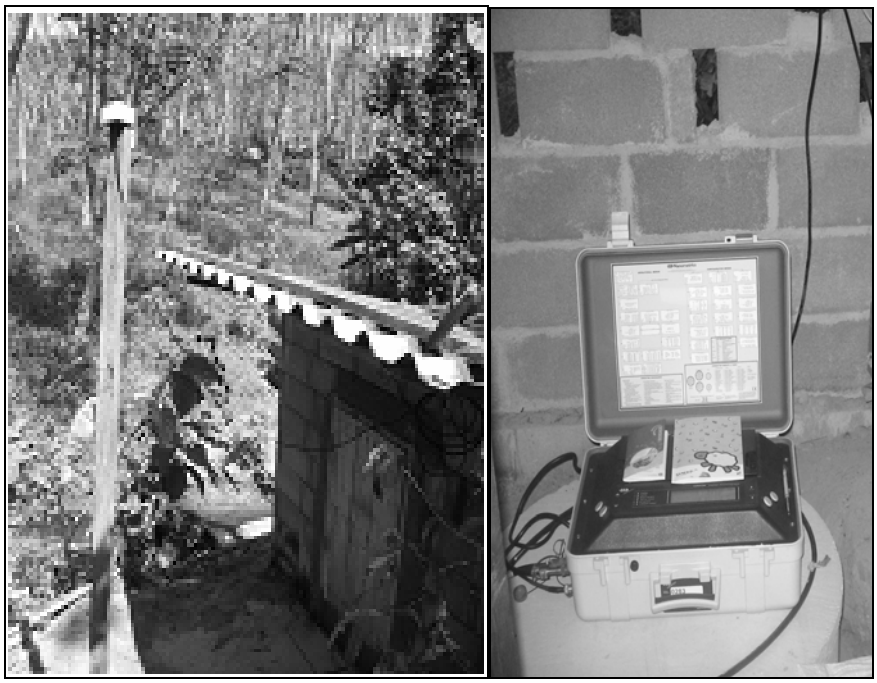

Figure 2.16 Left: Seismic station location near a small river with a small concrete shelter containing a concrete tube and the Orion portable seismograph and a GPS antenna in front. Right: Concrete shelter, where the Orion portable seismograph is protected in the concrete tube.

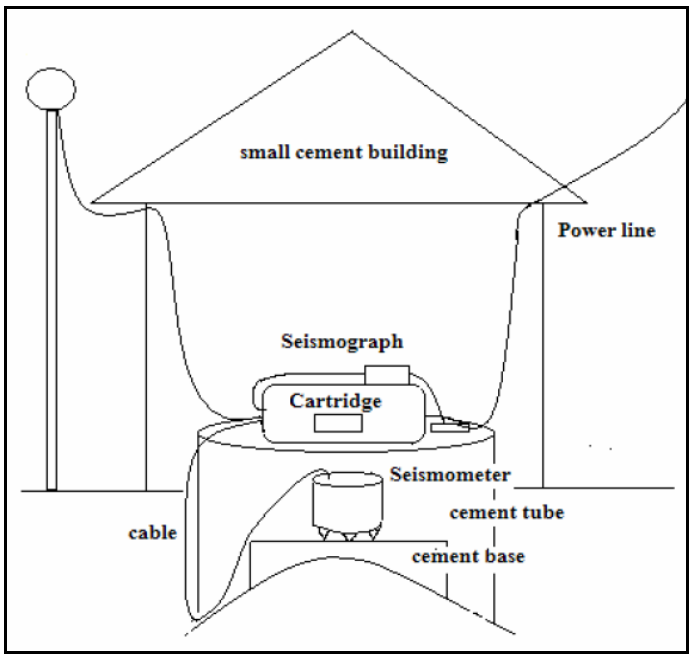

Figure 2.17 Schematic diagram of the seismic station, with the seismometer covered by a concrete tube and the seismometer inside a small house (after Dangmuan, 2008).

2.2.3 Data processing

Data processing steps

The data were transferred and processed as shown in Figure 2.18. The data from the Orion cartridge were in different files: the ringbuffer files x.she, x.shn, and the x.shz store the data of the E, N, and Z component. The x.soh file contains data about the state of health information of the seismological equipment.

The **soh file** was segregated using the **sohextrp** playback program in nmx/bin. The seismological time series data were separated from the ringbuffer files. The output file is in X-file format.

The program **response** generates a system response file, which corresponds with the station response information in the SEED file header (standard exchange of earthquake data).

The makeseed uses seed.rsp (output program) and X- file to generate the system response information.

The seed is read by rdseed program. IRIS, Incorporated Research Institutions for Seismology, developed the original UNIX-version of this program. Rdseed uses the seed data to create sac file and response file (RESP).

The Winquake software for identifying events, whereas the Seisan software utilizes seed and response file to analyze earthquake parameter, like P-wave and S-wave arrival time, amplitude for magnitude determination, and others.

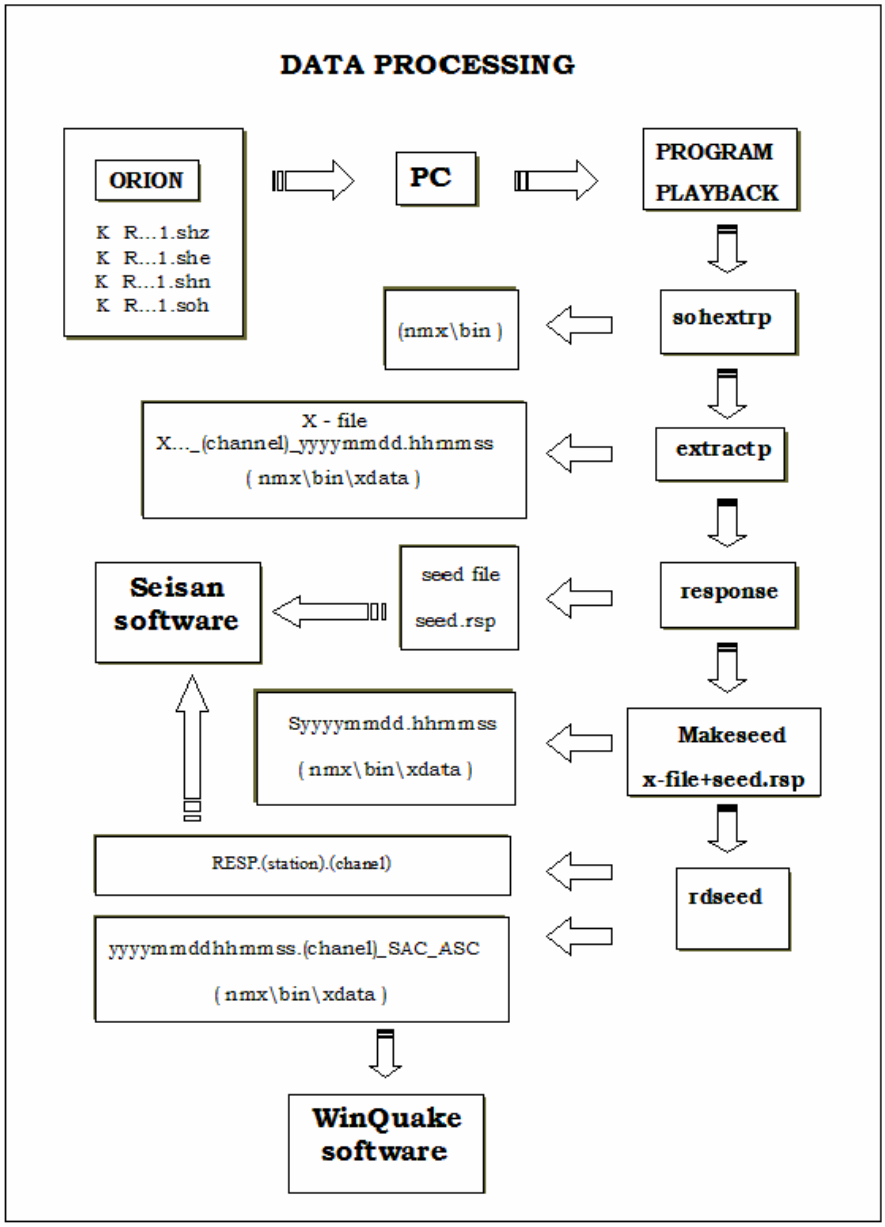

Figure 2.18 Flowchart of the stepwise processing of the seismological data (after Dangmuan, 2008).

2.2.4 Seismogram

The seismic events are displayed in Seisan software (Havskov and Ottemöller, 2005). The software can be freely downloaded from following website: ftp.geo.uib.no (129.177.554) for different operating platforms. The latest version is 8.3. For this study the version 8.1 was used.

The Seisan window has an option menu on the top, followed below by file information (Figure 2.19). The seismogram is displayed in the window below. A more detailed part of this seismogram can be additionally shown at the same time in a second window below. The x-axis for both seismograms windows is time in hours, minutes or seconds, which can be changed accordingly. The Y-axis shows the amplitude in counts.

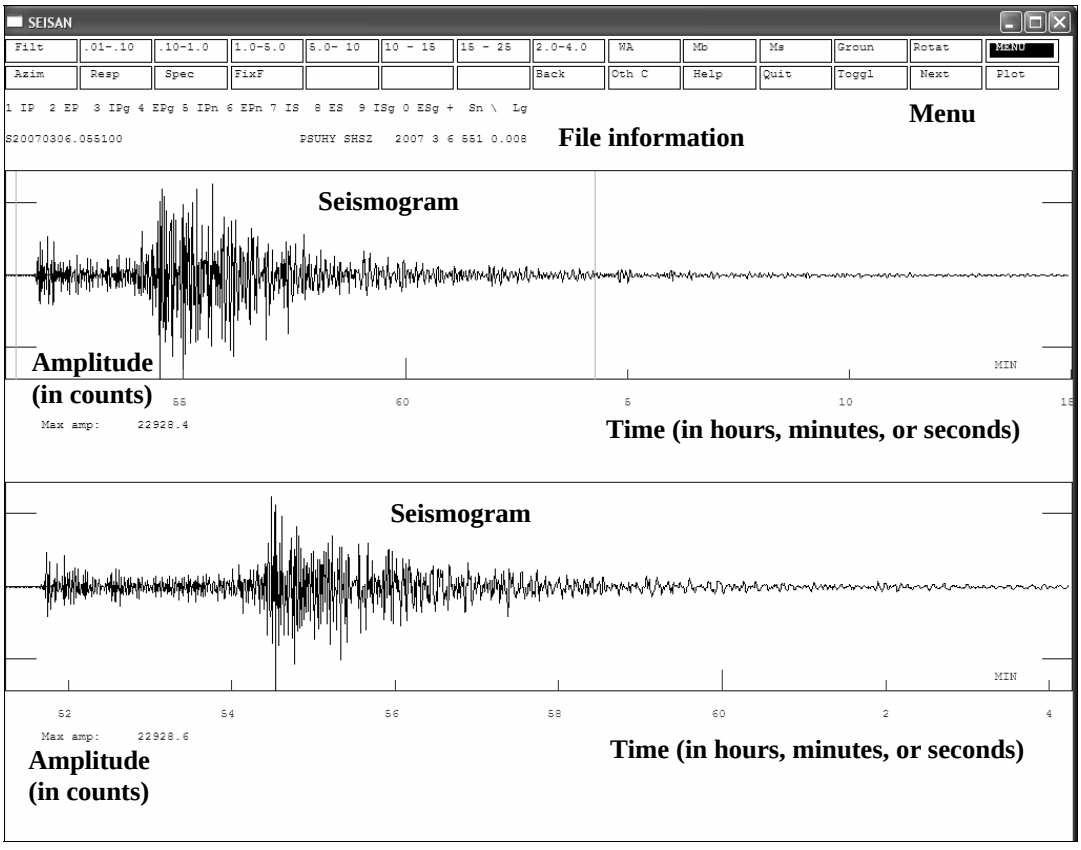

Figure 2.19 Seisan window showing a seismogram in Z-component of a seismic event recorded on 6 March 2007 (UTC time 05:48:51.31).

All three components of an event can be displayed in one window and therefore can be analyzed parallel as shown in Figure 2.20.

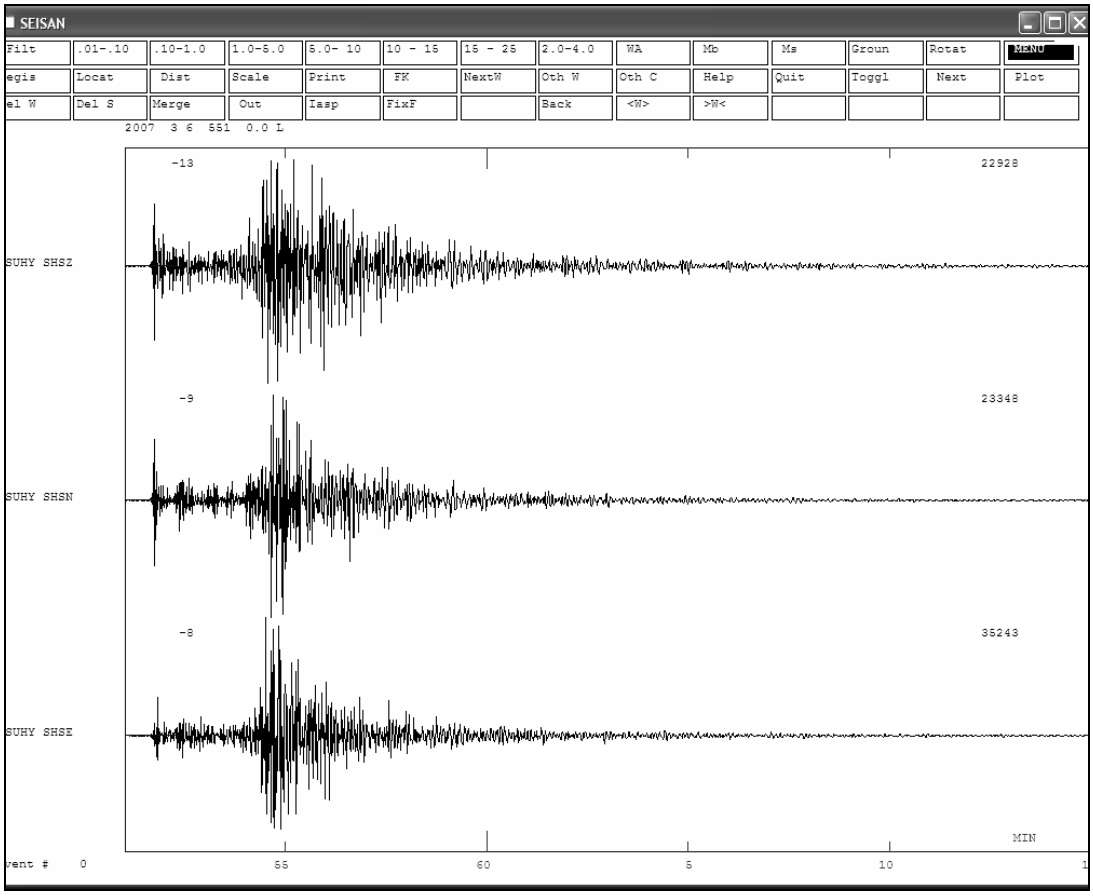

Figure 2.20 Seismogram of the Z-, E-, and N-component recorded on 6 March 2007 (UTC time 05:48:51.31). X-axis is the time in minutes; y-axis is the amplitude in counts.

2.2.5 Identification and separation of seismic events

The first step in the data analyzing process was the phase identification in the seismogram and to separate seismic noise from seismic events. The seismometer recorded all seismic events during the study time, teleseismic, regional earthquakes in the Andaman Sea, local earthquakes, man-made seismic events, and seismic noise. Therefore, the second step of the data analysis was the separation of the different types of events.

After the P- and S-phase identification and arrival time determination the regional seismic events related to the subduction zone in the Andaman Sea area and the teleseismic events were separated from local seismic events by using delta time, respectively distance. The regional and teleseismic events were usually located more than 500 km from the seismic stations (Setapong, 2007), which is equivalent to more than 50 seconds delta time using the refracted Pn- and Sn-phases. The local earthquakes and man-made seismic events were considered having a delta time with equal or less than 50 seconds between the refracted Pg- and Sg- phases (Figure 2.21).

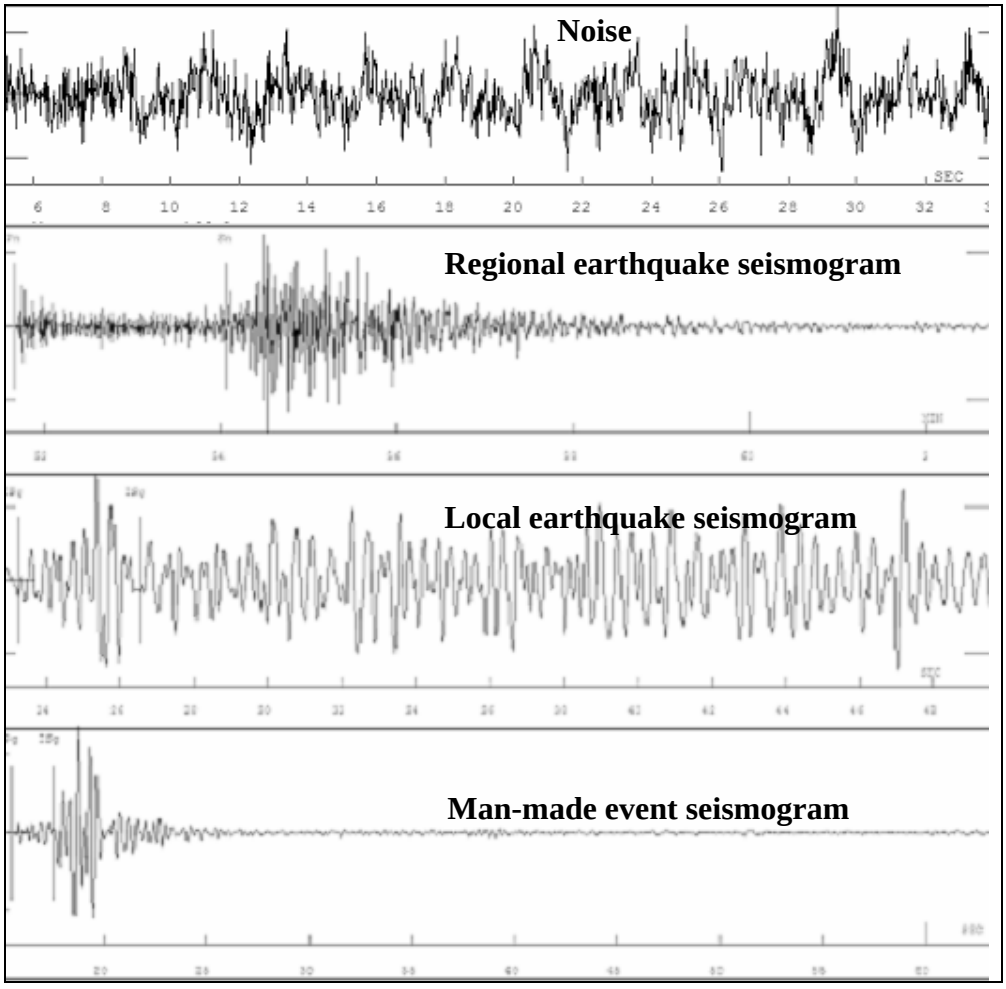

Figure 2.21 Seismogram showing the Z-component of the identification, phase separation and arrival time identification of regional earthquake in the Andaman Sea, local earthquakes, man-made seismic events; with X-axis is the time in minutes and seconds, y-axis is the amplitude in counts.

2.2.6 Distance determination of seismic events

For this study, no velocity model for Southern Thailand was available, so the depths and velocities of the Crustal and Upper Mantle layers were unknown. Therefore, the Jeffreys and Bullen (JB) velocity tables (Jeffreys and Bullen, 1967, 1970; see Appendix B1.2 and B1.3) were used for the distance determination of the seismic events (see Dangmuan, 2008). The distance between a seismic event and the station was determined using the delta time between the S- and P-wave arrival times and using the *Jeffreys and Bullen Seismological Tables*, showing delta time versus distance for certain depth of the seismic events. The P and S-wave arrival times were usually determined using seismograms with three component e.g. N-, E- and Z-component in this study (see Figure 2.22).

The depth for all seismic events in this study is set at 0 km or surface focus. The main reason was that the seismogram analysis did not allow a resolution of the depth. Because the depth of an earthquake is generally more accurate where the distance from the epicenter to the closest station is less than the calculated focal depth and the accuracy of focal depths usually increases as the number of picked S-phase arrivals increases (Trnkoczy et al., 2002). For this study, the local earthquakes were assumed crustal earthquakes with depths less than 30 km. The distances to the seismic stations were usually more than that.

For relatively shorter distances between seismic source and station, here less than 600 km, the delta time versus distance data can be represented for each phase in a linear graph as shown in Figure 2.22 (see also Table 2.1).

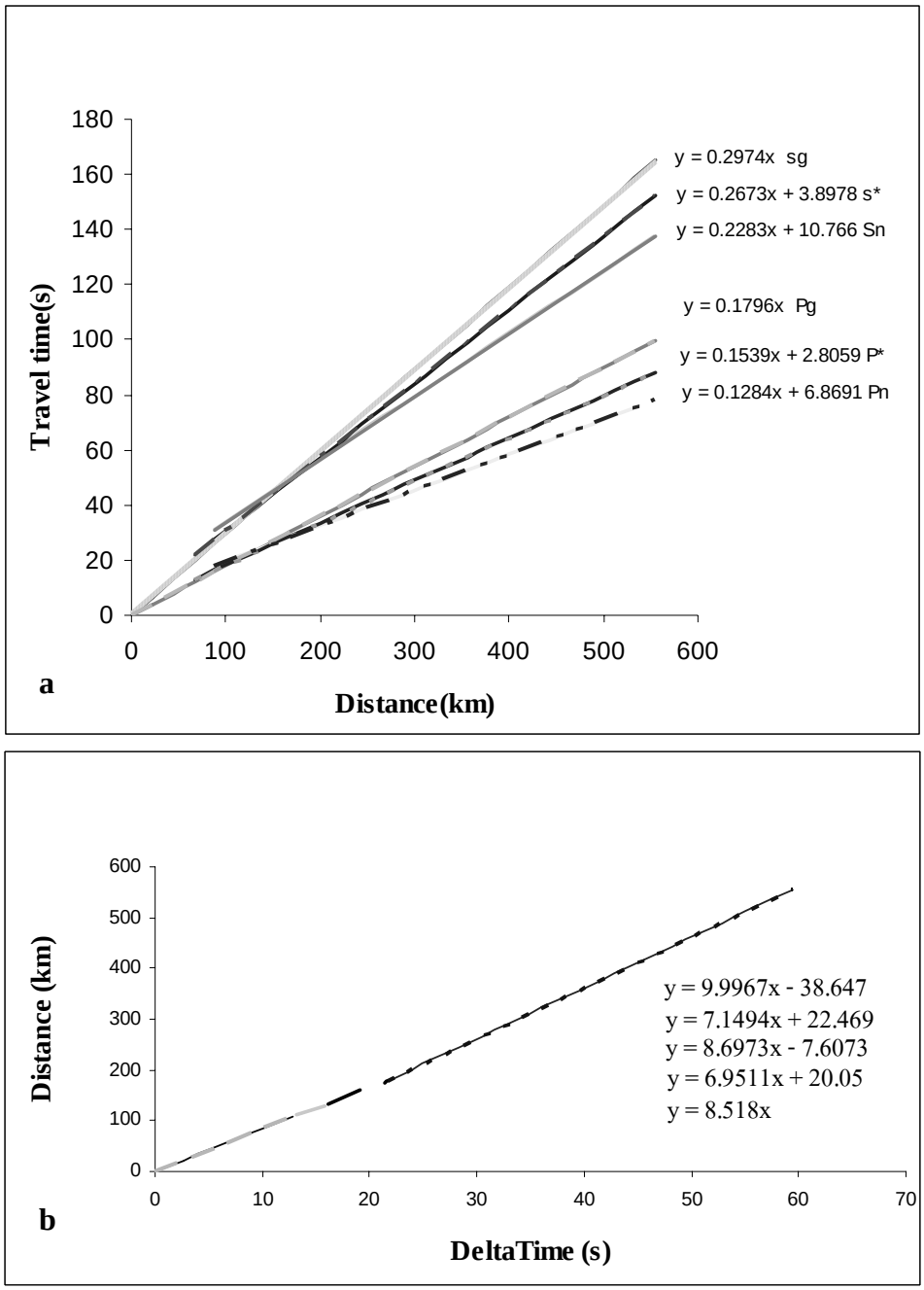

Figure 2.22 Relationship between delta time and distance for seismic events based on JB tables (a): The travel time (T) versus distance (d) for the different phases (b): Linear relationship between distance and delta time for different phases, direct and refracted waves.

Table 2.1: Delta time versus the distance for the seismic events based on Jeffreys and Bullen (1967).

Distance (y) (in km)	a	b	Delta time (x) (in sec)
y = 8.518x	8.518	0	0-12.87
y = 6.9511x + 20.05	6.951	20.05	12.87-15.76
y = 8.6973x - 7.6073	8.697	-7.607	15.76-19.16
y = 7.1494x + 22.469	7.149	22.469	19.16-21.54
y = 9.9967x - 38.647	9.997	-38.647	> 21.54

The determination of the distance from the delta time using the relationship in Table 2.1 are as following:

For the earthquake on 17 March 2007

P-wave arrival time = 19:05:23.24 UTC

S-wave arrival time = 19:06:04.20 UTC

Delta time = 40.96 sec

This seismic event has a delta time of more than 21.54 sec; therefore the distance can be calculated by the equation in the Table 2.1 as:

Distance (km) = (9.9967 km/s x 40.96 s) - 38.647km

= 370.818 km.

The earthquake location is 370.818 km away from the seismic station.

2.2.7 Determination of earthquake location

The earthquake location is determined using data from several stations and various distances from the epicenter location. In case, only one seismic station with a three-component seismometer is available, the location can be determined from the distance and the backazimuth (BAZ). However, the depth cannot be resolved with one station and is here set as zero.

Single station location

At any seismic station was possible to determined the earthquake location (epicenter) using the three-component data, north (N), east (E) and vertical (Z) component. The vector of the P- wave motion can be used to calculate the backazimuth to the epicenter. The ratio of amplitude A_E /A_N on the horizontal component is used to calculate the backazimuth: BAZ or azimuth (AZI) (Figure 2.23, Bormann and Wylegalla, 2002b) with

$$BAZ = \arctan A_E / A_N$$

The backazimuth can be determined from the first break of the P-wave arrival at all three components. The BAZ is the angle that measured clockwise from north. The BAZ is using the amplitudes of the N-, E- and Z-component and the direction of each component, up/plus (+) or down/minus (-). For example, the local earthquake recorded on 17 March 2007 (UTC time 19:04:28.75) in Table 2.2 and Figure 2.24 and 2.25.

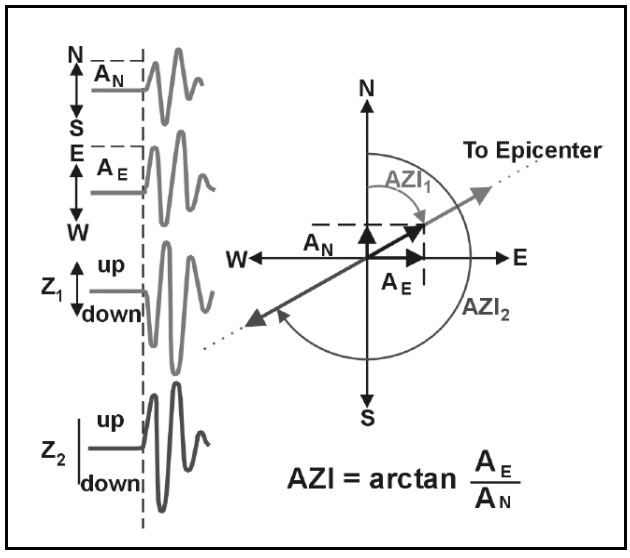

Figure 2.23 P-wave first motion in 3-component record (left) and backazimuth (AZI) to the epicenter (right), from Bormann and Wylegalla (2002).

Table 2.2: The direction for each component and the measured amplitude values for the N- and E-component for the 17 March 2007 (UTC time 19:04:28.75) earthquake, see also Figure 2.24.

Component	Direction	Movement direction	Amplitude(counts)
N	Minus	S	4.0
E	Minus	W	3.3
Z	Minus	down	

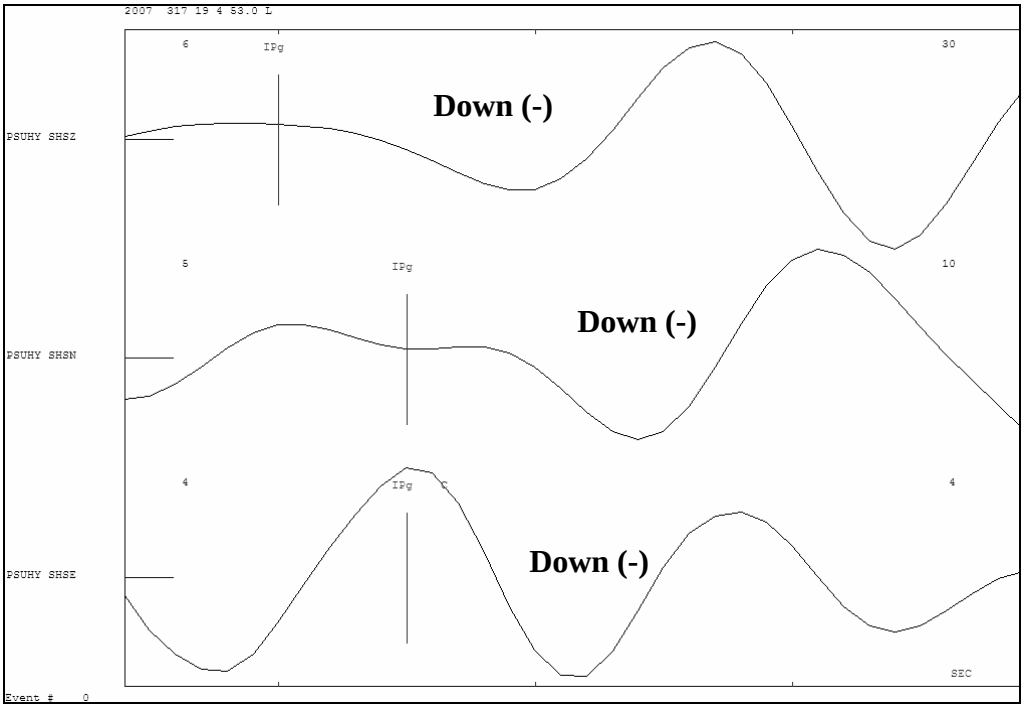

Figure 2.24 Seismogram of all three components with the first break of the earthquake recorded on 17 March 2007 (UTC time 19:04:28.75).

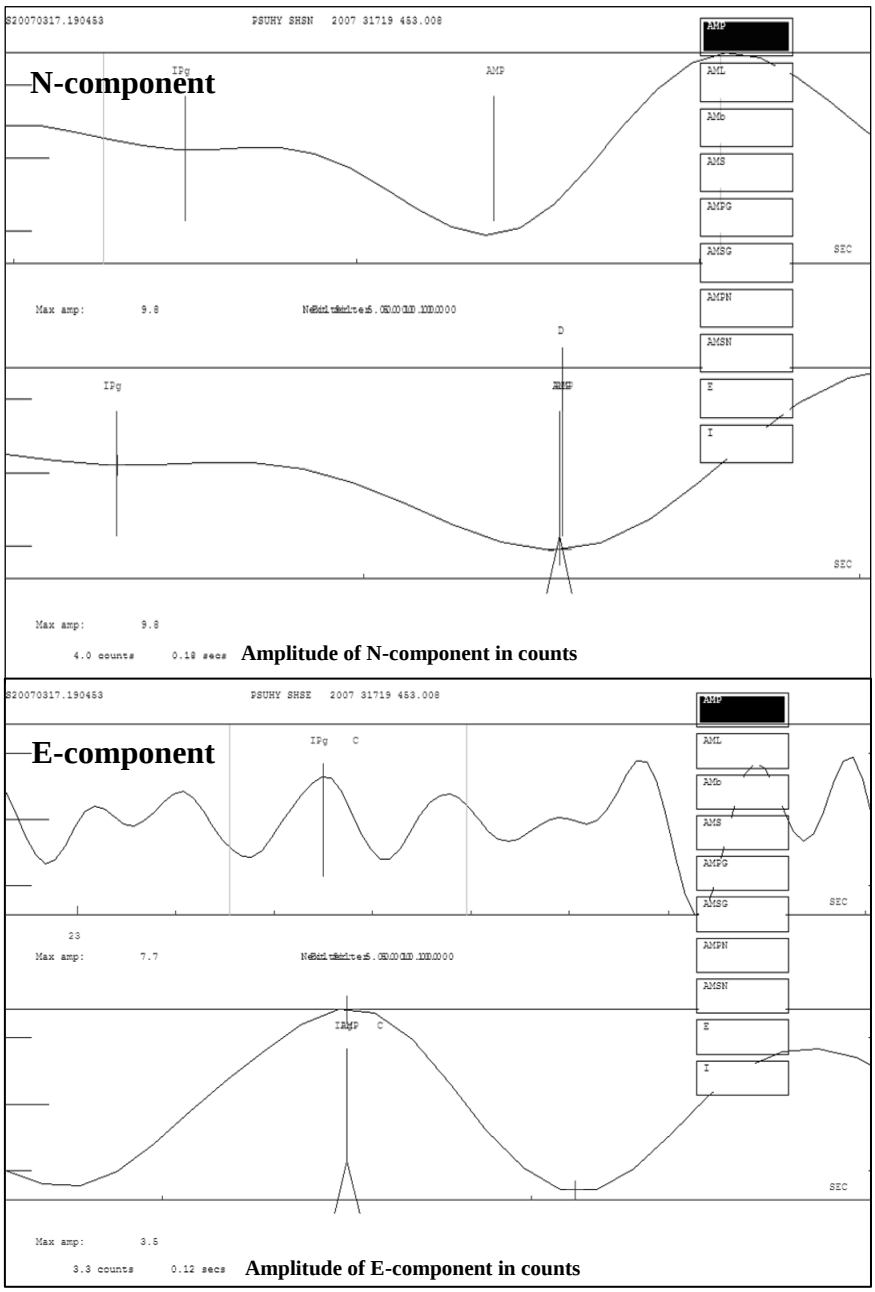

Figure 2.25 Seismograms of the 17 March 2007 (UTC time 19:04:28.75) earthquake. N- and E-components of the earthquake with the amplitude of the P-wave in the N-component of AN=4 counts and in the E-component of AE=3.3 counts.

Form the formation summarized in Table 2.2 a picture for the backazimuth and the earthquake location can be drawn (Figure 2.26). The direction N (–) is South, E (–) is West, and Z (–) is down. The vector sum of both horizontal

components provides the backazimuth angle. Then the Z-component has to be considered, showing where the first wave came from. For this example, the Z-component is down, which it means that the first wave "pulls" the surface at the seismometer down. Finally, the earthquake wave came from the SW, the location of earthquake.

$$\text{The backazimuth angle (BZI)} = 180^{o} + (\tan^{-1}\frac{AE}{AN})$$

$$= 180^{o} + (\tan^{-1}\frac{3.3}{4})$$

$$= 180^{o} + 39.52^{o}$$

$$= 219.52^{o}$$

The earthquake location can be found from the location of the seismic station (in this case, longitude and latitude) and distance and the backazimuth.

Location of seismic station: 98.66^{o}E and 8.55^{o}N

Delta latitude = (distance x cos 39.52 ^{o}) /111.32 km.
= (370.81 km x cos 39.52 ^{o})/111.32 km
= 2.57 ^{o} N

Delta longitude = (distance x sin39.52 ^{o}) /111.32 km.
= (370.81 km x sin 39.52 ^{o})/111.32 km
= 2.12 ^{o} E

Coordinates of earthquake recorded on 17 March 2007 are

Longitude = 98.66 – 2.12 = 96.54 ^{o} E

Latitude =8.55 – 2.57 = 5.98 ^{o} N

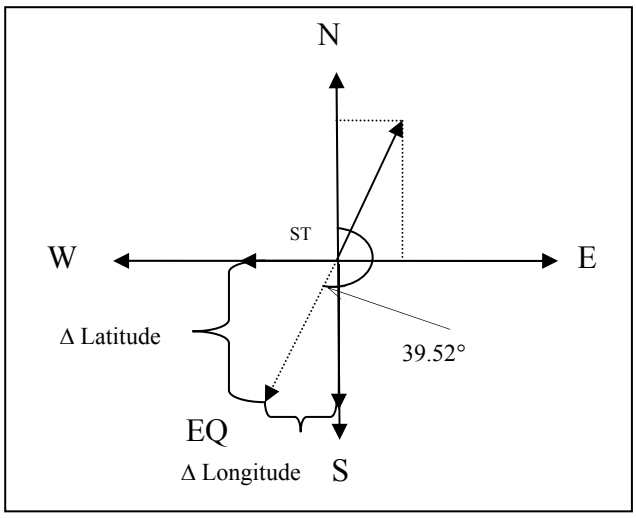

Figure 2.26 Earthquake on 17 March 2007: Relationship between the amplitude of the first P-wave for earthquake location determination with one three-component seismometer. For the data see text.

2.2.8 Origin time

The origin time is the time when the earthquake happened, and when both P-wave and S-wave started. The origin time of seismic event can be determined from the P- or S- wave arrival time and the distance-travel time relationship in the JB travel time table (see in Figure 2.22a). After the distance is determined from the delta time the travel time for each phase and the origin time can be found in the JB travel time tables (see Table 2.3). For example, see below the calculation of the origin time for the seismic event recorded on 17 March 2007, with the seismic phase to be Pn refracted at the Moho.

Table 2.3: Travel time versus the distance for the origin time of seismic events based on Jeffreys and Bullen (1967).

Travel time (y) (in sec)	**a**	**b**	**Distance (x) (in km)**	
y=0.1796x	0.1796	0	0-111.11	Pg
y=0.1539x + 2.8059	0.1539	2.8059	111.11-159.34	P^*
y=0.1284x + 6.8691	0.1284	6.8691	>159.34	Pn

Origin time = Time of P-wave arrival at station-Travel time of P-wave

= 19:05:23.24- 00:00:54.48

= 19:04:28.75 UTC

2.2.9 Magnitude

Local magnitude

For all seismic events in this study, the local magnitude (Ml) was determined. The local magnitude is applied for epicenter distances less than 5 degrees (Bormann, 2002). The local magnitudes are calculated as following

$$Ml = \log A_{max} - \log A_0 \qquad (2.2)$$

with A_{max} is the amplitude sum in mm, measured as zero to peak in the horizontal component (East and North component, $A_{max} = \sqrt{(E^2_{max} + N^2_{max})}$) with a Wood-Anderson seismograms and $- \log A_0$ is the correction or calibration values. In this study, the local magnitude was calculated following Hutton and Boore (1987):

$$- \log A_0 = 1.110 \log (R/100) + 0.00189 (R- 100) + 3 \qquad (2.3)$$

with R is the hypocentral distance in km, $R = \sqrt{(\Delta^2 + h^2)}$, Δ is the epicentral distance in km, h is hypocenter depth in km. If h = 0, zero depth, then $R = \Delta$. For data recorded on a Wood-Anderson seismograph the local magnitude can be calculated as

$$Ml = \log A_{max\,(mm)} + 1.110 \log (R/100) + 0.00189 (R- 100) + 3 \qquad (2.4)$$

In the Seisan software, the real ground displacement is calculated from the seismogram and the response information (Havskov and Ottemöller, 2005). In the real ground displacement window the amplitudes for the magnitude determination are

measured. Therefore, the local magnitude in formula Equation 2.4 has to be changed for real ground displacement using the Wood-Anderson magnification of 2080 $\pm$ 60. Rewriting Equation 2.4 for real ground displacement amplitudes (A_{max}) in nanometers (10^{-6} mm = 1 nm) the magnitude formula is (Dangmuan, 2008).

$$Ml = \log (A_{max\,(nm)}) + 1.110 * \log (R) + 0.00189*R - 2.09 \qquad (2.5)$$

where A_{max} is the sum of the amplitude in the East and North component (in nm) measured at the same time, with $A_{max} = \sqrt{(E_{max}^2 + N_{max}^2)}$, and R the hypocenter distance (in km).

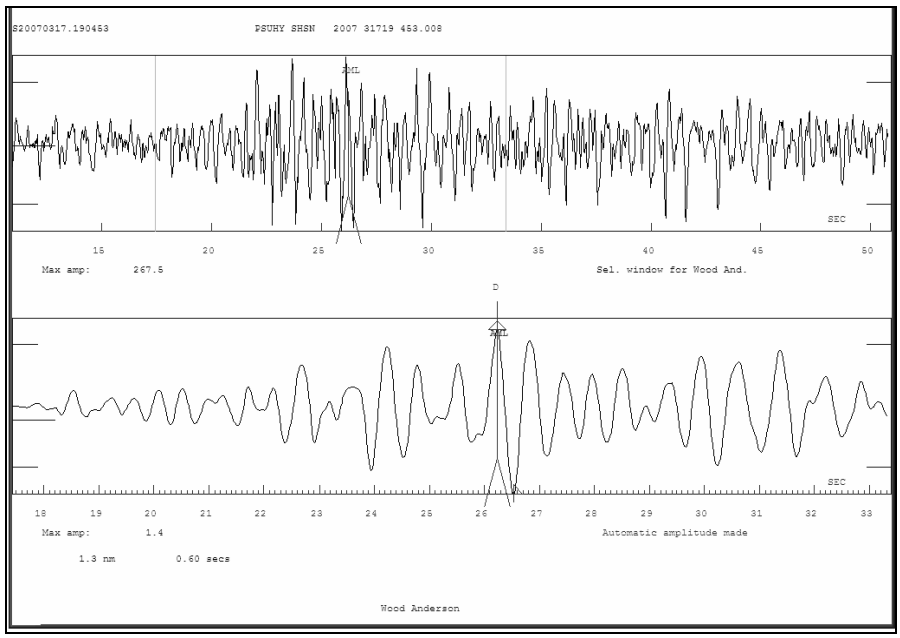

Figure 2.27 Seismogram of the local earthquake recorded on 17 March 2007 (UTC time 19:04:28.75) in the N-component with the maximum amplitude of 1.3 nm and a period of 0.60 sec.

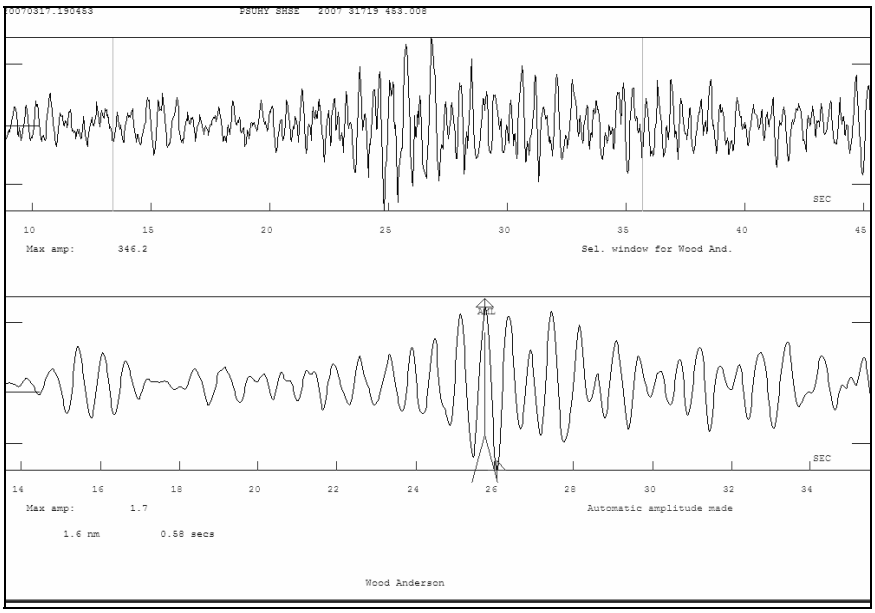

Figure 2.28 Seismogram of the local earthquake recorded on 17 March 2007 (UTC time) in the E-component with the maximum amplitude of 1.6 nm and a period 0.58 sec.

Determination of the local magnitude (after Hutton and Boore, 1987) for the earthquake on 17 March 2007 at 19:04:28.75 UTC (see also Figure 2.27 and 2.28):

Maximum amplitude in E component = 1.6 nm

Maximum amplitude in N component = 1.3 nm

$$\text{Vector sum} = \sqrt{E^2 + N^2} = 2.06$$

Local magnitude (Ml)

A_{sum} = 2.06 nm, distance = 124.2 km

$Ml = \log_{10} A_{sum} + 1.11 * \log_{10} D_{km} + 0.00189 * D_{km} - 2.09$

$Ml = \log_{10} 2.06 + 1.11 * \log_{10} 370.8 + 0.00189 * 370.8 - 2.09$

$Ml = 1.8$

Following this calculation, the local magnitude of the earthquake is Ml=1.8.

Body-wave magnitude

The body wave magnitude was calculated from the highest amplitude of the P-wave for earthquakes with an epicenter distance more than 5^o ($D \geq 5^o$) and the period of the waves ranges from $0.1 \leq T \leq 3.0$ sec following USGS (2005) by using the formula defined by Gutenberg and Richer (1956) in Equation 2.6 (see Setapong, 2006).

$$mb = \log(A/T)+Q(D,h) \qquad (2.6)$$

where *A* is the maximum ground amplitude in micrometer for events of with period *T* (in seconds), *Q* is a function for the body wave phase (Figure 2.29) dependent on the focal depth *(h)* as set at 30 km, and the epicenter distance *(D)* in degrees ($D \geq 5^o$). For the earthquake recorded on 6 March 2007 at 05:48:51.31 UTC time the seismograms and amplitude analysis are shown in Figure 2.30 and 2.31.

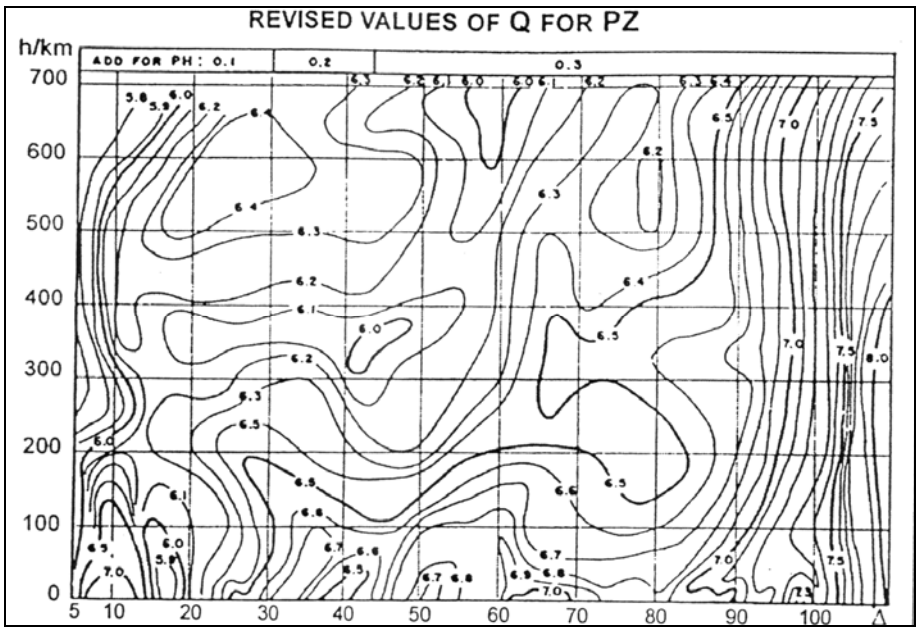

Figure 2.29 Q (Δ) values as function of distance Δ and source depth after Gutenberg and Richter (1956) for P-wave in vertical and horizontal components. These Q values are valid only when A is given in micrometer (μm).

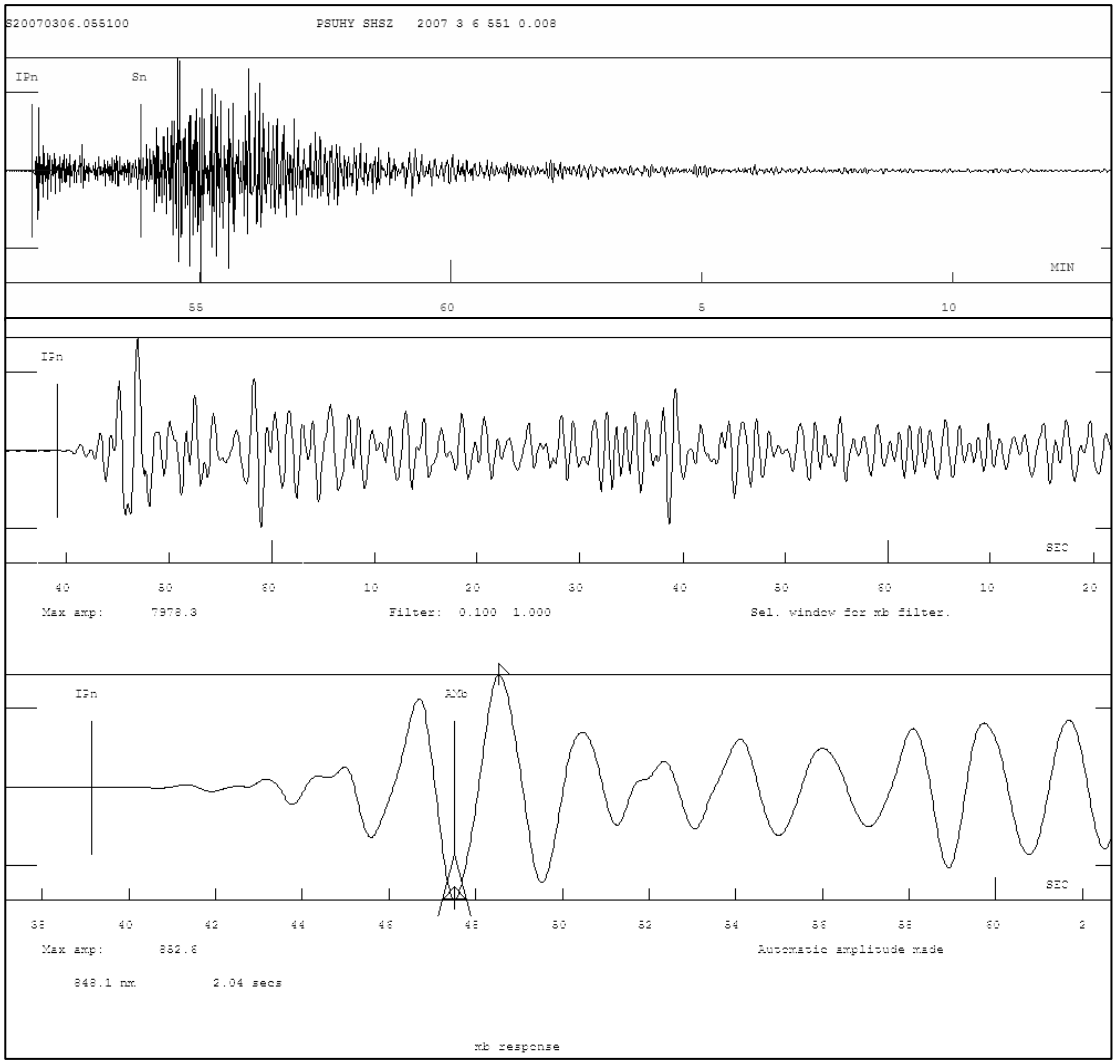

Figure 2.30 Seismogram of the vertical (Z-) component recorded on 6 March 2007 (05:48:51.31 UTC time) with the maximum ground displacement amplitude of 848.1 nm and a period of 2.04 sec of the P-wave used to determine the body-wave magnitude.

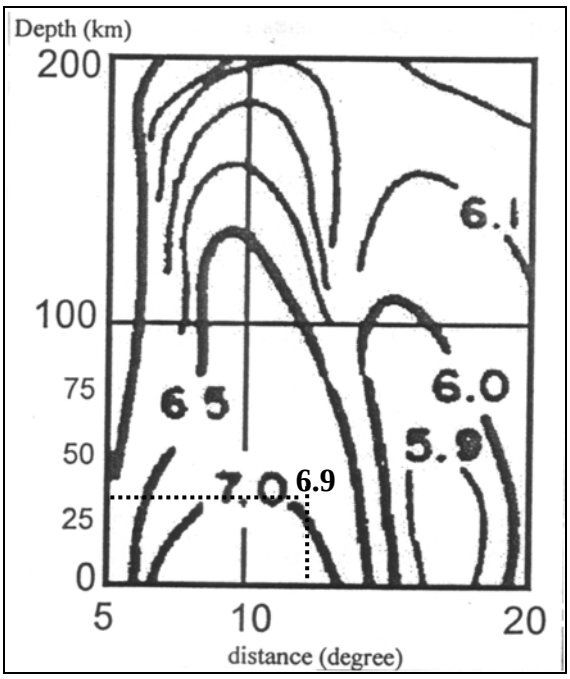

Figure 2.31 The Q (Δ) value for the vertical (Z-) component recorded on 6 March 2007 (05:48:51.31 UTC time) is 6.9 following Figure 2.30. The distance is 12.53 degrees and the depth is set at 30 km.

An example of the amplitude analysis for body-wave magnitude determination is shown in Figure 2.30, where the earthquake has a maximum amplitude of the P-wave of 0.8481 μm (848.1 nm), and a period of 2.04 sec (Figure 2.30, 2.31). The distance in degrees is 12.53 and the depth is 30 km. Therefore,

$$mb = \log(A/T)+Q(D,h)$$
$$= \log(0.8481/2.04)+6.9$$
$$= 6.5$$

Following this calculation, the body-wave magnitude of the earthquake is 6.5 mb

CHAPTER 3

RESULTS AND DISCUSSIONS

In the nearly four month period from 12 January to 20 May 2007 the radon concentration in soil gas and earthquake measurements were carried out. The results obtained are presented in this chapter.

3.1. Average radon concentration in soil gas at ten stations

The radon concentration in soil gas measurements were conducted at 10 stations, mainly in Thap Put District, Phang Nga Province, all distributed along the Khlong Marui Fault Zone within the study area. The results of the radon concentration were presented as the variation of cumulative alpha track over a week period, which was then separated in an average radon concentration in Bq/m^3/day. The radon emission data cover three months in the period from 28 January to 25 April 2007, altogether 12 weeks at 10 locations. To identify radon anomalies the data from each station were compared to each other over the period of measurement. The data in Table 3.1 show that for all 10 stations the 70 % confidence (7 in 10 stations) of the average radon concentration value of each station is ranged 221-362 kBq/m^3. Three locations have an average radon concentration value higher than the 70 % confidence; ST-10, ST-02, and ST-04 with 2,241, 627, and 602 kBq/m^3, respectively (see also Figure 2.8). At station ST10 at 8.46^o N and 98.57^o E, the radon concentration is in general higher than at other locations for every week (see Figure 3.1 and 3.2).

The first radon anomaly at ST-10 was in the interval from 11 March to 25 March 2007 of week 7 and week 8, which shows an increase from the mean value of 2,241 kBq/m^3 with more than one standard deviation of 971 kBq/m^3 to 3,251 and 3,728 kBq/m^3, respectively. In week 9, from 25 March to 1 April 2007, the radon value decrease (1,675 kBq/m^3) and a second radon anomaly can be seen in the interval from 1 April to 15 April 2007, week 10 and 11, with 2,782 and 3,615 kBq/m^3, respectively. The highest radon anomaly was in week 8, from 18 March to 25 March

2007, with 3,728 kBq/m^3 (see Figure 3.2). The comparison of the anomalies with all data is shown in Figure 3.4.

Table 3.1: Radon track in soil gas concentration data by solid-state nuclear track detectors using CR-39 plastic films for all ten stations in Phang Nga Province with mean and standard deviation.

Site Number	Longitude (degree East)	Latitude (degree North)	Radon concentration (kBq/m^3)	
			Mean	Stdev
ST-01	98.66	8.55	253	88
ST-02	98.67	8.58	627	264
ST-03	98.65	8.55	314	97
ST-04	98.67	8.53	602	255
ST-05	98.65	8.51	211	113
ST-06	98.60	8.55	362	103
ST-07	98.63	8.50	262	68
ST-08	98.65	8.47	357	110
ST-09	98.59	8.47	254	70
ST-10	98.57	8.46	2,241	971

Table 3.2: Cumulative one week alpha track radon concentrations (kBq/m^3) at ten different stations in Phang Nga Province over a 12-week period from 28 January to 25 April 2007.

Time (week)	Radon concentration (kBq/m^3)									
	ST-01	ST-02	ST-03	ST-04	ST-05	ST-06	ST-07	ST-08	ST-09	ST-10
1	256	677	184	288	280	276	271	312	319	723
2	173	117	222	471	431	406	383	224	332	1903
3	235	302	226	399	235	205	306	275	152	1716
4	169	504	248	-	325	324	223	256	240	1466
5	289	1177	530	-	329	361	-	332	321	2179
6	213	481	277	450	226	272	-	269	275	1619
7	101	678	269	299	162	324	302	277	133	3251
8	268	610	328	631	61	392	260	346	258	3728
9	329	725	350	892	146	586	153	500	323	1675
10	432	780	416	870	134	505	264	504	236	2782
11	339	760	379	746	100	330	287	509	287	3615
12	231	713	339	969	95	358	167	483	172	-

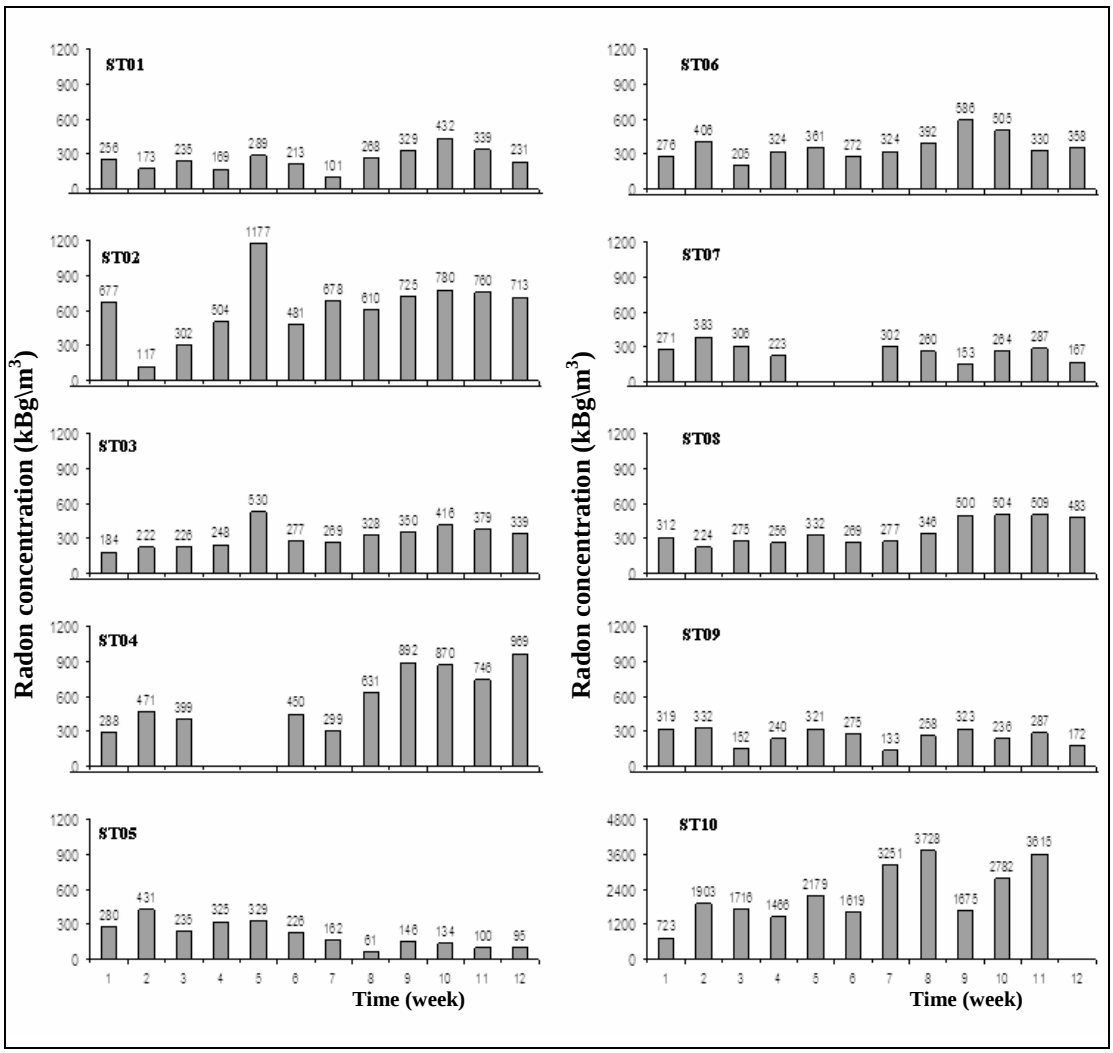

Figure 3.1 Cumulative one week alpha track radon concentrations (kBq/m^3) for the ten stations in Phang Nga Province over a 12-week period from 28 January to 25 April 2007.

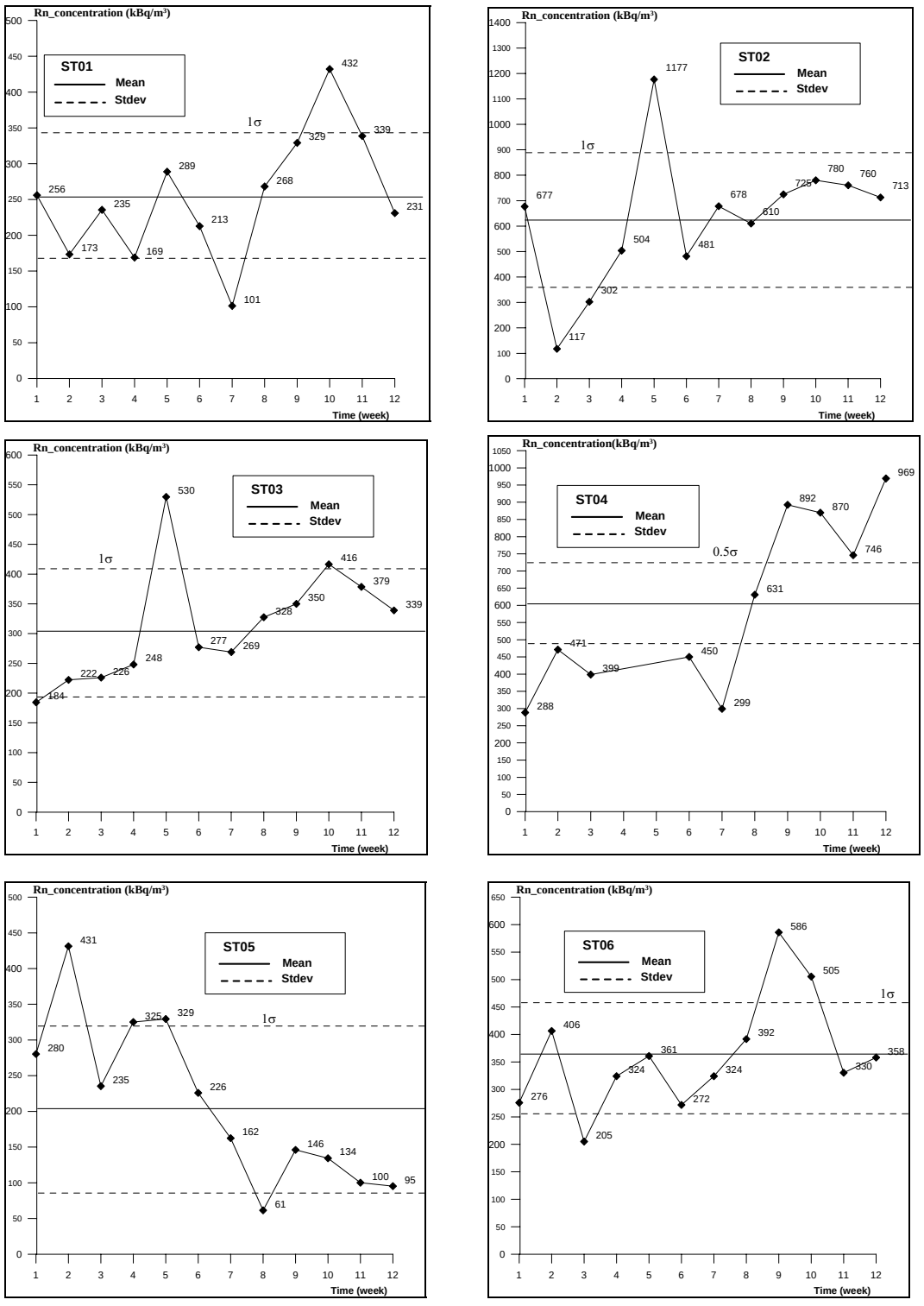

Figure 3.2 Radon concentrations in soil gas (kBq/m^3) for each week over the 12-week measurement period from 28 January to 25 April 2007 for six stations, ST01 to ST06, with mean and standard deviation.

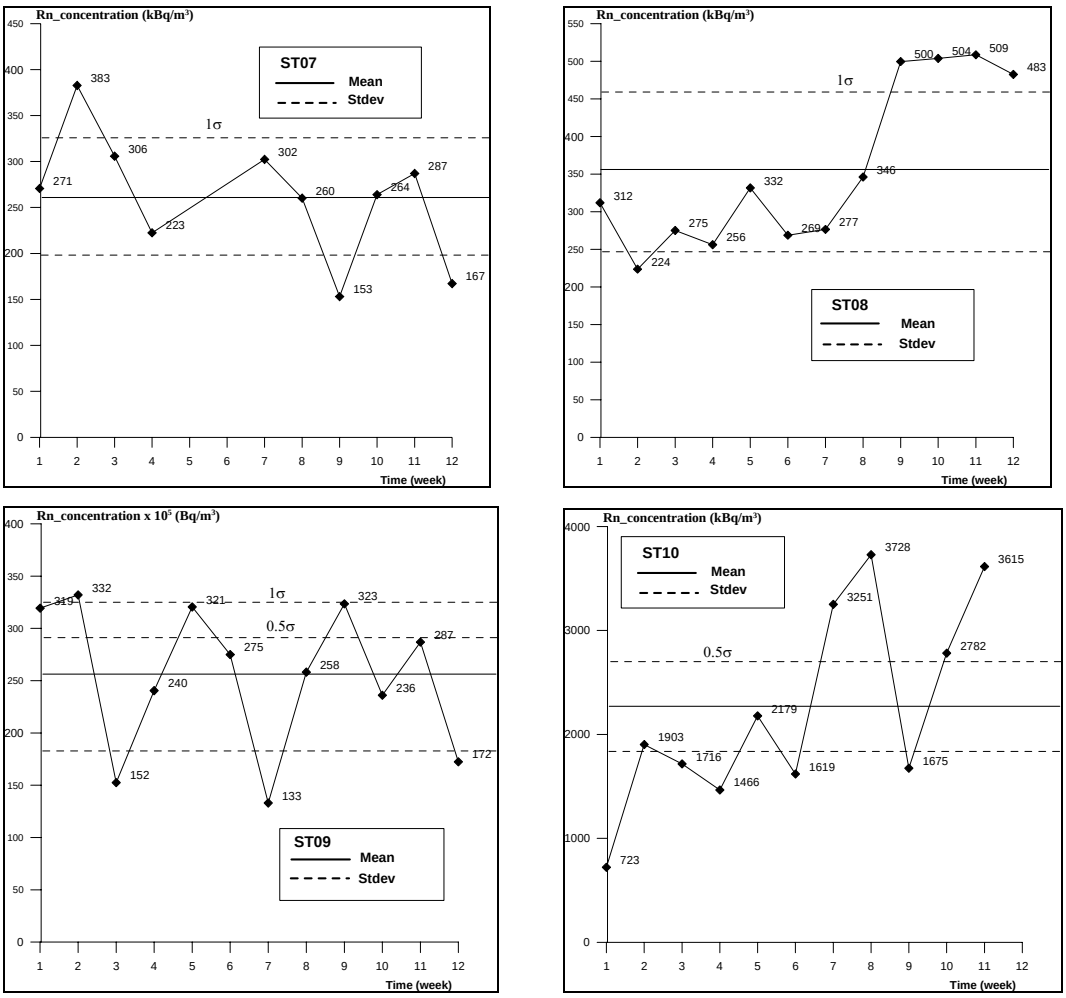

Figure 3.3 Radon concentrations in soil gas (kBq/m^3) for each week over the 12-week measurement period from 28 January to 25 April 2007 for four stations, ST07 to ST10, with mean and standard deviation.

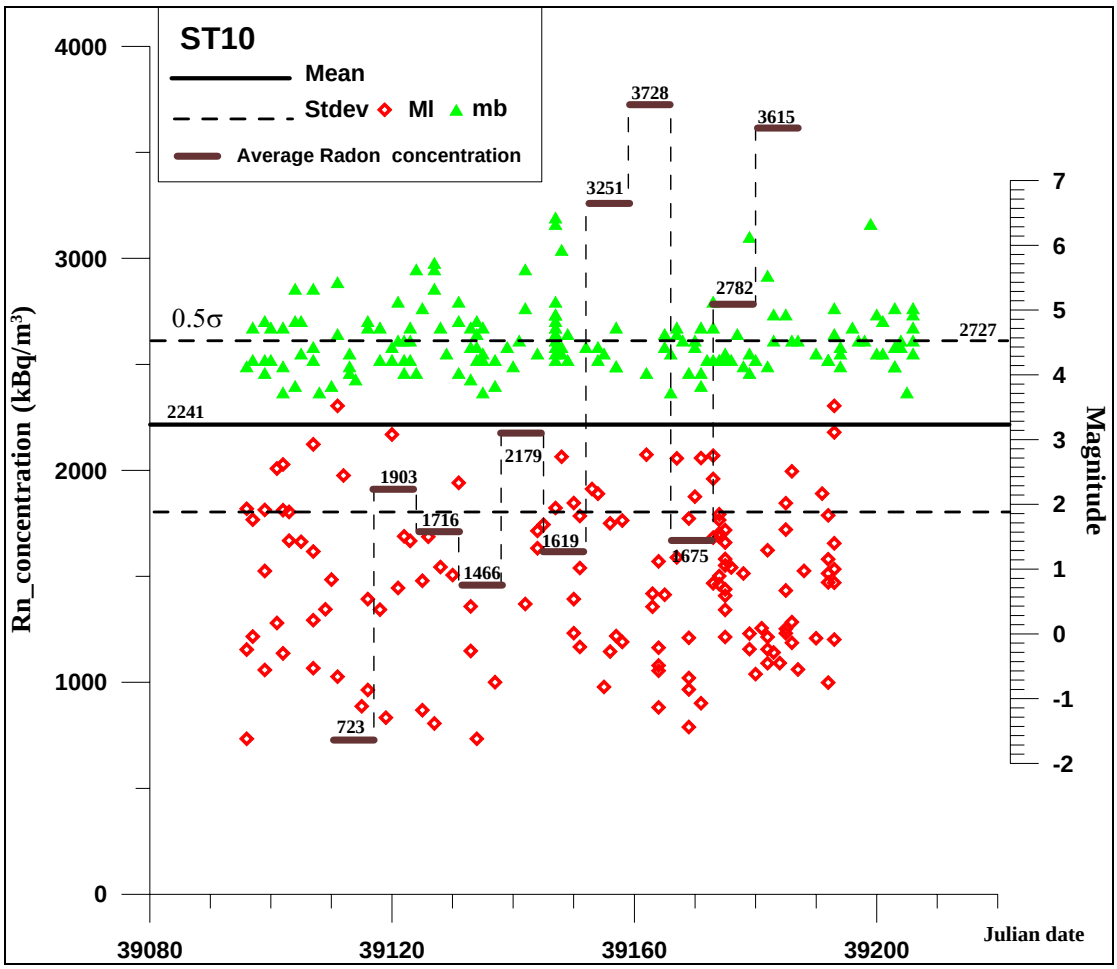

Figure 3.4 The average radon concentration in soil gas (kBq/m^3) of station ST10 between 28 February (39110 Julian Calendar date) and 25 April 2007 (39197 Julian Calendar date) in one-week intervals (equal one bar) with mean and standard deviations. Diamonds are occurrence time (in UTC) and magnitude (Ml) of local earthquakes; triangles are occurrence time (in UTC) and magnitude (mb) of regional earthquakes (from USGS, 2008).

Figure 3.4 shows the radon concentrations in soil gas at station ST10 in correlation to the occurrence and magnitude of local and regional earthquakes for the same period of time, as well as before and after. The average radon concentration in the week 1, 2, 3, 4, 5, 6, and 9 are less than the mean value. A radon peak with a radon anomaly can be observed when the radon values start to increase by 0.5σ from

the mean value in week 7 from March 11 to 18 March 2007 (39152-39159, Julian date Calendar) with 3,251 kBq/m^3. The maximum radon value occured in week 8 from 18 March to 25 March 2007 (39159-39166, Julian date Calendar) with 3,728 kBq/m^3. The increase can be realeted to a possible influence of the pressure and stress increases in the subsurface. After that, an increase in the number of seismic events can be obserevd correlating to a lower peak in the radon data in week 9, with 1,675 kBq/m^3. The numbers of local earthquakes occurred in this period are 14 events with a local magnitude (Ml) ranging from -1.4 to 2.8 and 16 regional earthquakes occurred with a body-wave magnitude (mb) from 3.8 to 5.1.

Further, in week 10 from 1 to 8 April 2007 (39173-39180, Julian date Calendar), 19 local events with Ml ranging from -0.6 to 1.8 and 12 regional events with mb 4.0 to 6.1 occurred. That might be an effect from the highest radon anomaly in week 8.

Finally, in week 11 from 8 to 15 April 2007 (39180-39187, Julian date Calendar) the radon anomaly increased again, with 16 local events with ml ranging from -0.5 to 2.5 occurred in the same time interval, as well as 11 regional events with mb from 4.1 to 5.5. It can be seen that the locations of local earthquakes occurred along the KMF zone, closer and further, and that this relates to a higher average radon anomaly shortly after week 7 to 11 in the area between 7º N to 9º N and 98º E and 99.5 º E as shown in Figure 3.5.

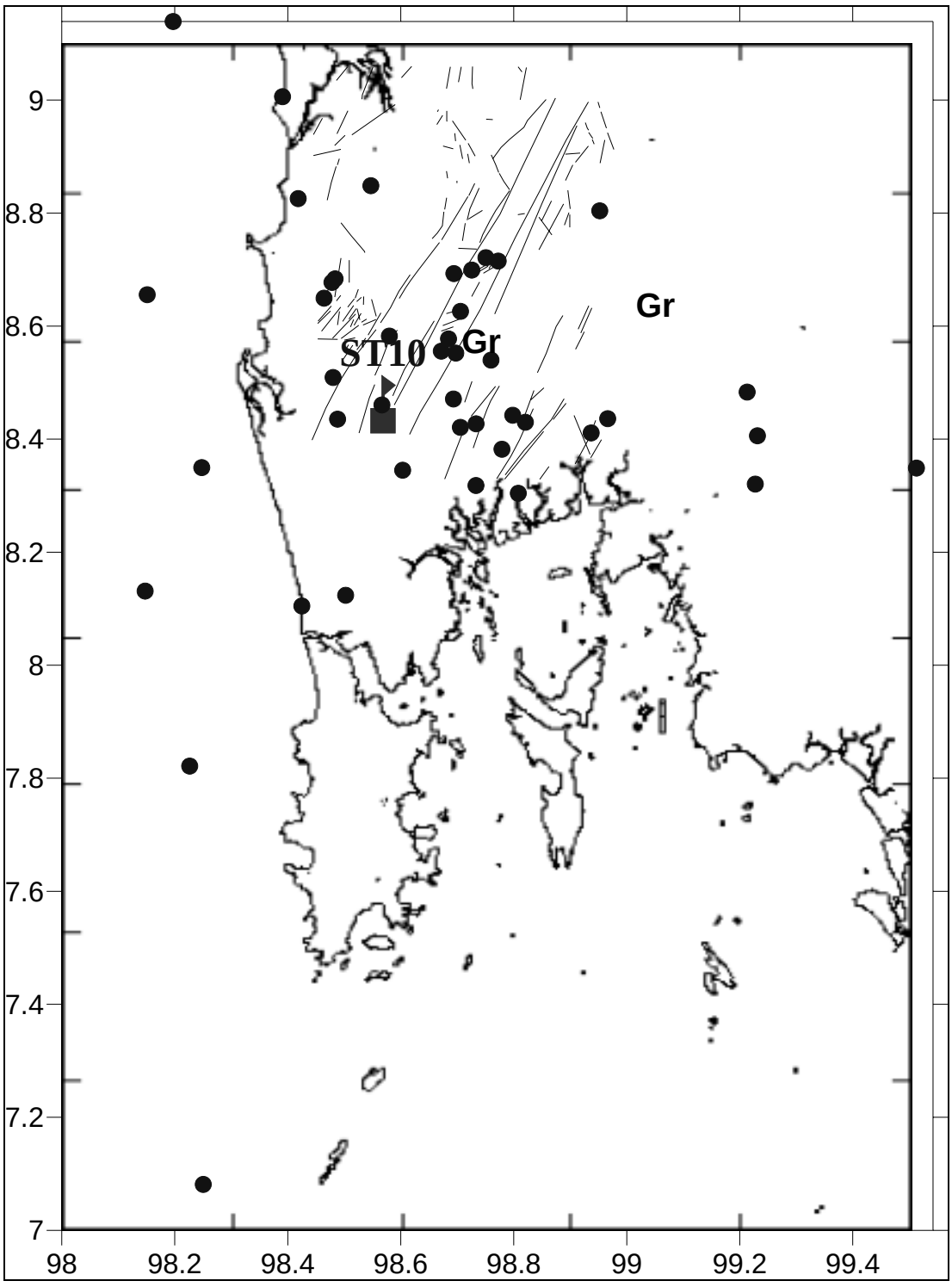

Figure 3.5 Locations of local earthquakes shortly after the week 7-11 of the average radon anomaly in the area between 7º N to 9º N and 98º E to 99.5 º E.

3.2. Automatic monitoring of radon concentration in soil gas

The Radon Progeny Monitor (RPM-256 UGF, Czech Republic) measured the radon that originates continuously by radioactive decay from its parent product from the natural radioactive elements uranium thorium and radium in rocks and soil in the subsurface. In this study the RPM-256 was used at two sites, for monitoring over a longer period of time and for spot check. Firstly, monitoring was done continuously at seismic station in Khok Charoen Village, Thap Put District, Phang Nga Province, and secondly spot check was carried out on the road covering three districts, Phanom, Kiriratnikom, and Phunphin District in Surat Thani Province.

3.2.1 Radon and meteorological measurements

The soil gas radon was determined by measuring the α-decays of radon and its progeny with the RPM-256 Radon Progeny Monitor continuously. The α-decays were reported in counts as shown in Figure 3.6, for a period between 7 February (39120 Julian Calendar date) and 18 May 2007 (39220 Julian Calendar date). However, due to data loss there is no continuous record available, as shown in Figure 3.6.

Further, the meteorological parameters P (barometric pressure) and T (temperature) were provided by the Thai Meteorological Department (TMD), which were used for investigating their effect on the temporal radon variations by statistical tests. First, the measured values of P and T from 7 February to 5 May 2007, and the radon measured from February 12 to 29 April 2007 were correlated as shown in Figure 3.6. To identify radon anomalies the daily average were used.

An increase from the mean value by 0.5σ can be seen in the interval from February 12 to 23 March 2007 (39125-39164), by 1σ in the interval from 3 April to 12 April 2007 (39164-39184), and by 0.5 σ in the interval from 25 April to 29 April 2007 (39197-39201). From the comparison of the anomalies with the P and T data, it can be seen that the meteorological parameters have less effect on the peaks of the soil gas radon concentration, because the measurements were taken at 1 m depth as suggested by Wattananikorn et al. (1998).

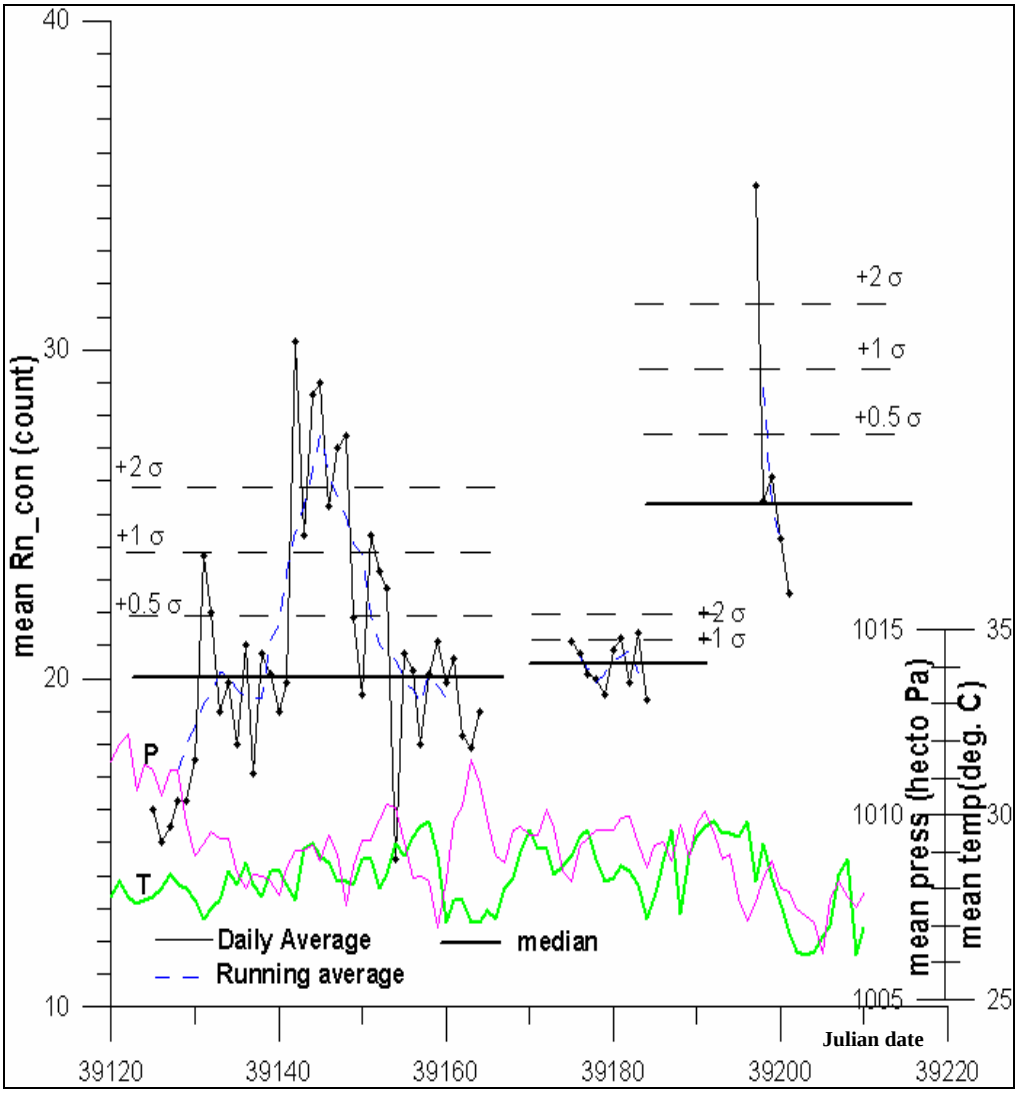

Figure 3.6 Radon concentration in soil gas at 1 m depth (in counts, daily average) in correlation to the meteorological parameters P (barometric pressure, hPa) and T (temperature, °C) for the period between 7 February (39120 Julian Calendar, Thai date) and 18 May 2007 (39220 Julian Calendar, Thai date). Mean and standard deviations are given for each continuous recording.

From the available continuous radon data the interval from 12 February to 23 March 2007 (39125-39164) shown in Figure 3.7 covered the longest period of time and showed two significant radon anomalies.

The first one was on 18 February 2007 at 15:48:53 (Universal Coordinate Time, UTC +7 hrs = Thai Time) with 54 counts/10 minute every 3-hour interval. The second anomaly occurred on 1 March 2007 at 14:34:35 UTC with 91 counts/10 minute. The median radon value for this period is 20 counts/10 minute, with one standard deviation of 7.61 counts/10 min.

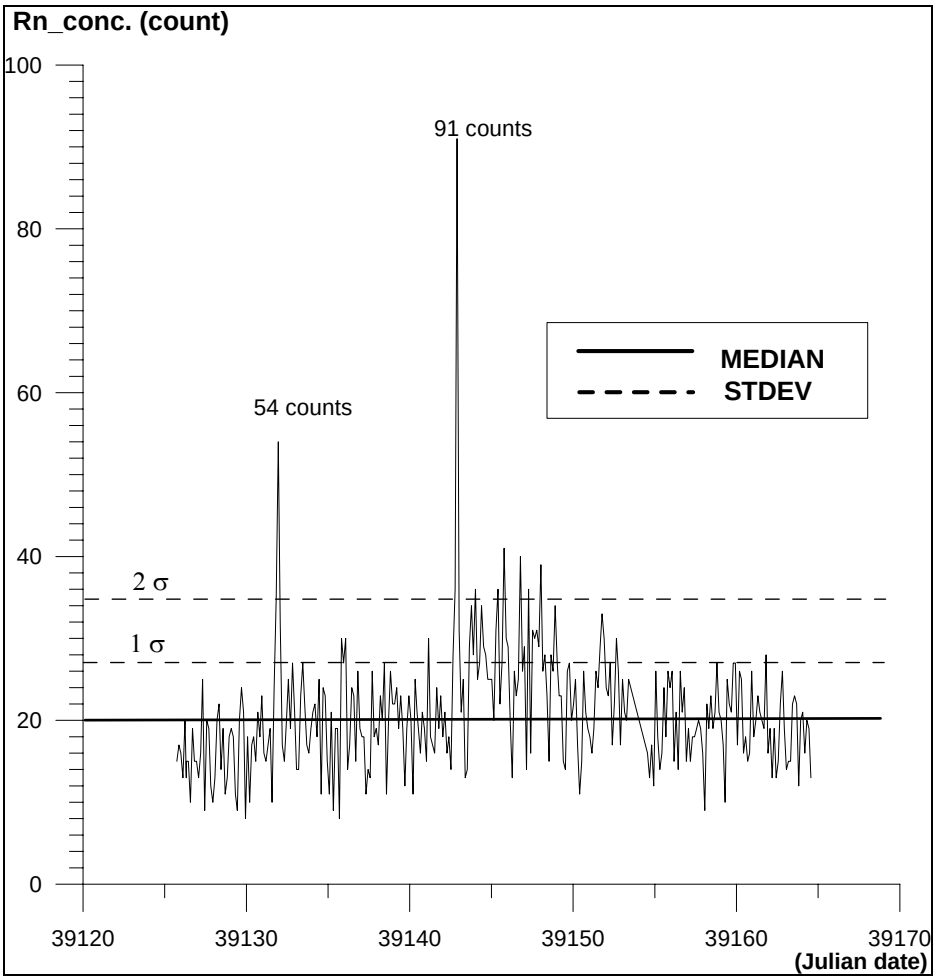

Figure 3.7 Radon concentration in soil gas (in counts/10 minute.) between 12 February (39125 Julian Calendar, Thai date) and 23 March 2007 (39164 Julian Calendar, Thai date) with median and standard deviations. Two clear peaks with significant increase in the radon values can be seen, on 18 February (54 counts/10 minute) and 1 March 2007 (91 counts/10 minute).

3.3 Radon on the road

The Radon Progeny Monitor (RPM-256) was further used for the measurement of the radon along public roads every 1 km to detect the position of the Khlong Marui Fault (KMF) Zone and to identify monitoring sites in the KMF zone. The measurements covered three districts, Phanom, Kiriratnikom and Phunphin District in Surat Thani Province, with 108 sampling points along 116 km altogether, from 470849 E and 978097 N to 529150 E and 1001505 N (Figure 3.8).

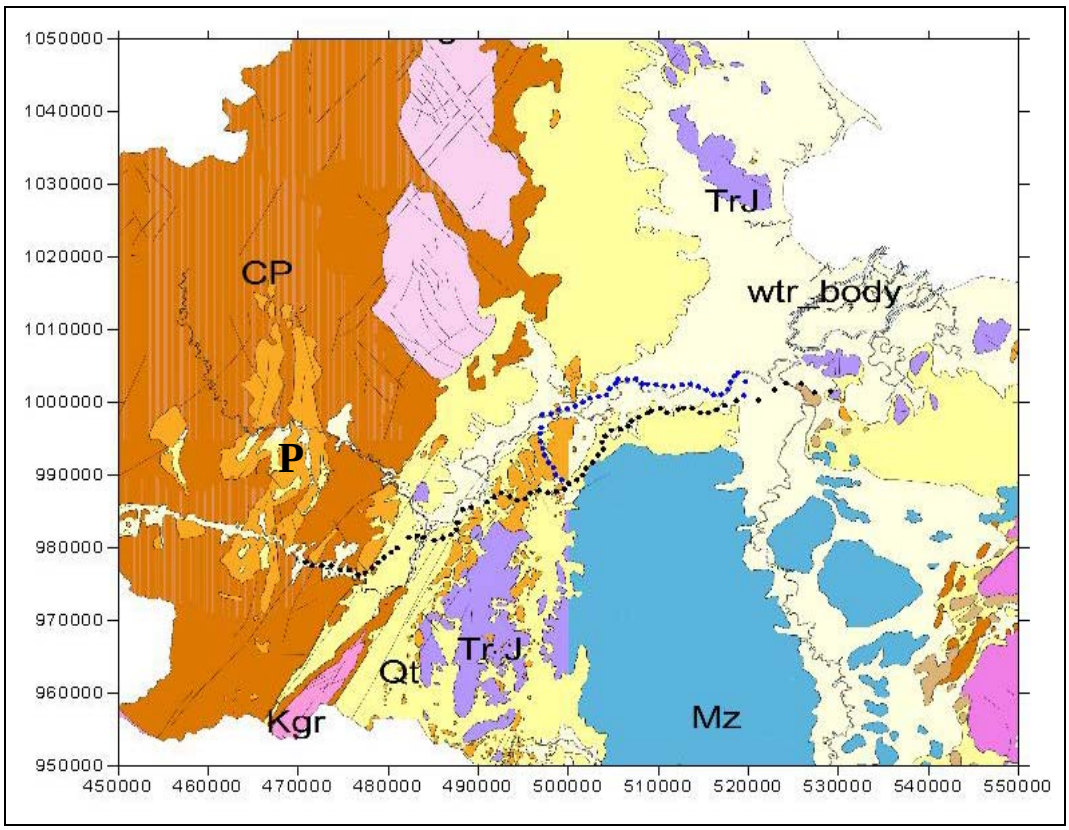

Figure 3.8 The sampling location of the spot checks for soil gas radon along roads from 470849 E 978097 N to 529150 E 1001505 N in Surat Thani Province with geology base map; CP = Carboniferous, P = Permian, Qt = Quaternary, Kgr = Cretaceous, Tr J = Triassic- Jurassic and Mz = Mesozoic.

The RPM-256 automatically measured the radon concentration in soil gas for 5 minutes counting time with air pumping on, so called spot checks. The whole measurements were carried out in five days, spot check 1-12 on 12 March 2007, spot check 13-27 on 23 April 2007, spot check 28-67 on 24 April 2007, spot check 68-83 on 18 May 2007, and spot check 84-108 on 19 May 2007.

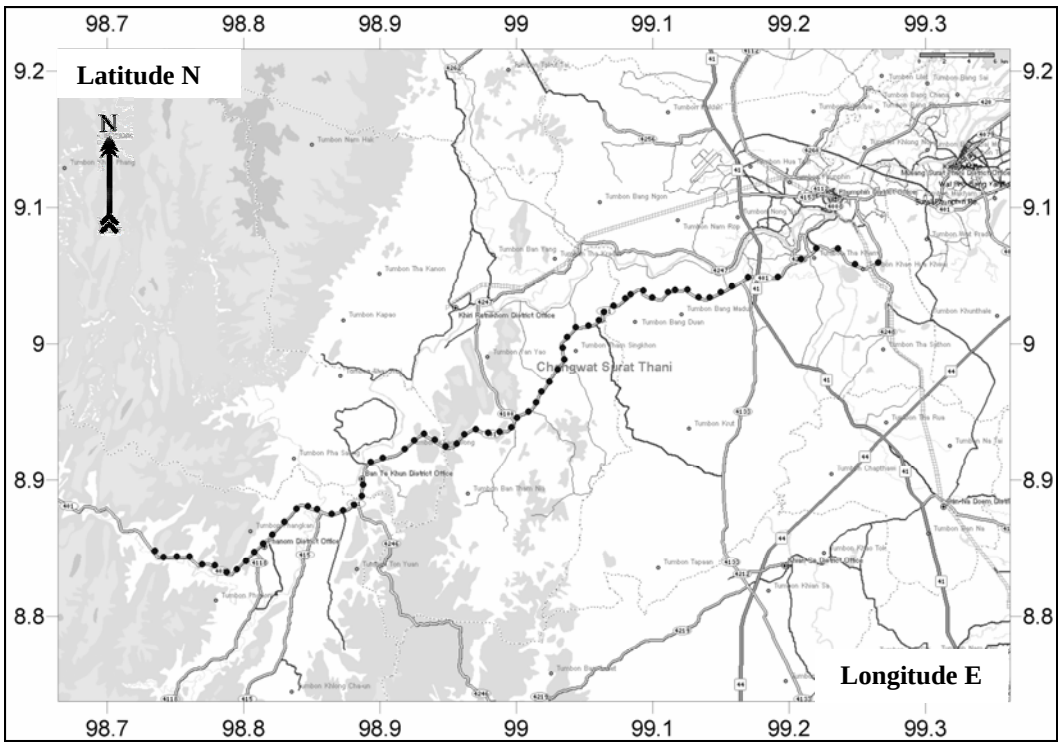

Figure 3.9 The sampling locations of the spot check measurements of soil gas radon along public road no. 401 in Surat Thani Province with terrain base map.

From the data along the public road no. 401 three radon anomalies could be identified shown in Figure 3.10. All anomalies are located in an area with Permian limestone (P) outcrops (see Figure 3.8), with the first highest one at spot check 26, measured on 23 April 2007 with 109 counts. The second highest anomaly measured on 24 April 2007 with 198 counts and the third anomaly measured on 24 April 2007 with 132 counts at spot check 30. The median radon value for this period is 30 counts, with one standard deviation of 30.73 counts as indicated in Figure 3.10.

It is possible, that the radon anomaly is related to the karst characteristic of the Permian limestone. As radon is a gas that can move easily through underground cavities or fractures in the limestone created by the karst weathering, even from much deeper regions of the subsurface. From the limestone the radon can move through the pore spaces between grains of the soil to the surface. At other spot checks with sedimentary rocks of Carboniferous and Quaternary age the above lying soil might be more impermeable due to higher clay content. There fore, it is more difficult for radon to move to the surface than through the fractures and pores of the limestone.

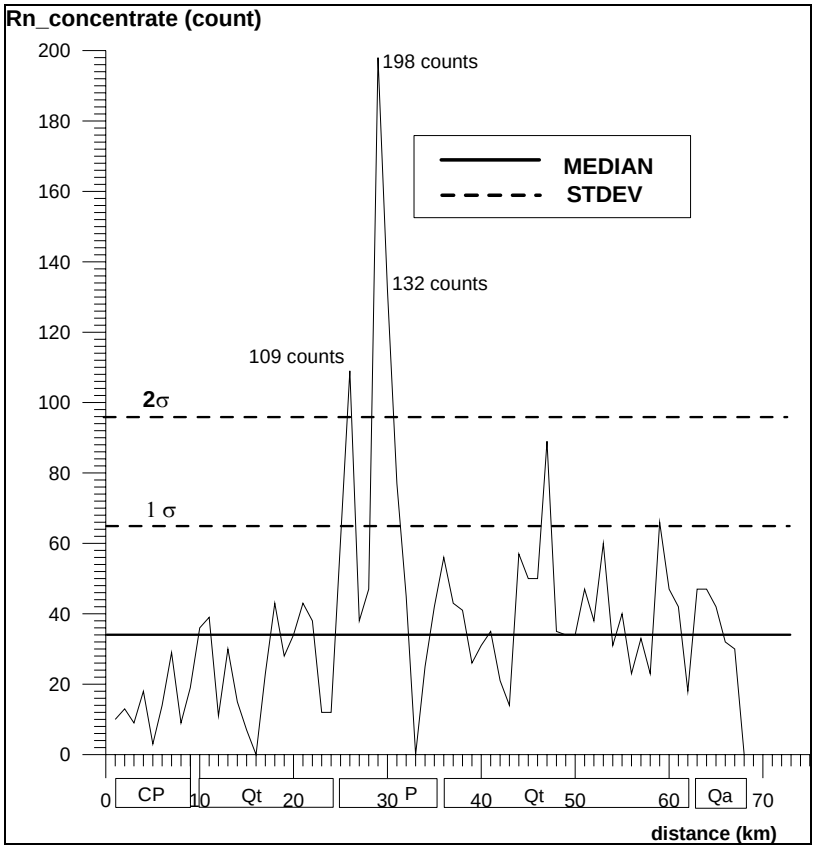

Figure 3.10 Radon anomalies of spot check measurements along the public road no. 401 in Surat Thani Province with the near surface to surface rock type. Distance in km, Radon in counts (per 5 min), see also Figure 3.9.

However, a more in-depth analysis of this anomaly cannot be carried out until a detailed survey in this area is conducted.

3.4 Seismic events

From 14 January to 21 April 2007, the short period seismic station in Thap Put could detect 226 seismic events. They occurred in areas between -4.36°N to 16.47°N and 87.66°E to 111.14°E. Among all events are 58 regional earthquakes with a magnitude range from 3.2 to 6.5 body-wave magnitude (mb). Further, there are 135 local earthquakes, with a magnitude range from -1.6 to 3.5 local magnitude (Ml). Additionally, 33 man-made events were determined with a magnitude range from -2.3 to 2.2 (Ml), probably blasting from rock quarries (see Dangmuan, 2008). The seismic events are listed in Table 3.3 and the distribution is shown in Figure 3.11.

Table 3.3: Summary of seismic events from 14 January to 21 April 2007.

Month	**Magnitude of seismic events (Ml – local magnitude, mb – body wave magnitude)**									**Sum of events**
	Local earthquakes			**Regional earthquakes**			**Blasting or man-made events**			
	event	**Ml min**	**Ml max**	**event**	**mb min**	**mb max**	**event**	**Ml min**	**Ml max**	
January	24	-0.7	3.5	10	4.4	5.8	9	-0.6	0.2	**43**
February	20	-2.3	3.1	15	3.7	5.7	11	-2.3	0.5	**46**
March	39	-1.6	2.8	22	3.2	6.5	7	-0.3	0.2	**68**
April	52	-0.8	3.1	11	3.5	5.6	6	-0.8	2.2	**69**
sum	**135**	**-1.6**	**3.5**	**58**	**3.2**	**6.5**	**33**	**-2.3**	**2.2**	**226**

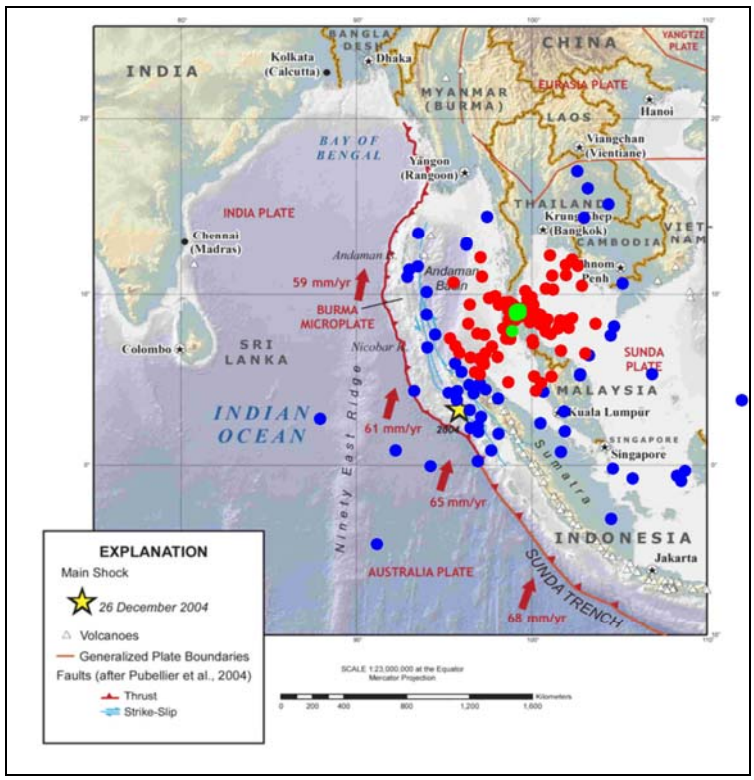

Figure 3.11 Locations of all earthquakes from 14 January to 21 April 2007 detected by the short period seismometer. Blue circle symbols represent regional EQ, red circles are local EQ and green circles are blasting event.

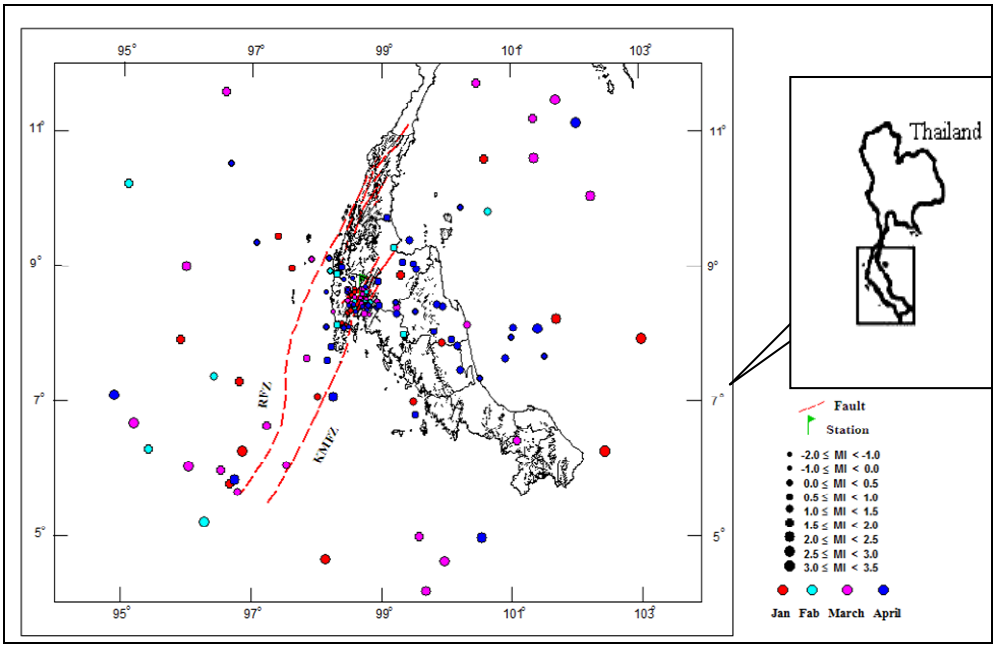

Figure 3.12 Locations of the local earthquakes from 14 January to 21 April 2007 in relation to their magnitudes (circle size) and origin time (colors).

3.4.1 Local earthquakes

The local earthquake occurred in an area between 4.19°S and 11.73°N and 94.89°E to 103.00°E. There are 135 local earthquakes, with a magnitude range from -1.6 to 3.5 local magnitudes (Ml) on the Richter Scale. Their origin time, location and magnitude are listed in Table 3.4 and the distribution in relation to the magnitude is shown in Figure 3.12. Local earthquakes are less than 500 km apart from the monitoring station.

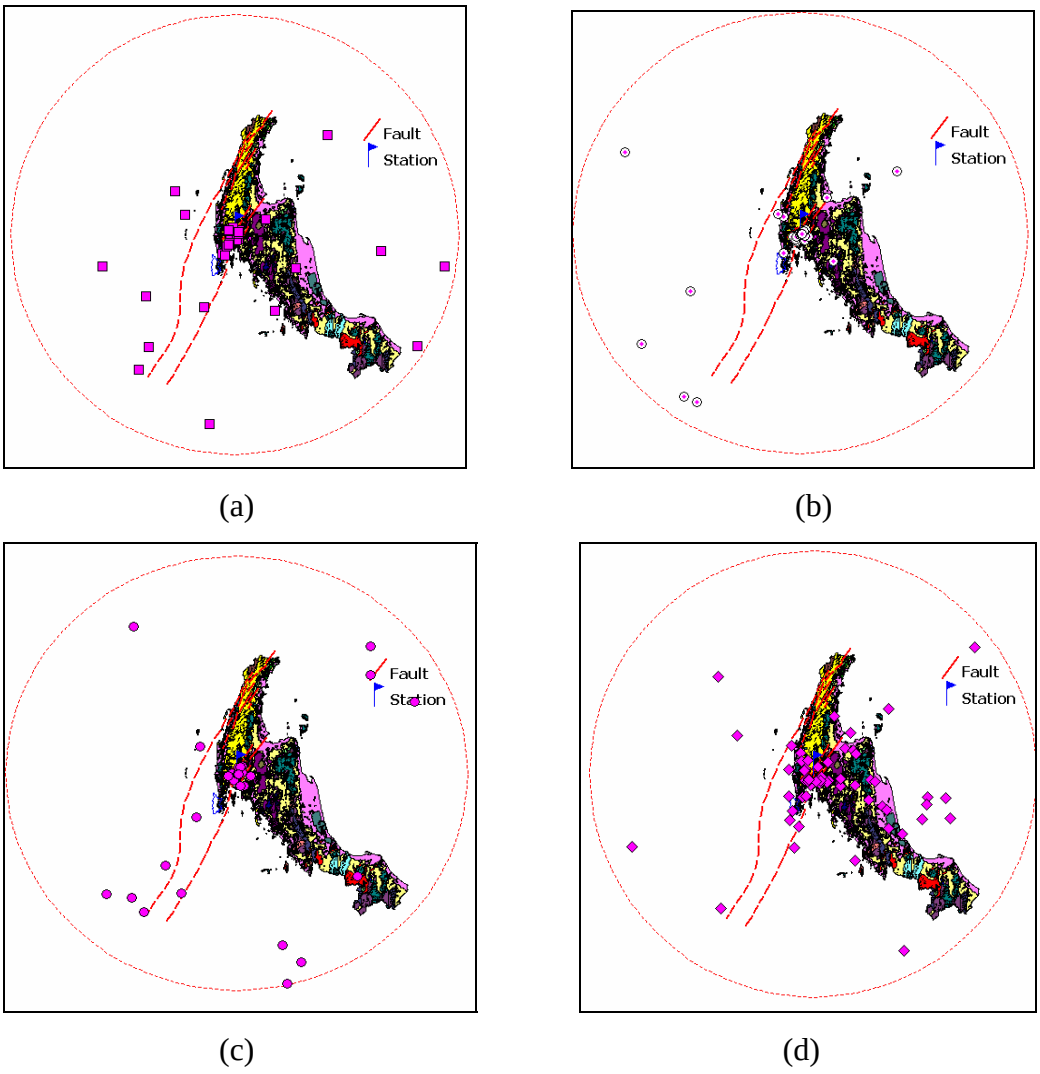

Figure 3.13 Locations of local earthquakes in Southern Thailand from 14 January to 21 April 2007 in relation to their magnitudes. The dashed lines represent the Ranong and Khlong Marui Fault Zone. (a) January, (b) February, (c) March, and (d) April.

3.4.2 Regional earthquakes

The regional earthquake occurred in an area between 4.36 °S and 16.47 °N and 87.66° E to 111.14° E. There are 58 regional earthquakes with a magnitude ranging from mb 3.2 to 6.5. Their origin time, location and magnitude are listed in Table 3.5 and the distribution of the regional earthquakes is shown in Figure 3.13. However, in the records of the short period seismic station in Thap Put from 14 January to 21 April 2007 less regional events (distance from station more than 500 km) could be identified than listed in the USGS database (179 earthquakes, Figure 3.15, USGS, 2008).

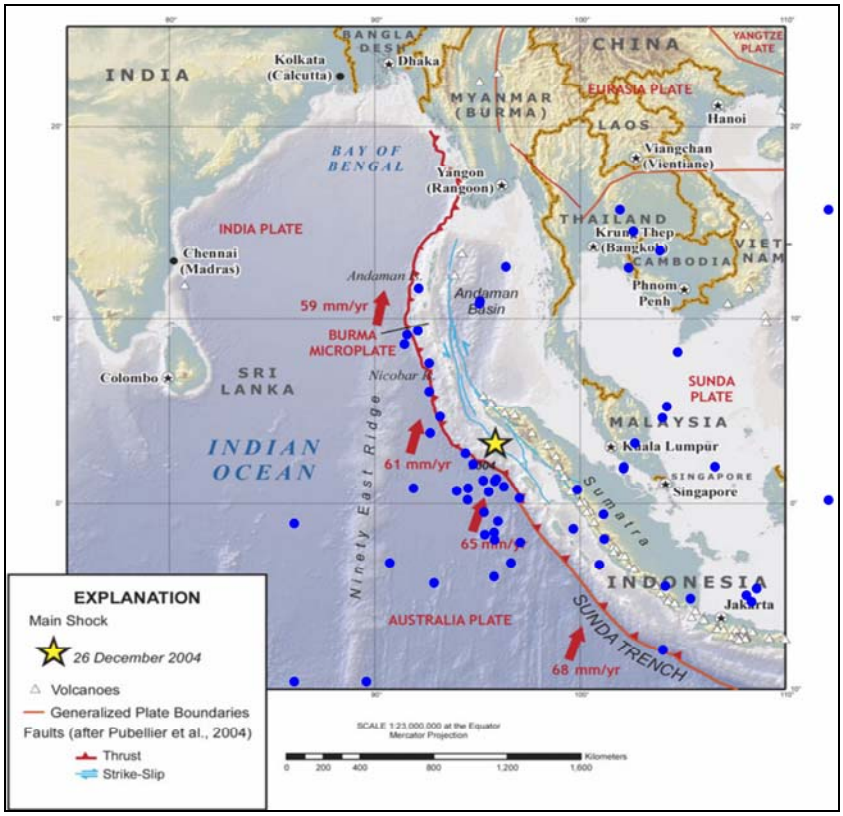

Figure 3.14 Locations of all regional earthquakes events detected by the short period seismometer, based on data from 14 January to 21 April 2007.

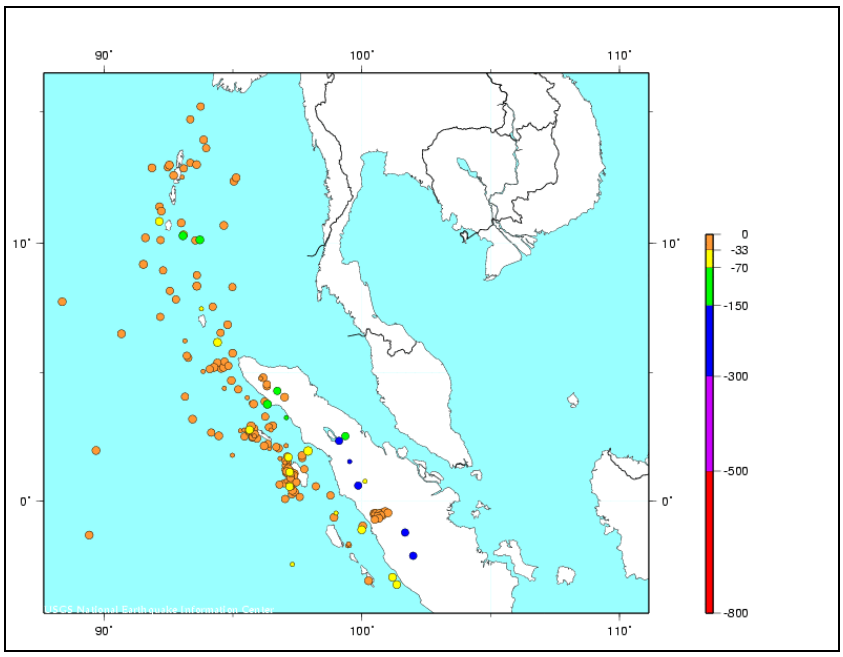

Figure 3.15 Locations of all 179 regional earthquakes events from 14 January to 21 April 2007 after USGS (USGS, 2008).

The discrepancy in the locations between this study and the USGS data comes from the method of location determination (Figure 3.14 and 3.15). As the USGS locations are the result of numerous data from several seismic stations in the region and around the world, the locations in this study depend only on one station and the backazimuth method. For further interpretation the USGS data are used in this work.

The majority of the regional earthquakes occurred along the Sunda Subduction Zone (SSZ) and the adjacent fracture zones (FracZ). These earthquakes are related to the stress increase and stress release as the Indian-Australian Plate subducts under the Sunda Plate which is a part of the Eurasian Plate (USGS, 2005).

3.4.3 Man-made events

From all the recorded seismic events during the measurement period from 14 January to 21 April 2007, altogether 33 man-made events were determined and separated with a magnitude range from Ml -2.3 to 2.2 (see also Dangmuan, 2008).

They occurred at the similar daytime at around 4.00 and 10.00 UTC time or 11:00 in the morning and 17:00 in the afternoon Thai time, and in the same area.

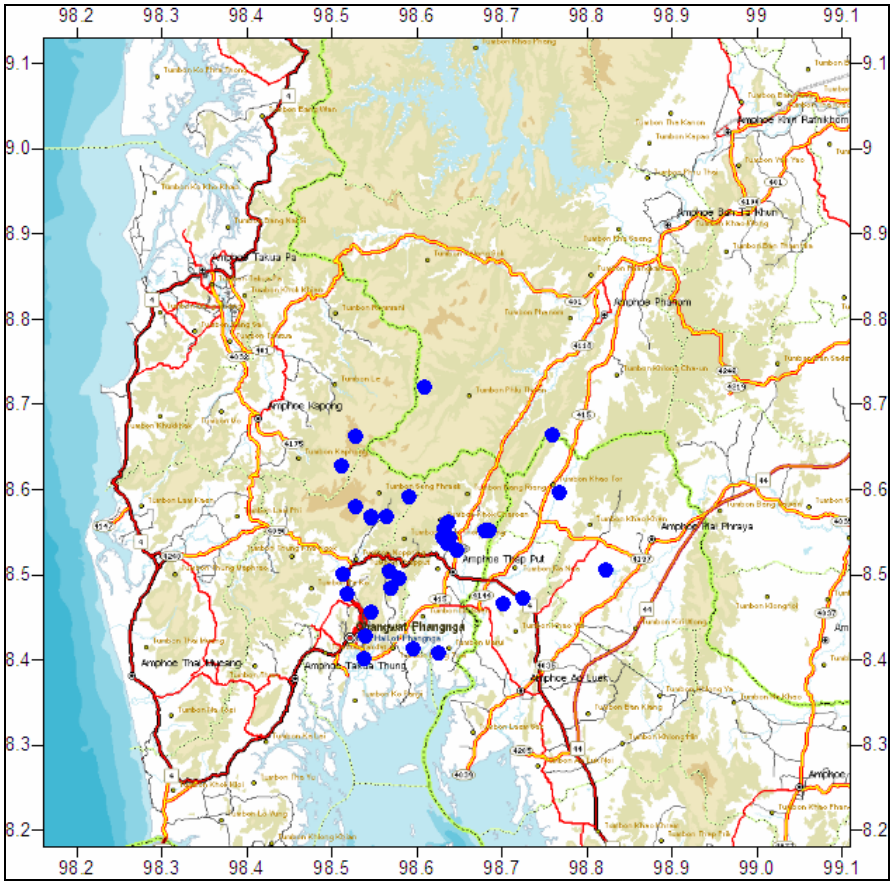

Figure 3.16 Locations of man-made events during the measurement period from 14 January to 21 April 2007, altogether 33 man-made events.

3.5 Earthquake precursor

Beyond the interest in the literature on identifying geophysical precursors to predict earthquakes, such as changes in the P-wave velocity, changes in ground tilt and uplift, decrease in electrical resistivity of rocks, changes of underground water level fluctuations and increase in radon emissions, there are obvious reasons to find earthquake precursors and consequently to predict earthquakes.

The results of this study present a correlation of the occurrence of earthquakes related to fluctuations and increases in soil gas radon emissions along a

fault zone see as shown in Figure 3.16. The radon emission data cover a period between 12 February (39125 Julian Calendar, UTC date) and 29 April 2007 (39201 Julian Calendar, UTC date) and are plotted in Figure 3.17 together with the occurrence time and magnitude of the local and regional earthquakes.

There are two clear radon anomalies, the first on 18 February 2007 at 15:48:53 (Universal Coordinate Time, UTC +7 hrs = Thai Time) with 54 counts/ 10 minute in 3-hour interval. The second anomaly occurred on 1 March 2007 at 14:34:35 UTC with 91 counts/10 minute. The average radon value for this period is 20 counts/10 minute, with one standard deviation of 7.43 counts/10 minute.

After the first radon anomaly until the second one the number of local earthquakes went down, only four (see Figure 3.17). There were 23 regional earthquakes between the two anomalies, but the magnitudes of these earthquakes dropped significantly after the 18 February radon anomaly. However, just before the second radon anomaly there were two earthquakes with higher magnitude (mb $\geq$ 5) again.

After the second and higher radon anomaly, there was a smaller increase in the number of local earthquakes. About 5.5 days after the anomaly, a local earthquake with a higher magnitude, Ml 2.7, occurred (local earthquake No. 6 in Figure 3.18, see Table 4.1). Following then was a period with more local earthquakes, between 7.5 and 9.3 days after the anomaly. Then, after a 1.4-day gap, two earthquakes with Ml 2.2 occurred (No. 13 and 14). For the regional earthquakes there only three earthquakes until the 6 March, and then on the 6 March there were 15 earthquakes, with the highest magnitude on 6 March 03:49 UTC with mb 6.4 (regional earthquake No 5 in Figure 3.18, see Table 4.1).

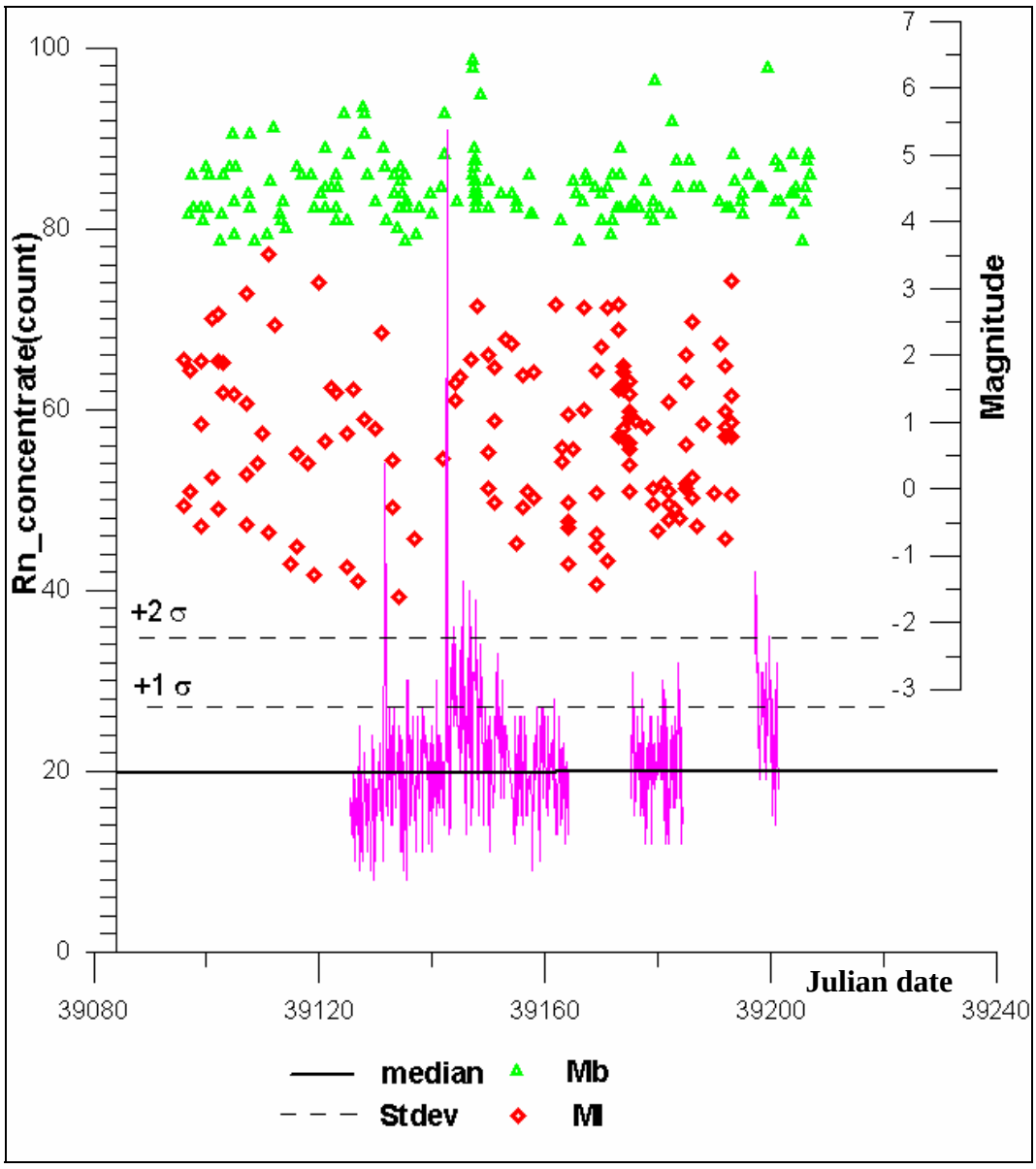

Figure 3.17 Radon concentration in soil gas (in counts/10 min., every 3 hrs) between 12 February (39125 Julian Calendar, UTC date) and 29 April 2007 (39201 Julian Calendar, UTC date) with median and standard deviations. Diamonds are occurrence time (in UTC) and magnitude (Ml) of local earthquakes; triangles are occurrence time (in UTC) and magnitude (mb) of regional earthquakes (from USGS, 2008).

Figure 3.18 shows the locations of the local and regional earthquakes from 1 March (shortly before the radon anomaly) and 16 March 2007. After this day, there was a gap of five days without any regional earthquake. Many of the local earthquakes that occurred after the second radon anomaly are located along the Khlong Marui Fault Zone on the land; however, others were located in the Andaman Sea and Gulf of Thailand.

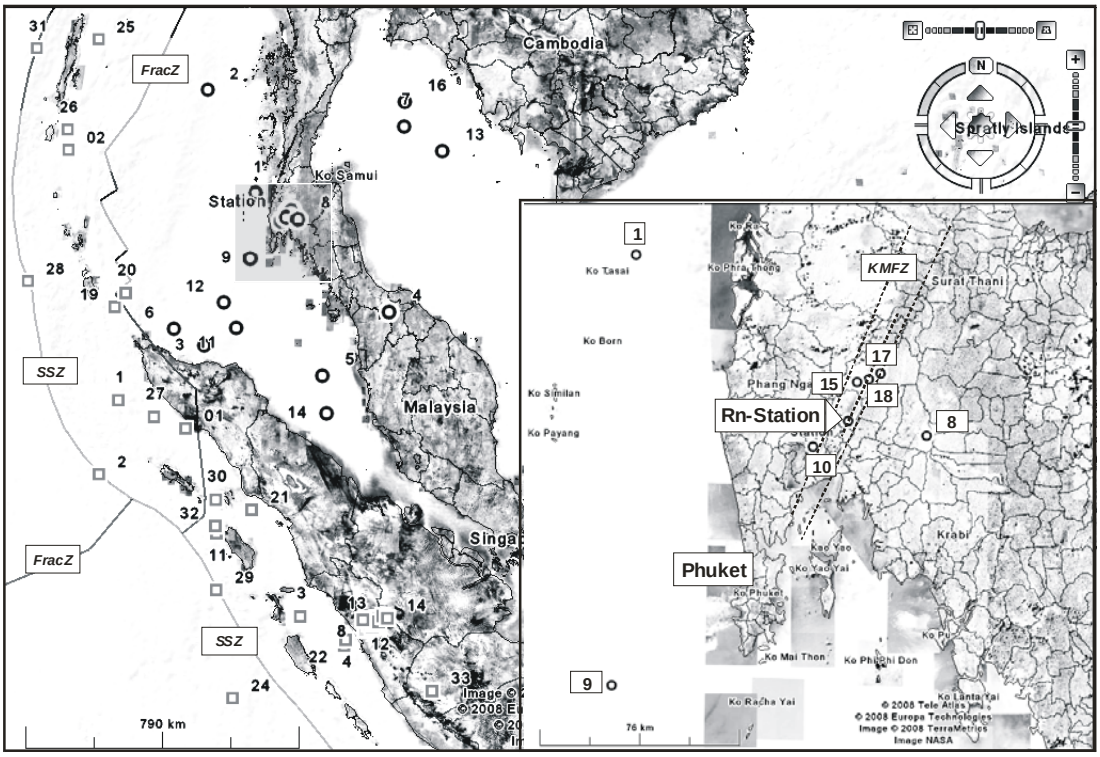

Figure 3.18 Locations of local and regional earthquakes shortly before and after the second radon anomaly on 1 March 2007, 21:34 UTC. Squares indicate regional events with 01 and 02 before, and 1 to 33 after the radon anomaly. Circles are local events with 1-18 after the radon anomaly. Further event details are given in Table 4.1. Rn-Station - radon measurement station, SSZ - Sunda Subduction Zone, FracZ - Fracture Zone, KMFZ - Khlong Marui Fault Zone. The right lower box is a magnification of the area around the measurement station. Map based on and copyright by Google™ Earth 2008.

CHAPTER 4

CONCLUSION AND RECOMMENDATION

The identification of a clear earthquake related signals related to radon anomalies has been difficult because there are many complications and influence, for example the earth's tides, barometric pressure, temperature, rainfall, tectonic processes and other factors. As the influences of the tectonic activity on the permeability of aquifers or crack patterns in the earth's crust are difficult to estimate so it is difficult to find significance in the temporal variations of the radon related to earthquake activities.

However, many researchers are interested in the relationship between a change in the concentration of radon and the occurrence earthquakes, especially radon anomalies as earthquake precursors. Until today, earthquake-related radon anomalies have been detected at distances in the order of hundreds of kilometres from the epicenter, but so far they have been proved to be unreliable as earthquake predictors.

Also, it is important to observe and interpret the influences of other factors (e.g. geological, meteorological) upon the emission of radon from the ground as most, if not all, of this work has been hampered on two counts. Firstly, is the use of the radon detectors (e.g. track-etch and continuous by RPM-256), which often have an exposure over a certain period of time, e.g. hours, days, weeks, or months. Secondly, very few researchers have monitored radon and earthquake using for both real-time detectors and record more than one location simultaneously.

As for this study the radon on the road has only a limited number of measurements in one time at the study area and only at one location at a time. Whether then the radon variations are highly localized or more widespread cannot be determined. Sources of localized variations include vibrations induced by trains, street-traffic and building activities, for example, at distances up to several tens of meters, dependent upon factors such as type of vibration and type of bedrock. Sources of more widespread variations include earthquakes and large explosions.

In the study the meteorological parameters P (barometric pressure) and T (temperature) were taken into account before identifying radon anomalies.

The analysis here using a statistical test could show that the meteorological data have no obvious effect on the temporal radon variations. The meteorological effect to soil gas radon anomalies here is negligible, as the radon emission was measured at 1 m depth.

According to present study the earthquake radon precursor relationship outlined in Chapter 3 and shown in Figure 3.4, the average radon concentration in the interval period time week 1, 2, 3, 4, 5, 6 and 9 is less than the mean value of 2,241 kBq/m^3 with one standard deviations of 971 kBq/m^3. Further, in the ST10 station has a highest radon anomaly in week 8 from 18 March to 25 March 2007 with 3,728 kBq/m^3. Here it would be better to have continuous radon monitoring like at the Thap Put Station.

Using the continuous measurement of the concentration of radon in soil gas precursor for earthquake activities might be able to be identified, as it is done in this study. Two days after the first anomaly, there was a slight increase in the number of regional earthquakes, which lasted for three days. The number of local earthquakes on the other side dropped. However, further correlation here is difficult as the second and higher radon anomaly occurred 10 days after the first one. The second radon anomaly can be seen as precursor for the sharp increase in regional earthquake activities about 4.5 to 5.8 days later and around 11.4 to 15 days later. An increase in the local earthquake numbers is coming about 7.5 to 9.3 days after the radon anomaly (see Table 4.1), with one earthquake (Ml 2.7) before and two earthquakes (Ml 2.2) after this period. The earthquake and radon data indicate that there might be a relationship between the local and regions earthquakes, suggesting a possible (stress/strain) relationship between the Sunda Subduction Zone and the fault zones in Southern Thailand. Longer-term measurements of earthquake activities and radon emissions would be preferable, several months or better several years, as this earth related processes have a longer period time scale.

In the future, it might be possible to use radon gas variations as a possible method for earthquake warning in the study area.

Table 4.1: Details of the earthquake activities after the second radon anomaly on 1 March 2007 21:34 UTC. See also map in Figure 3.18 for the locations.

Date of occurrence of radon anomaly	Earthquake occurrence				Magnitude		Epicenter distance from radon station (km)		Radon anomaly	Radon anomaly from avg. value	Delta time between Rn anomaly and EQ (Precursor time, days)	
	Local EQ (Ml)	Map O	Regional EQ (mb)	Map □	(Ml)	(mb)	(Ml)	(mb)	(Counts)	σ	(Ml)	(mb)
1/3/2007			01/03/07 02:01:07.00	01		5.6		590	91	> 2 σ		-12.56 hrs
14:34:35.00	01/03/07 15:20:05.00	1	01/03/07 05:08:20.74	02	0.5	5	104	651			0.76 hr	-9.44 hrs
39142.61	03/03/07 00:07:31.50	2	03/03/07 07:39:32.03	1	1.6	-	410	640			1.40	1.71
in Julian	03/03/07 22:05:26.57	3	03/03/07 10:09:19.65	2	1.3	4.3	382	822			2.31	1.82
Calendar	04/03/07 21:26:05.59	4	05/03/07 04:22:50.97	3	1.7		358	1002			3.29	3.58
UTC date	06/03/07 18:21:06.10	5	06/03/07 03:23:15.13	4	1.9	4.7	408	1069			5.16	4.53
	07/03/07 01:24:46.75	6	06/03/07 03:49:38.90	5	2.7	6.4	403	1025			5.45	4.55
	09/03/07 03:29:30.70	7	06/03/07 04:28:35.79	6	2.0	-	377	1052			7.54	4.58
	09/03/07 07:55:46.58	8	06/03/07 05:49:25.43	7	0.0	6.3	31	1026			7.72	4.64
	09/03/07 17:48:43.81	9	06/03/07 06:18:09.35	8	0.5	-	135	1025			8.13	4.66
	10/03/07 09:57:54.70	10	06/03/07 08:13:39.51	9	-0.2	4.6	17	1027			8.81	4.74
	10/03/07 17:15:05.08	11	06/03/07 08:49:50.38	10	1.0	4.9	303	1035			9.11	4.76
	10/03/07 21:23:12.98	12	06/03/07 09:34:03.12	11	1.8	4.8	265	814			9.28	4.79
	12/03/07 06:15:07.67	13	06/03/07 10:08:53.58	12	2.2	4.4	430	1038			10.65	4.82
	13/03/07 03:22:53.42	14	06/03/07 12:53:06.86	13	2.2	5.1	498	1025			11.53	4.93
	14/03/07 10:40:30.00	15	06/03/07 15:22:17.67	14	-0.8	4.5	15	1033			12.84	5.03
	15/03/07 06:13:31.00	16	06/03/07 16:02:13.99	15	1.7	4.2	419	1027			13.65	5.06
	15/03/07 10:38:10.00	17	06/03/07 16:23:52.93	16	-0.3	4.9	21	1037			13.84	5.08
	16/03/07 10:09:30.00	18	06/03/07 17:37:21.30	17	0.0	4.3	17	1037			14.82	5.13
			06/03/07 20:14:50.33	18		4.6		1048				5.24
			07/03/07 01:14:10.69	19		4.3		511				5.44
			07/03/07 01:24:37.55	20		4.4		469				5.45
			07/03/07 10:53:37.59	21		5.9		737				5.85
			08/03/07 22:36:12.57	22		4.6		1083				7.33
			08/03/07 22:39:45.02	23		4.2		1050				7.34

Table 4.1(cont.): Details of the earthquake activities after the second radon anomaly on 1 March 2007 21:34 UTC. See also map in Figure 3.18 for the locations.

Date of occurrence of radon anomaly	Earthquake occurrence				Magnitude		Epicenter distance from radon station (km)		Radon anomaly	Radon anomaly from avg. value	Delta time between Rn anomaly and EQ (Precursor time, days)	
	Map			Map								
	Local EQ (Ml)	O	Regional EQ (mb)	□	(Ml)	(mb)	(Ml)	(mb)	(Counts)	σ	(Ml)	(mb)
1/3/2007			08/03/07 23:51:51.58	24	-			1232	91	$> 2\sigma$		7.39
14:34:35.00			11/03/07 06:09:00.33	25	4.4			749				9.65
39142.61 in			13/03/07 00:12:16.41	26	4.4			676				11.40
1/3/2007			13/03/07 03:22:43.73	27	-			609				11.53
			13/03/07 20:42:49.41	28	4.2			736				12.26
			14/03/07 00:54:43.16	29	4.3			957				12.43
			14/03/07 20:52:38.31	30	-			731				13.26
			16/03/07 07:19:42.83	31	4.7			895				14.70
			16/03/07 10:07:15.52	32	4.1			796				14.81
			16/03/07 14:15:47.48	33	4.1			1243				14.99

REFERENCES

Al-Tamimi, M.H. and Abumurad, K.M. 2001. Radon anomalies along faults in North of Jordan. Radiation Measurements. 34: 397-400.

Alter, W.H. and Fleischer, R.L. 1981. Passive integrating radon monitor for environmental monitoring. Health Physics. 40: 693-697.

Baird, A. and Bosence, D. 1993. The sedimentological and diagenetic evolution of the Ratburi Limestone, Peninsular Thailand. Journal of Southeast Asian Earth Sciences. 8: 173-180.

Bilham, R. 2005. A Flying Start, Then a Slow Slip. Science. 308: 1126-1127.

Bilham, R., Engdahl, E.R., Feldl, N. and Satyabala S.P. 2005. Partial and Complete Rupture of the Indo-Andaman plate boundary 1847-2004. Seismological Research Letters [online]. Available from:http://cires.colorado.edu/~bilham/IndonesiAndaman2004_files/Andaman SRL4Mar.pdf.

Bodansky, D., Robkin, M.A. and Stadler D.R. 1987. Indoor Radon and Its Hazards. University of Washington Press: USA.

Bormann, P. 2002. EX 3 .1: Magnitude determinations Global. In: Bormann, P. (Ed) 2002. IASPEI: New manual of Seismological Observatory Practice 2, GeoForschungsZentrum Potsdam, Germany 8.

Bormann, P. and Wylegalla, K. 2002. EX 11.2: Earthquake location at teleseismic distances by hand from 3-component records. In: Bormann, P. (Ed) 2002. IASPEI: New manual of Seismological Observatory Practice 2, GeoForschungsZentrum Potsdam, Germany 10.

Bormann, P., Baumbach, M Bock G., Grosser, H., Choy, G.L. and Boatwringht, J, 2002. Chapter 3: Seismic sources and source parameter. In: P. Bormann. (Ed) 2002. IASPEI New Manual of Seismological observatory Practice 1, GeoForschungsZentrum Potsdam, Germany 1-94.

Briais, A., Patriat, P., Tapponnier, P., 1993. Updated interpretation of magnetic anomalies and seafloor spreading stages in the South China Sea: implications for the Tertiary tectonics of Southeast Asia. Journal of Geophysical Research. 98: 6299-6328.

Brill, A.B.1994. Radon Update. The Journal of Nuclide Medicine. 35, 2.

Bunopas, S. 1981. Paleogeographic history of western Thailand and adjacent part of Southeast Asia: A plate tectonic interpretation. Ph.D. thesis, Victoria University of Wellington, New Zealand.

Bunopas, S., Jungyusuk, N. and Khositanont, 1991. Summary of geology of Southern Thailand. In: Southern Thailand: Lithophile mineral deposits (Ranong-Takua Pa-Phuket), The Seventh Regional Conference on Geology, Mineral and Energy Resources of Southeast Asia and The Third Symposium IGCP 282: Rare Metal Granitoids. Geological Excursion Guidebook No. 2, by Nakapadungrat, S., Jungyusuk, N., Putthapiban, P., Kosuwan, S. and Chaimanee, N., pp1–13.

Burton, C.K., 1974. Peninsular Thailand. Geological Society. London, Special Publications. 4: 301-315.

CGS, 2008. California Geological Survey [online]. Available from: http://206.170.189.143/CGS/minerals/hazardous_minerals/radon/index.htm [3 June 2008].

Chyi, L.L., Chou, C.Y., Yang, F.T. and Chen, C.H. 2001. Continuous radon measurements in faults and earthquake precursor pattern recognition. Western Pacific Earth Science. 2: 227-246.

Chyi, L.L., Chou, C.Y., Yang, F.T. and Chen, C.H. 2002. Automated radon monitoring of seismicity in a fault zone. Geofisica Internacional. 4: 507-511.

Cobbing, E.J., Mallick, D.I.J., Pitfield, P.E.J. and Teoh, L.H., 1986. The granites of the Southeast Asian Tin Belt. Journal of the Geological Society. London, 143: 537–550.

Cothern, C.R., James, E., Smith, Jr. 1987. Environmental Radon. Plenum Press: New York.

Cummins, P. and Leonard, M. 2004. Small Threat but Warning Sounded for Tsunami Research. AUSGEO News, 75: (September).

Curray, J.R, Emmel, F.J., Moore D.G. and Raitt R.W. 1982. Structure, Tectonics and Geological History of the North eastern Indian Ocean: The Ocean basins and Margins. Ed.A.E.M.Nairn and EG. Stehli: Plenum Publishing Corporation, 6: 399-450.

Dangmuan, S. 2008. Seismic study of Southern Thailand after the 26 December 2007 Sumastra Andaman Earthquake. Master of Science Thesis in Geophysics, Prince of Songkla University, Hatyai, Thailand.

Dasgupta, S. 1992. Seismotectonics and stress distribution in the Andaman Plate. Mem. Journal of the Geological Society. India, 23: 319-334.

DMR, 2005. Sinkhole map in southern part of Thailand from June 1995 to June 2005. Department of Mineral Resource. Bangkok, Thailand.

DMR, 1982. Geological Map of Thailand, Scale 1:250,000.

DMR, 2006. Geological Map of Thailand, Scale 1:50,000.

Düerrast, H, Dangmuan, S. and Lohawijarn, W. 2007. Khlong Marui and Ranong Fult Zones in Southern Thailand Re-Activated The 26 December 2004 Mw 9.3 Sumatra- Andaman Earthquake. GEOTHAI'07 International Conference on Geology of Thailand: Towards Sustainable Development and Sufficiency Economy. pp.141-144.

Durrani, S.A., Ili´c, R., 1997. Radon Measurements by Etched TrackDetectors. World Scientific Publishing Co. Pte. Ltd, Singapore.

Einarssón, P., Theodórsson, P., Hjartardóttir, A.R. and Guðjónsson, I.G. 2008. Radon Changes Associated with the Earthquake Sequence in June 2000 in the South Iceland Seismic Zone. Pure and Applied Geophysics. 165: 63-74.

England, P., Houseman, G. 1986. Finite strain calculations of continental deformation 2. Comparison with the India–Asia collision zone. Journal of Geophysical Research 91: 3664–3676.

Garson, M.S., Mitchell, A.H. 1970. Transform faulting in the Thai Peninsula. Nature. 22: 45–47.

Garson, M.S., Young, B., Mitchell, A.H.G. and Tait, B.A.R. 1975a. The geology of the tin belt in Peninsular Thailand around Phuket, Phangnga, and Takua Pa. In: Overseas Memoir of the Institute of Geological Sciences. 1:112

Garson, M.S., Young, B., Mitchell, A.H.G. and Tait, B.A.R. 1975b. Geological map of Phuket/Phannga/Krabi, 1:125,000. In: Garson, M.S., Young, B., Mitchell, A.H.G. and Tait, B.A.R., the geology of the tin belt in Peninsular Thailand around Phuket, Phangnga, and Takua Pa. In: Overseas Memoir of the Institute of Geological Sciences. 1:112

Ghosh D., Deb A., Sengupta, R., Patra, K.K. and Bera, S. 2007. Pronounced soil – radon anomaly – Precursor of recent earthquakes in India. Radiation Measurements. 42: 466-471.

Gutenberg, B., Richter, C.F. 1956. Magnitude and energy of earthquake. Annali di Geoficica. 9: 1-15.

Gutenberg, B., Richter, C.F., 1956. Earthquake Magnitude, Intensıty, Energy and Accelaration, Bull. Seismology Society. of America, 32, 3: (July).

Hall, R., Morley, C.K., 2004. Sundaland Basins, continent–ocean interactions within East Asian marginal seas. Geophysical Monograph Series 149: 55–85.

Hamblin, W.K., and Christiansen, E.H. 2001. Earth's dynamic systems, 9th Ed., Chapter 7, Bringham Young University Provo, Utah.

Havskov, J., and Ottemöller, L. 2005. SEISAN: The earthquake analysis software Version 8.1. 254. Bergen University Norway.

HPS: Health Physics Society. Specialists in radiation safety. Founded 1956 update 2008 http://hps.org.

Hutton, L.K. and Boore, D.M. 1987. The M_L scale in Southern California. Bull. Seismology Society. Am., 77, 6: 2074-2094.

Intawong, A., 2006. The structural evolution of Tertiary sedimentary basins in Southern Thailand and their relationship to the Khlong Marui Fault. Unpublished Ph.D. Thesis, Royal Holloway, University of London, UK.

Jeffreys, H., and Bullen, K.E. 1967. Seismological tables. In: Smith & Ritche LTD, London.

Jeffreys, H., and Bullen, K.E. 1970. Seismological Tables, British Association for the Advancement of Science. Gray Milne Trust, London 50 pp.

Jo´nsson, S. and Einasson, P. 1996. Radon anomalies and earthquakes in the South Iceland Seismic Zone 1977–1993. In Seismology in Europe (ed. Thorkelsson, B. et al.), European Seismology. Commission, Reykjavı´k, pp. 247–252.

Kamesh, R.K.A., Ramprasad, T., Rao, P.S., Rao, B.R. and Varghese, J. 2004. New insights into the tectonic evolution of the Andaman basin, northeast Indian Ocean, Earth Planet. Science Letters. 221: 145-162.

Khan, P.K. and Chakraborty, P.P. 2005. Two phase opening of Andaman Sea: a new seismotectonic insight, Earth and Planet. Science letters. 229: 259-271.

Lay, T., Kanamori, H., Ammon, C.J., Nettles, M., Ward, S.N., Aster, R.C., Beck, S.L., Bilek, S.L., Brudzinski, M.R., Butler, R., DeShon, H.R., Ekström, G., Satake, K., and Sipkin S. 2005. The Great Sumatra-Andaman Earthquake of 26 December 2004. Science 308: 1127-1133.

Makofske W.J. and Edelstein, M.R. 1988. Ramapo College Institute Environmental Studies Contributor William J. Makofske, Michael R. Edelstein Published by William Andrew Inc.

Metcalfe, I. 2002. Permian tectonic framework and palaeogeography of SE Asia. Journal of Asian Earth Sciences 20: 551–566.

Metcalfe, I., 2006. Palaeozoic and Mesozoic tectonic evolution and palaeogeography of East Asian crustal fragments: the Korean Peninsula in context. Gondwana Research 9: 24–46.

Morley, C.K., 2001. Combined escape tectonics and subduction rollback-back arc extension: a model for the evolution of Tertiary rift basins in Thailand, Malaysia and Laos. Journal of the Geological Society, London 158: 461–474.

Morley, C.K., 2002. A tectonic model for the Tertiary evolution of strike-slip faults and rift basins in SE Asia. Tectonophysics 347: 189–215.

Morley, C.K., and Westaway, R. 2006. Subsidence in the super-deep Pattani and Malay basins of Southeast Asia: a coupled model incorporating lower-crustal flow in response to post-rift sediment loading. Basin Research 18: 51–84.

NCRP, 1984. Report No. 78. Evaluation of occupational and environmental exposures to radon and radon daughters in the United States.

NCRP, 1987. Report No. 93. Ionizing radiation exposure of the population of the United States.

Newcomb, K.R and McCann, W.R. 1987. Seismic history and seismotectonics of the Sunda Arc. Journal of Geophysical Research. 92: 421.439.

Ni, S., Kanamori, H. and Helmberger, D. 2005. Energy radiation from the Sumatra earthquake. Nature 434: 582.

Nutalaya, P., Sodsri, S. and Arnold, E.P. 1985. Seismicity Data of Thailand and Adjacent Areas. (Part B) in Arnold, E.P. (ed.) Thailand, Series on Seismology Volume II, Southeast Asia Association of Seismology and Earthquake Engineering, 403 pp, ISBN 974-8202-13-5.

Nutlaya, P. and S. Sodsri 1984. Earthquake Data of Thailand and Adjacent Areas Supplementary data, The Asian Institute of Technology, Bangkok, Thailand.

Ortiz, M. and Bilham, R. 2003. Source area and rupture parameters of the 31 December 1881 Mw = 7.9 Car Nicobar earthquake estimated from tsunamis recorded in the Bay of Bengal. Journal of Geophysical Research 108 (B4) 2215http://cires.colorado.edu/~bilham/Andaman.pdf.

Packham, G.H. 1993. Plate tectonics and the development of sedimentary basins of the dextral regime in western Southeast Asia. Journal of Southeast Asian Earth Sciences 8: 497–511.

Pigott, J.D. and Sattayarak, N. 1993. Aspects of sedimentary basin evolution assessed through tectonic subsidence analysis. Example: northern Gulf of Thailand. Journal of Southeast Asian Earth Sciences 8: 407–420.

Planini´c, J., Radoli´c, V. and Lazanin, Ž. 2001. Temporal variations of radon in soil related to earthquakes. Applied Radiation and Isotopes. 55: 267–272.

Polachan, S. 1988. The geological evolution of the Mergui Basin, S.E. Andaman Sea, Thailand. Unpublished Ph.D. Thesis, Royal Holloway and Bedford New College, University of London, 218 pp.

Polachan, S., Pradidtan, S., Tongtaow, C., Janmaha, S., Intarawijitr, K., and Sangsuwan, C. 1991. Development of Cenozoic basins in Thailand. Marine and Petroleum Geology 8: 84–97.

Poobrasert, S. 1987. Country Report on Earthquake Preparedness in Thailand, Report on Geodetic and geophysical Activities of the Thai National Committee on Geodesy and Geophysics period 1983-1986, Paper Subrnitted by the Royal Thai Survey Department, Thailand.

Pritchard H.M. and Gesell T.F. 1981. An estimate of population exposure due to radon in public water supplies in the area of Houston, Texas. Health Physics 41:599-606.

Rangin, C., Klein, M., Roques, D., Le Pichon, X., and Van Trong, L., 1995. The Red River fault system in the Tonkin Gulf, Vietnam. Tectonophysics 243: 209-222.

Robert, B., Cowan, H., Dalziell, E., Evans, N., O'Leary, M., Rush, B. and Lawrence Y. 2005. Survey of Impacts on the Andaman coast, Southern Thailand. Bulletin of the New Zealand Society for Earthquake. 38, 3: 123-147.

Robert, R.B. 2005. Inside an Earthquake: Geologists Penetrate Fault Zone 2 Miles Down. LiveScience. 04 August 2005 .

Searle, M.P., 2006. Role of the Red River Shear zone, Yunnan and Vietnam, in the continental extrusion of SE Asia. Journal of the Geological Society, London 163: 1025–1036.

Sercel, 2002. Mark Product L-4 Seismometer. Sercel Inc., USA.

Setapong, N. 2007 Magnitude of Aftershock of the M_w 9.3 Sumatra-Andaman Earthquake Record at the Temporary PSU Seismic Station in Phang Nga, Thailand. Master of Science Thesis in Geophysics, Prince of Songkla University, Hatyai, Thailand.

Sirijarukul, S. 2000. The investigation of radon gas in ground water around Songkhla lake basin using nuclear track etching technique. Master of Science Thesis in Physics, Prince of Songkla University, Hatyai, Thailand.

Stein, S. and Okal, E.A. 1978. Seismicity and tectonics of the Ninety east Ridge Area: evidence for internal deformation of the Indian Plate, Jour, of Geophysical Research, 83:2233-2246. Storey C.B., 1995. The role of mantle plumes in continental break up: case histories from Gondwanaland, Nature, 377:28.

Stein, S. and Wysession, M. 2003. Earthquake. In: An introduction to Seismology. Blackwell Publishing Ltd.

Stranden, E., Kolstad, A.K., Bjorn, L. 1984. Radon exhalation: Moisture and temperature dependence. Health Physics. 47: 480-484.

Tapponnier, P., Peltzer, G., Armijo, R. 1986. On the mechanics of the collision between India and Asia. In: Coward, M.P., Ries, A.C. (Eds.), Collision Tectonics. Geological Society Special Publication. 19: 115–157.

TMD, 2008. Recent earthquakes. Thai Meteorological Department. [online]. Available from: http://www.tmdseismology.com [20 May 2008]

Trnkoczy, A., Havskov, J., and Ottemöller, L. 2000. Chapter 8: Seismic Networks In: Bormann, P. (Ed) 2002. IASPEI: New manual of Seismological Observatory Practice 1, GeoForschungsZentrum Potsdam, Germany 1-59.

Ulamov, V.I. and Mavashev, B.Z. 1967. On fore – runners of a strong tectonic earthquakes. Dokl. USSR Academy of Science. 176: 319-322.

USGS, 2005. Summary of Magnitude 9.0 Sumatra-Andaman Islands Earthquake & Tsunami Sunday, December 26, 2004 at 00:58:53 UTC [online]. Available from:http://neic.usgs.gov/neis/bulletin/neic_slav_ts.html [1 September 2007]

USGS, 2005. Summary of Magnitude 9.0 Sumatra-Andaman Islands Earthquake & Tsunami Sunday, December 26, 2004 at 00:58:53 UTC [online]. Available from:http://neic.usgs.gov/neis/bulletin/neic_slav_ts.html [1 September 2007]

USGS, 2008. Earthquake data Search. United States Geological Survey [online]. Available from: http://neic.usgs.gov/neis/epic/epic.html. [15 April 2008].

Vigny, C., Simons, W.J.F., Abu, S., Bamphenyu, R., Satirapod, C., Choosakul, N., Subarya, C., Socquet, A., Omar, K., Abidin, H.Z., and Ambrosius, B.A.C. 2005. Insight into the 2004 Sumatra−Andaman earthquake from GPS measurements in southeast Asia. Nature 436: 201-206 [online]. Available from:http://www.nature.com/nature/journal/v436/n7048/full/nature03937.html

Watkinson, I., Chris, E., and Hall, R. 2008. The kinematic history of the Khlong Marui and Ranong Faults, southern Thailand. Structural Geology. [Online]. Available from:http://doi:10.1016/j.jsg.2008.09.001.

Wattananikorn, K., Kanaree, M. and Wiboolsake, S. 1998. Soil gas radon as an earthquake precursor: some considerations on data improvement. Radiation Measurements. 29: 593-598.

APPENDICES

APPENDIX A
RADON DATA

APPENDIX A1

STANDARD CALIBRATION CURVE

Determination of the standard calibration curve using the normal equation for 1 m depth. It can be determined from the original data of counting track shown in Table A1.1.

Table A1.1: Original data of counting track in close system over 7 and 14 days.

Volume code	In the 7 day close system		In the 14 day close system	
	Rn-conc. (Bq/m^3)	track density/cm^2	Rn-conc. (Bq/m^3)	track density/cm^2
Background	0	389.17	0	389.17
1	563.62	412.50	563.62	469.17
2	1699.58	525.83	1699.58	577.50

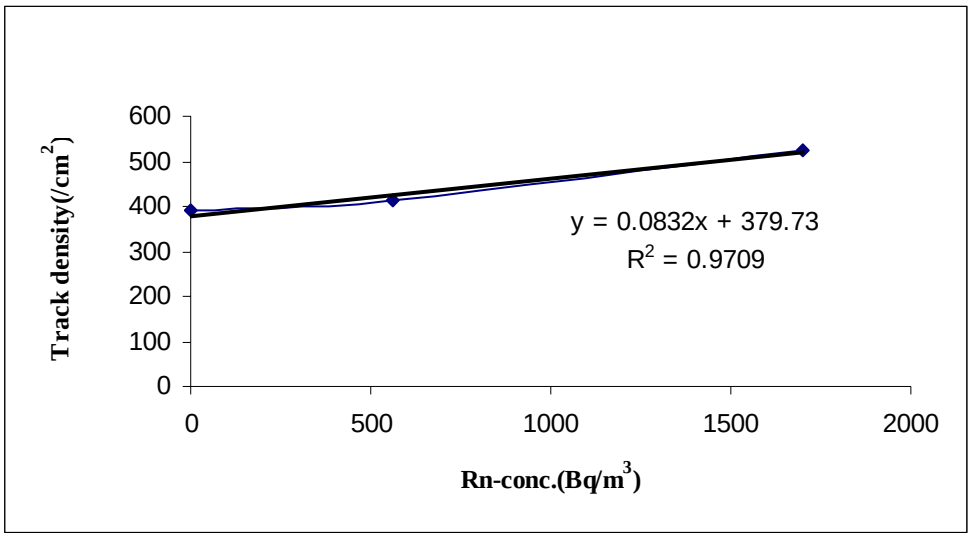

Figure A1.1 Original data of counting track in the 7 day close system.

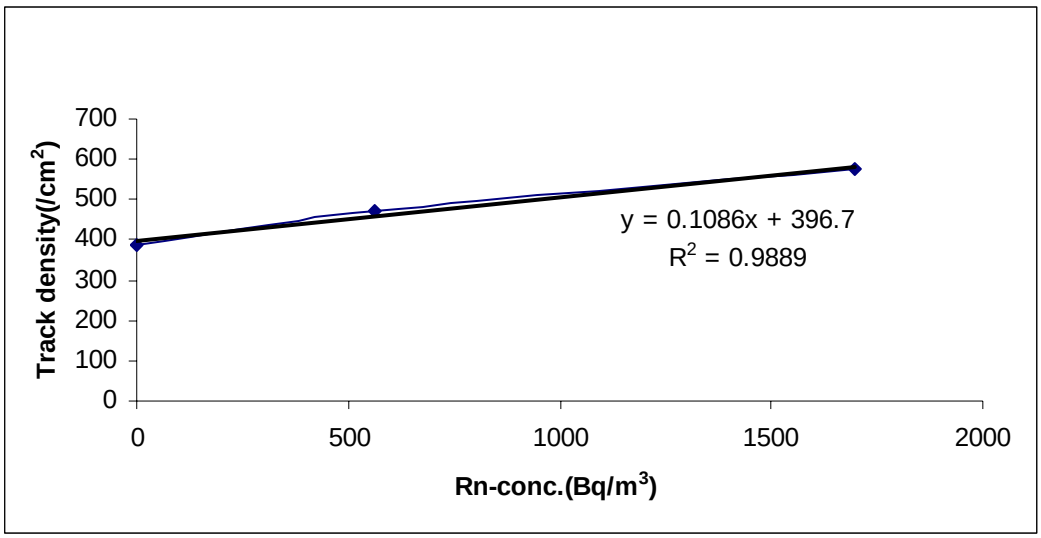

Figure A1.2 Original data of counting track in the 14 day close system.

Form Figure A1.1 in close system over 7 days, take a linear equation that is;

$$y = 0.0832x + 379.73 \qquad \text{(A1-1)}$$

Thus as

$$TD\ (Track/cm^2) = 0.0832\ Rn\text{-}conc.\ (Bq/m^3) + 379.73 \qquad \text{(A1-2)}$$

$$Rn\text{-}conc. = (TD - 379.73) \times \left(\frac{1}{0.0832}\right) \qquad \text{(A1-3)}$$

$$= (TD - 379.73) \times 12.01923$$

$$Corr.TD = (TD - 379.73)$$

In this study, the measured background track density is 389.17 per cm^2, which is different from the fitted background value (379.73) given by the regression method in the equation (A1-1). When the corrected track density at the background was calibrated to zero. Therefore, the new radon concentrations in soil gas can be calculated using equation A1-4;

$$Rn\text{-}conc. = Corr.TD \times 12.01923 \qquad \text{(A1-4)}$$

Table A1.2: Corrected track density after equation A1-4 in close system over 7 days.

Rn-conc. (Bq/m^3)	Tracks Density ($Tracks/cm^2$)	X = New Rn-conc. (Bq/m^3)	Y = Corrected TD. ($Tracks/cm^2$)
0.00	389.17	0.00	0.00
563.62	412.50	280.45	23.33
1699.58	525.83	1642.63	136.67

Plot the relationship between Corrected Track densities with New Radon concentration.

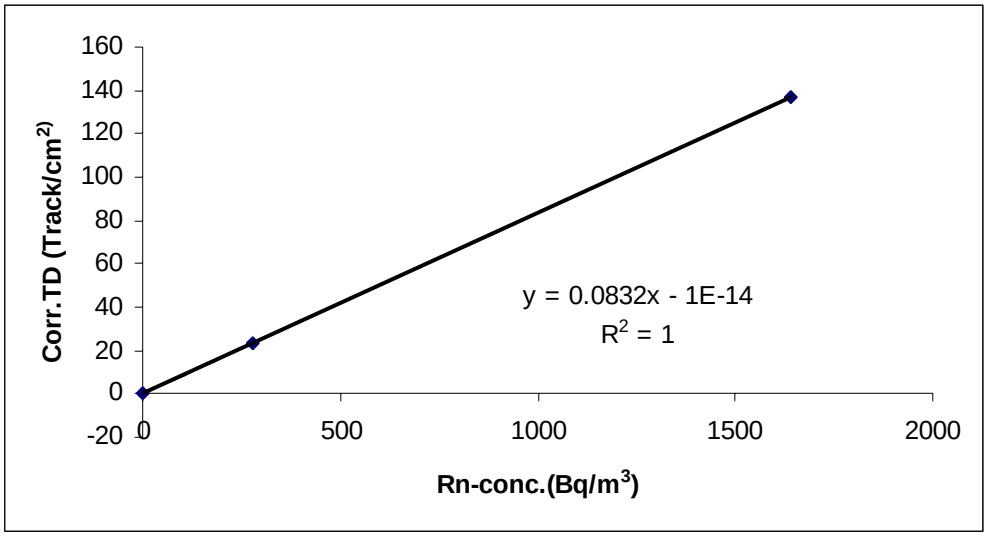

Figure A1.3 Corrected track density data and radon concentration of counting track in the 7 day close system.

Hence, from Figure A1.3 the radon concentration in Bq Bq/m^3/day unit can be found.

Rn-conc. per 7 days = 12.01923x Corr.TD (A1-5)

If,

Rn-conc. per day = 84.13461x Corr.TD (in Bq/m^3/day unit) (A1-6)

Similar is the close system over 14 days as shown the Figure A1.2. The linear equation is;

$$y = 0.1086x + 398.70 \quad \text{(A1-7)}$$

Thus as

$$TD\ (Track/cm^2) = 0.1086\ Rn\text{-}conc.\ (Bq/m^3) + 398.70 \quad \text{(A1-8)}$$

$$Rn\text{-}conc = (TD - 398.70) \times \left(\frac{1}{0.1086}\right) \quad \text{(A1-9)}$$

$$= (TD - 398.70) \times 9.208103$$

$$orr.TD = (TD - 398.70)$$

Further, the measured background track density is 389.17 per cm^2, which is different from the fitted background value (398.70) given by the regression method in the equation (A1-7). When the corrected track density at the background was calibrated to zero. Therefore, the new radon concentrations in soil gas can be calculated using equation A1-10;

$$Rn\text{-}conc. = Corr.TD \times 9.208103 \quad \text{(A1-10)}$$

Table A1.3: Corrected track density in equation A1-10 in close system over 14 days.

Rn-conc. (Bq/m^3)	Tracks Density ($Tracks/cm^2$)	X = New Rn-conc. (Bq/m^3)	Y = Corrected TD. ($Tracks/cm^2$)
0.00	389.17	0.00	0.00
563.62	412.50	736.65	80.00
1699.58	525.83	1734.19	188.33

Plot the relationship between Corrected Track densities with New Radon concentration.

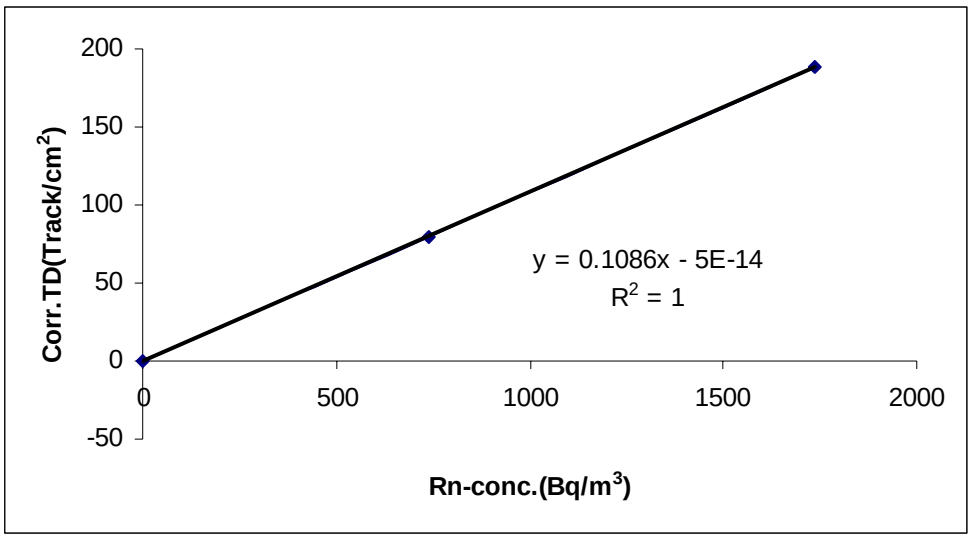

Figure A1.4 Corrected track density data and radon concentration of counting track in the 14 day close system.

Hence, from the Figure A1.4 the radon concentration in Bq Bq/m^3/day unit can be found.

Rn-conc. per 14 days = 12.01923x Corr.TD (A1-11)

If,

Rn-conc. per day = 128.9134x Corr.TD (A1-12)

Therefore, A-13 is the equation for 1 m dept in Bq/m^3/day unit. It can be determined from equation A1-6 and A1-12, following in A1-13.

$$RnConc.(Bq/m^3) = \frac{106.524 \times Corr.TD(Tracks/cm^2)}{ExposureTime(day)} \qquad \text{(A1-13)}$$

APPENDIX A2

RADON DATA ALONG THE ROAD

Table A2: Data from 68 stations along the public road no. 401 detected with RPM-256; Takua Pa – Phunphin road.

Order of Spot check	Date dd/mm/yy	Time hh:mm:ss.0	Radon emission (counts)	Location in WGS-84	
				Latitude	longitude
1	12.03.07	14:03:20	10	8.85	98.73
2	12.03.07	14:16:25	13	8.85	98.73
3	12.03.07	14:28:18	9	8.84	98.74
4	12.03.07	14:55:44	18	8.84	98.75
5	12.03.07	16:22:29	3	8.84	98.76
6	12.03.07	16:37:28	14	8.84	98.77
7	12.03.07	16:49:17	29	8.84	98.78
8	12.03.07	17:02:38	9	8.83	98.79
9	12.03.07	17:23:38	19	8.83	98.79
10	12.03.07	17:40:30	36	8.84	98.80
11	12.03.07	17:52:48	39	8.85	98.81
12	12.03.07	18:10:37	11	8.85	98.81
13	23.04.07	13:05:45	30	8.86	98.82
14	23.04.07	13:29:29	15	8.87	98.83
15	23.04.07	13:39:28	7	8.88	98.84
16	23.04.07	13:49:47	0	8.88	98.85
17	23.04.07	14:01:10	23	8.88	98.85
18	23.04.07	14:11:25	43	8.88	98.86
19	23.04.07	14:21:45	28	8.88	98.87
20	23.04.07	14:32:46	34	8.88	98.88
21	23.04.07	14:44:11	43	8.89	98.89
22	23.04.07	14:58:49	38	8.90	98.89
23	23.04.07	15:25:45	12	8.91	98.89
24	23.04.07	15:39:23	12	8.92	98.90
25	23.04.07	15:50:10	61	8.92	98.92
26	23.04.07	16:03:20	109	8.93	98.93
27	23.04.07	16:16:20	38	8.93	98.93
28	24.04.07	9:02:14	47	8.93	98.94
29	24.04.07	9:14:23	198	8.93	98.95
30	24.04.07	9:25:06	132	8.92	98.95
31	24.04.07	9:37:17	77	8.93	98.96
32	24.04.07	9:47:56	45	8.93	98.96
33	24.04.07	10:04:54	0	8.94	98.97
34	24.04.07	10:38:40	25	8.93	98.98
35	24.04.07	10:53:42	42	8.94	98.99
36	24.04.07	11:04:37	56	8.94	99.00

Table A2: (continued)

Order of Spot check	Date dd/mm/yy	Time hh:mm:ss.0	Radon emission (counts)	Location in WGS-84	
				Latitude	longitude
37	24.04.07	11:15:58	43	8.95	99.00
38	24.04.07	11:26:10	41	8.95	99.01
39	24.04.07	11:37:12	26	8.96	99.01
40	24.04.07	11:49:37	31	8.96	99.02
41	24.04.07	12:00:15	35	8.97	99.02
42	24.04.07	12:10:17	21	8.98	99.03
43	24.04.07	12:21:13	14	8.99	99.04
44	24.04.07	12:32:04	57	9.00	99.03
45	24.04.07	13:18:57	50	9.01	99.04
46	24.04.07	13:31:41	50	9.01	99.04
47	24.04.07	13:42:58	89	9.01	99.05
48	24.04.07	13:55:33	35	9.02	99.06
49	24.04.07	14:06:49	34	9.02	99.06
50	24.04.07	14:22:07	34	9.03	99.07
51	24.04.07	14:33:56	47	9.03	99.08
52	24.04.07	14:47:40	38	9.04	99.08
53	24.04.07	15:00:38	60	9.04	99.09
54	24.04.07	15:21:09	31	9.03	99.10
55	24.04.07	15:36:22	40	9.04	99.11
56	24.04.07	15:48:49	23	9.04	99.12
57	24.04.07	16:03:25	33	9.04	99.13
58	24.04.07	16:17:13	23	9.03	99.13
59	24.04.07	16:32:26	66	9.03	99.14
60	24.04.07	16:46:29	47	9.04	99.15
61	24.04.07	17:02:22	42	9.04	99.16
62	24.04.07	17:17:15	18	9.05	99.17
63	24.04.07	17:30:23	47	9.05	99.19
64	24.04.07	17:41:42	47	9.06	99.21
65	24.04.07	17:55:24	42	9.07	99.22
66	24.04.07	18:06:29	32	9.07	99.24
67	24.04.07	18:19:49	30	9.06	99.25
68	18.05.07	15:23:55	0	9.06	99.27

APPENDIX B
EARTHQUAKE DATA

APPENDIX B1

TRAVELTIME TABLE

Table B1.1: Traveltime versus distances for different phases for local earthquakes after Jeffreys and Bullen (1967, 1970).

Seismological Table
Near Earthquake Phase
Time of Transmission for Surface Focus

Pg			Pn			Sg			Sn		
Distance (degree)	Travel-time m	s	Distance (degree)	Travel-time m	s	Distance (degree)	Travel-time m	s	Distance (degree)	Travel-time m	s
0.00	0	0.000	0.80	0	18.355	0.00	0	0.001	0.80	0	31.275
0.28		5.507	1.05		21.894	0.34		11.378	1.12		39.255
0.55		11.014	1.30		25.433	0.69		22.755	1.43		47.236
0.83		16.521	1.54		28.973	1.03		34.133	1.75		55.217
1.10		22.028	1.79		32.512	1.38		45.511	2.07	1	3.198
1.38		27.535	2.04		36.051	1.72		56.888	2.39		11.179
1.66		33.042	2.29		39.591	2.07	1	8.266	2.70		19.160
1.93		38.549	2.54		43.130	2.41		19.644	3.02		27.140
2.21		44.056	2.79		46.669	2.76		31.021	3.34		35.121
2.48		49.563	3.03		50.209	3.10		42.399	3.66		43.102
2.76		55.070	3.28		53.748	3.45		53.777	3.97		51.083
3.03	1	0.577	3.53		57.287	3.79	2	5.154	4.29		59.064
3.31		6.084	3.78	1	0.827	4.14		16.532	4.61	2	7.045
3.59		11.591	4.03		4.366	4.48		27.910	4.92		15.025
3.86		17.099	4.28		7.905	4.83		39.287	5.24		23.006
4.14		22.606	4.52		11.445	5.17		50.665	5.56		30.987
4.41		28.113	4.77		14.984	5.52	3	2.043	5.88		38.968
4.69		33.620	5.02		18.523	5.86		13.420	6.19		46.949
4.97		39.127	5.27		22.063	6.21		24.798	6.51		54.930
5.24		44.634	5.52		25.602	6.55		36.176	6.83	3	2.911
5.52		50.141	5.77		29.141	6.90		47.553	7.14		10.891
5.79		55.648	6.01		32.681	7.24		58.931	7.46		18.872
6.07	2	1.155	6.26		36.220	7.59	4	10.309	7.78		26.853
6.34		6.662	6.51		39.759	7.93		21.686	8.10		34.834
6.62		12.169	6.76		43.299	8.28		33.064	8.41		42.815
6.90		17.676	7.01		46.838	8.62		44.442	8.73		50.796
7.17		23.183	7.26		50.377	8.97		55.819	9.05		58.776
7.45		28.690	7.50		53.917	9.31	5	7.197	9.37	4	6.757
7.72		34.197	7.75		57.456	9.66		18.575	9.68		14.738
8.00		39.704	8.00	2	0.995	10.00		29.952	10.00		22.718

Table B1.2: Travel times for different seismic phases for a surface focus in relation to different distances in degree (here up to 2.6 degree, Jeffreys and Bullen, 1967). Pg, Sg are direct waves, P*, S* are refracted at upper-lower crust boundary, Pn, Sn are refracted at crust-mantle boundary.

Δ	**Pg**		**P***		**Pn**		**Sg**		**S***		**Sn**	
	min	**sec**	**min**	**sec**	**min**	**sec**	**min**	**sec**	**min**	**sec**	**min**	**sec**
0	0	0.0	0	(2.8)	0	(6.8)	0	0.0	0	(3.9)	0	(10.7)
0.2		4.0						6.6				
0.4		8.0		(9.6)				13.2				
0.6		12.0		13.1				19.8		21.7		
0.8		16.0		16.5		18.3		26.4		27.7		31.0
1.0		20.0		19.9		21.1		33.0		33.6		36.1
1.2		23.9		23.3		23.9		39.6		39.5		41.2
1.4		27.9		26.7		26.8		46.3		45.5		46.3
1.6		31.9		30.2		29.6		52.9		51.4		51.3
1.8		35.9		33.6		32.5		59.5		57.4		58.4
2.0		39.9		37.0		35.4	1	6.1	1	3.3	1	1.5
2.2		43.9		40.4		38.3	1	12.7	1	9.2	1	6.6
2.4		47.9		43.8		41.2	1	19.3	1	15.2	1	11.7
2.6		51.9		47.3		44.0	1	25.9	1	21.1	1	16.7

Table B1.3: Traveltime versus distances of different phases near earthquake after Jeffreys and Bullen (1967, 1970).

degree	distance	Pg	Sg	Pn	Sn	P*	S*	Sg-Pg	Sn-Pn	S*-P*
0.0	0.0	0.0	0.0					0.0		
0.2	22.2	4.0	6.6					2.6		
0.4	44.4	8.0	13.2					5.2		
0.6	66.7	12.0	19.8			13.1	21.7	7.8		8.6
0.8	88.9	16.0	26.4	18.3	31.0	16.5	27.7	10.4	12.7	11.2
1.0	111.1	20.0	33.0	21.1	36.1	19.9	33.6	13.0	15.0	13.7
1.2	133.3	23.9	39.6	23.9	41.2	23.3	39.5	15.7	17.3	16.2
1.4	155.6	27.9	46.3	26.8	46.3	26.7	45.5	18.4	19.5	18.8
1.6	177.8	31.9	52.9	29.6	51.3	30.2	51.4	21.0	21.7	21.2
1.8	200.0	35.9	59.5	32.5	56.4	33.6	57.4	23.6	23.9	23.8
2.0	222.2	39.9	66.1	35.4	61.5	37.0	63.3	26.2	26.1	26.3
2.2	244.4	43.9	72.7	38.3	66.6	40.4	69.2	28.8	28.3	28.8
2.4	266.7	47.9	79.3	41.2	71.7	43.8	75.2	31.4	30.5	31.4
2.6	288.9	51.9	85.9	44.0	76.7	47.3	81.1	34.0	32.7	33.8
2.8	311.1	55.9	92.5	46.9	81.8	50.7	87.1	36.6	34.9	36.4
3.0	333.3	59.8	99.1	49.7	86.9	54.1	93.0	39.3	37.2	38.9
3.2	355.6	63.8	105.7	52.5	92.0	57.5	98.9	41.9	39.5	41.4
3.4	377.8	67.8	112.3	55.4	97.1	60.9	104.9	44.5	41.7	44.0
3.6	400.0	71.8	118.9	58.2	102.1	64.4	110.8	47.1	43.9	46.4
3.8	422.2	75.8	125.6	61.1	107.2	67.8	116.8	49.8	46.1	49.0
4.0	444.4	79.8	132.2	63.9	112.2	71.2	122.7	52.4	48.3	51.5
4.2	466.7	83.8	138.8	66.7	117.3	74.6	128.6	55.0	50.6	54.0
4.4	488.9	87.8	145.4	69.6	122.4	78.0	134.6	57.6	52.8	56.6
4.6	511.1	91.8	152.0	72.4	127.4	81.5	140.5	60.2	55.0	59.0
4.8	533.3	95.8	158.6	75.3	132.5	84.9	146.5	62.8	57.2	61.6
5.0	555.6	99.8	165.2	78.1	137.5	88.3	152.4	65.4	59.4	64.1

APPENDIX B2

ORDER OF EARTHQUAKE EVENTS

Table B2.1 Earthquakes occurred in January 2007 with Date (dd/mm/yy), Origin time (UTC), Location (latitude, longitude) and magnitude of local (Ml), regional (mb) and man-made (Ml) events. Ml – local magnitude; mb – body-wave magnitude.

Order	dd/mm/yy	Origin time	Longitude	Latitude	Ml	mb	Blasting
1	14/1/2007	4:01:44.72	98.59	8.59			-0.4
2	14/1/2007	10:26:12.54	98.53	8.60	-0.2		
3	14/1/2007	18:02:53.83	95.91	7.91	1.9		
4	15/1/2007	10:27:17.33	98.40	8.18	0.0		
5	15/1/2007	6:13:54.05	95.28	3.67		4.5	
6	15/1/2007	9:58:54.89	98.55	8.46			0.1
7	15/1/2007	18:25:10.98	100.58	10.61	1.8		
8	16/1/2007	4:01:53.36	98.57	8.50			-0.4
9	17/1/2007	5:54:07.07	96.66	5.80	1.9		
10	17/1/2007	7:58:52.13	93.81	-0.02		5.8	
11	17/1/2007	10:27:29.07	98.58	8.69	-0.6		
12	17/1/2007	20:05:11.38	92.62	10.95		5.1	
13	17/1/2007	23:25:52.12	97.41	9.46	1.0		
14	19/1/2007	2:48:18.40	96.86	6.27	2.6		
15	19/1/2007	10:07:13.05	98.48	8.33	0.2		
16	20/1/2007	2:51:16.38	103.00	7.92	2.6		
17	20/1/2007	4:04:06.25	98.72	8.47			-0.3
18	20/1/2007	9:49:20.34	98.70	8.47			-0.6
19	20/01/07	10:12:14.35	98.74	8.58	-0.3		
20	20/1/2007	17:24:14.86	96.81	7.31	1.9		
21	21/1/2007	11:33:22.82	99.29	8.89	1.9		
22	21/1/2007	17:38:18.04	99.48	7.01	1.4		
23	22/1/2007	1:47:53.01	102.64	6.16		4.4	
24	22/1/2007	16:44:33.61	96.00	3.11		5.3	
25	23/1/2007	3:41:16.69	95.30	4.18		4.6	
26	23/1/2007	4:41:38.32	101.98	16.47		5.7	
27	23/1/2007	17:26:53.80	99.92	7.88	1.4		
28	24/1/2007	4:03:42.09	98.54	8.40			-0.1
29	24/1/2007	9:57:10.24	98.76	8.66			-0.4
30	25/1/2007	7:38:58.98	98.14	4.67	2.9		
31	25/1/2007	10:18:19.48	98.59	8.65	-0.5		
32	25/1/2007	11:04:21.27	98.01	7.09	1.3		

Table B2.1**:** (continued)

Order	dd/mm/yy	Origin time	Longitude	Latitude	Ml	mb	Blasting
33	25/1/2007	14:47:51.62	98.45	8.15	0.2		
34	25/1/2007	15:17:41.50	91.86	0.87		5.7	
35	26/1/2007	3:59:02.67	98.61	8.72			0.2
36	27/1/2007	16:06:21.40	98.53	8.36	0.4		
37	28/1/2007	4:08:51.07	98.53	8.66			0
38	28/1/2007	11:54:39.48	97.61	8.99	0.8		
39	28/1/2007	16:53:07.82	104.50	10.17		4.6	
40	29/1/2007	6:03:32.38	102.43	6.27	3.5		
41	29/1/2007	7:52:53.66	98.74	8.62	-0.7		
42	29/1/2007	19:48:39.14	94.07	7.32		5.7	
43	30/1/2007	21:45:21.53	101.69	8.24	2.4		

Table B2.2: Earthquakes occurred in February 2007 with Date (dd/mm/yy), Origin time (UTC), Location (latitude, longitude) and magnitude of local (Ml), regional (mb) and man-made (Ml) events. Ml – local magnitude; mb – body-wave magnitude.

Order	dd/mm/yy	Origin time	Longitude	Latitude	Ml	mb	Blasting
1	010207	09:51:45.53	98.51	8.50			-0.64
2	010207	09:52:24.00	98.58	8.50			-0.41
3	020207	07:57:47.11	98.76	8.44	-1.12		
4	030207	00:49:38.73	98.31	8.91	0.54		
5	030207	04:11:47.72	98.64	8.54			-1.99
6	030207	08:59:46.42	98.59	8.40	-0.86		
7	030207	20:31:54.32	92.51	10.53		5.15	
8	050207	09:26:08.96	98.20	8.95	0.38		
9	060207	10:13:45.15	98.76	8.65	-1.29		
10	070207	02:41:42.75	96.28	5.22	3.08		
11	070207	04:11:20.41	98.63	8.54			0.46
12	080207	01:41:48.31	96.48	4.50		4.01	
13	080207	01:56:17.93	98.32	8.15	0.71		
14	090207	11:07:27.14	95.42	6.30	1.51		
15	100207	00:11:14.69	96.42	7.38	1.44		
16	110207	10:47:36.48	95.19	5.72		5.63	
17	120207	02:17:15.01	99.34	8.00	0.82		
18	120207	04:43:36.74	96.45	2.22		5.10	
19	120207	03:59:59.92	98.64	8.56			-1.45
20	120207	07:57:24.68	98.75	8.42	-1.18		
21	130207	19:26:46.94	95.08	10.23	1.50		
22	140207	03:33:55.67	98.56	8.44	-1.38		
23	140207	04:06:32.71	98.63	8.55			-1.42
24	140207	04:14:32.99	98.64	8.56			-1.55
25	140207	19:49:45.03	96.44	0.27		5.74	
26	140207	20:12:04.10	95.97	4.52		5.62	
27	140207	20:46:30.70	97.20	0.87		5.63	
28	150207	18:36:16.18	100.64	9.83	1.03		
29	170207	00:11:42.51	99.19	9.30	0.91		
30	180207	10:45:24.10	97.60	1.79		5.55	
31	180207	12:26:04.90	96.04	2.12		4.66	
32	180207	13:47:31.53	96.55	5.10	2.33		
33	180207	17:45:30.46	100.09	4.13		3.78	
34	190207	05:30:24.28	93.64	6.61		3.67	

Table B2.2: (continued)

Order	dd/mm/yy	Origin time	Longitude	Latitude	Ml	mb	Blasting
35	190207	09:54:59.29	98.64	8.54			-2.29
36	200207	08:10:29.58	98.83	8.49	0.42		
37	200207	14:31:31.54	98.75	8.52	-0.26		
38	200207	20:00:52.37	102.13	5.06		3.89	
39	210207	06:35:08.63	95.80	12.33		3.81	
40	210207	06:50:26.11	98.58	8.50	-1.62		
41	210207	9:23:09.10	95.82	12.43		4.84	
42	220207	11:13:47.72	96.88	4.25		4.29	
43	240207	09:54:06.98	98.65	8.53			-1.49
44	240207	19:57:36.97	98.73	8.61	-0.75		
45	250207	04:02:32.40	98.68	8.55			-1.83
46	270207	03:57:26.96	98.68	8.55			-1.58
35	190207	09:54:59.29	98.64	8.54			-2.29
36	200207	08:10:29.58	98.83	8.49	0.42		
37	200207	14:31:31.54	98.75	8.52	-0.26		
38	200207	20:00:52.37	102.13	5.06		3.89	
39	210207	06:35:08.63	95.80	12.33		3.81	
40	210207	06:50:26.11	98.58	8.50	-1.62		
41	210207	9:23:09.10	95.82	12.43		4.84	
42	220207	11:13:47.72	96.88	4.25		4.29	
43	240207	09:54:06.98	98.65	8.53			-1.49
44	240207	19:57:36.97	98.73	8.61	-0.75		
45	250207	04:02:32.40	98.68	8.55			-1.83
46	270207	03:57:26.96	98.68	8.55			-1.58

Table B2.3: Earthquakes occurred in March 2007 with Date (dd/mm/yy), Origin time (UTC), Location (latitude, longitude) and magnitude of local (Ml), regional (mb) and man-made (Ml) events. Ml – local magnitude; mb – body-wave magnitude.

Order	dd/mm/yy	Origin time	Longitude	Latitude	Ml	mb	Blasting
1	01/03/07	2:01:07.62	97.57	3.75		5.06	
2	01/03/07	5:08:25.71	93.60	9.69		5.35	
3	01/03/07	15:20:34.69	97.92	9.12	0.46		
4	02/03/07	3:59:08.41	98.55	8.57			-0.28
5	03/03/07	0:07:31.50	96.59	11.62	1.59		
6	03/03/07	3:58:13.34	98.55	8.57			-0.13
7	03/03/07	22:05:26.57	96.78	5.67	1.32		
8	04/03/07	21:26:05.59	101.08	6.42	1.69		
9	06/03/07	3:48:43.72	107.53	-0.56		5.70	
10	06/03/07	5:48:51.31	105.07	-0.71		6.51	
11	06/03/07	8:48:56.53	103.86	-2.95		5.09	
12	06/03/07	9:33:43.27	101.07	0.79		4.36	
13	06/03/07	12:52:08.46	107.98	-0.27		5.06	
14	06/03/07	16:22:59.17	87.66	2.62		4.57	
15	06/03/07	17:36:20.62	107.76	-0.84		4.47	
16	06/03/07	18:21:06.10	99.57	5.00	1.94		
17	07/03/07	1:24:46.75	96.03	6.05	2.73		
18	07/03/07	10:53:36.24	99.93	2.38		5.53	
19	08/03/07	22:35:06.68	111.14	3.65		4.32	
20	09/03/07	3:29:30.70	101.35	10.63	2.02		
21	09/03/07	3:33:01.91	102.56	15.52		5.31	
22	09/03/07	4:00:36.87	98.56	8.57			-0.27
23	09/03/07	7:55:46.58	98.93	8.51	0.01		
24	09/03/07	17:48:43.81	97.85	7.65	0.54		
25	10/03/07	9:57:54.70	98.54	8.47	-0.20		
26	10/03/07	17:15:05.08	97.54	6.07	1.02		
27	10/03/07	21:23:12.98	97.23	6.65	1.82		
28	12/03/07	6:15:07.67	102.24	10.05	2.24		
29	13/03/07	0:12:21.37	96.96	13.93		4.54	
30	13/03/07	3:22:53.42	99.67	4.19	2.17		
31	13/03/07	9:09:08.32	106.15	5.13		5.34	
32	14/03/07	10:40:47.05	98.69	8.69	-0.82		
33	15/03/07	6:12:48.55	101.35	11.21	1.71		
34	15/03/07	10:38:26.13	98.77	8.72	-0.27		

Table B2.3: (continued)

Order	dd/mm/yy	Origin time	Longitude	Latitude	Ml	mb	Blasting
35	16/03/07	3:58:04.43	98.77	8.60			-0.18
36	16/03/07	10:09:47.07	98.73	8.70	-0.03		
37	17/03/07	7:46:34.67	98.81	8.30	-0.12		
38	17/03/07	17:46:54.79	104.03	7.76		5.08	
39	17/03/07	19:04:28.75	96.54	5.98	1.75		
40	20/03/07	9:43:09.48	98.60	8.41			-0.25
41	21/03/07	19:16:26.64	99.96	4.64	2.77		
42	22/03/07	6:10:52.53	90.83	-4.36		4.49	
43	22/03/07	23:33:48.97	98.48	8.51	0.42		
44	22/03/07	23:53:51.65	98.73	8.32	0.62		
45	23/03/07	2:54:56.28	98.67	8.56	-1.13		
46	23/03/07	15:06:28.00	98.70	8.55	-0.49		
47	23/03/07	15:06:31.32	98.68	8.58	-0.57		
48	23/03/07	15:11:00.68	98.76	8.54	-0.21		
49	23/03/07	22:42:23.08	99.23	8.41	1.12		
50	24/03/07	11:59:44.97	98.48	8.68	0.60		
51	25/03/07	4:58:12.33	103.73	14.64		5.73	
52	25/03/07	4:00:44.03	98.51	8.63			0.24
53	25/03/07	18:27:12.43	95.53	5.24		3.85	
54	26/03/07	3:03:45.47	102.36	13.89		4.53	
55	26/03/07	4:00:04.96	98.53	8.58			0.22
56	26/03/07	10:02:40.15	101.70	11.50	2.71		
57	26/03/07	16:56:25.86	100.32	8.16	1.18		
58	28/03/07	6:43:21.06	93.59	8.44		3.22	
59	28/03/07	13:04:17.50	98.69	8.47	-1.44		
60	28/03/07	15:41:18.16	100.47	11.73	1.78		
61	28/03/07	19:25:29.84	98.58	8.58	-0.86		
62	28/03/07	19:26:22.40	98.73	8.43	-0.68		
63	28/03/07	21:28:17.36	98.25	8.35	-0.06		
64	29/03/07	1:35:46.84	92.90	4.18		4.50	
65	29/03/07	23:50:44.04	95.99	9.01	2.12		
66	30/03/07	19:48:49.45	101.29	1.93		5.17	
67	30/03/07	22:45:52.65	95.20	6.69	2.71		
68	30/03/07	23:58:36.79	98.71	8.63	-1.07		

Table B2.4 Earthquakes occurred in April 2007 with Date (dd/mm/yy), Origin time (UTC), Location (latitude, longitude) and magnitude of local (Ml), regional (mb) and man-made (Ml) events. Ml – local magnitude; mb – body-wave magnitude.

Order	dd/mm/yy	Origin time	Longitude	Latitude	Ml	mb	Blasting
1	01/04/07	2:58:23.58	98.95	8.80	0.78		
2	01/04/07	4:29:33.26	96.55	4.58		3.53	
3	01/04/07	5:08:42.48	96.47	1.90		4.62	
4	01/04/07	7:09:08.53	94.81	4.07		5.21	
5	01/04/07	17:17:56.75	100.54	4.99	2.39		
6	01/04/07	20:49:24.24	101.41	8.08	2.75		
7	01/04/07	20:55:05.56	103.84	7.27		5.06	
8	01/04/07	23:06:44.77	101.03	8.11	1.49		
9	02/04/07	3:53:58.18	98.63	8.41			-0.24
10	02/04/07	5:43:04.84	100.08	7.92	0.89		
11	02/04/07	10:58:59.95	99.51	8.35	1.85		
12	02/04/07	12:11:48.04	101.51	7.68	1.76		
13	02/04/07	12:45:06.67	99.52	6.81	0.77		
14	02/04/07	19:48:01.97	101.00	7.95	1.55		
15	02/04/07	23:29:57.84	100.50	7.35	1.50		
16	03/04/07	3:41:48.39	98.20	9.14	1.60		
17	03/04/07	3:47:23.85	98.39	9.01	0.59		
18	03/04/07	19:50:30.92	99.81	8.05	0.69		
19	03/04/07	20:25:59.20	100.17	7.84	1.41		
20	03/04/07	20:29:48.35	100.21	7.48	1.06		
21	03/04/07	20:37:19.62	97.07	9.36	0.37		
22	03/04/07	22:27:29.24	98.42	8.83	-0.05		
23	03/04/07	0:49:34.85	99.23	8.32	1.16		
24	04/04/07	4:00:43.61	98.52	8.48			0.29
25	04/04/07	6:44:18.75	99.84	8.46	1.03		
26	04/04/07	11:09:35.93	103.96	-0.15		5.32	
27	06/04/07	18:58:07.45	98.97	8.44	0.93		
28	07/04/07	0:19:14.25	98.49	8.44	-0.23		
29	07/04/07	1:25:16.00	93.10	11.13		4.27	
30	07/04/07	4:01:36.25	98.57	8.49			-0.09
31	07/04/07	5:12:50.92	98.42	8.10	0.01		
32	07/04/07	9:53:02.30	98.35	7.51			2.23
33	08/04/07	2:41:34.46	98.48	8.68	-0.62		
34	08/04/07	3:38:13.01	96.21	4.03		3.86	

Table B2.4: (continued)

Order	dd/mm/yy	Origin time	Longitude	Latitude	Ml	mb	Blasting
35	09/04/07	2:36:06.26	98.94	8.41	0.09		
36	10/04/07	9:57:49.40	98.82	8.51			-0.76
37	10/04/07	10:22:28.08	98.60	8.34	-0.24		
38	10/04/07	10:34:26.72	98.55	8.85	-0.05		
39	10/04/07	10:49:38.07	98.75	8.72	-0.45		
40	10/04/07	11:53:12.98	99.54	8.99	1.29		
41	10/04/07	13:56:55.51	93.13	12.99		5.63	
42	11/04/07	5:41:11.24	98.78	8.38	-0.29		
43	11/04/07	6:42:21.58	102.14	5.12		4.08	
44	11/04/07	12:26:26.89	101.25	3.03		4.23	
45	12/04/07	3:58:50.44	98.54	8.43			-0.02
46	12/04/07	10:28:49.91	98.82	8.43	-0.45		
47	13/04/07	6:01:16.18	96.68	10.55	1.61		
48	13/04/07	12:20:56.63	96.62	2.72		4.71	
49	13/04/07	12:57:45.15	98.17	7.63	0.67		
50	13/04/07	12:58:59.00	98.80	8.44	0.08		
51	13/04/07	14:31:45.97	98.25	7.08	2.02		
52	13/04/07	18:43:41.28	98.15	8.13	0.01		
53	14/04/07	6:14:14.43	98.15	8.66	-0.14		
54	14/04/07	6:26:38.12	94.89	7.10	2.51		
55	14/04/07	19:09:00.66	99.21	8.48	0.18		
56	15/04/07	10:40:15.61	98.71	8.42	-0.55		
57	16/04/07	17:22:05.68	98.23	7.82	0.97		
58	18/04/07	18:17:25.08	98.50	8.12	-0.07		
59	19/04/07	10:47:31.39	96.74	5.86	2.17		
60	20/04/07	0:32:32.92	99.43	9.40	1.15		
61	20/04/07	0:36:49.76	99.08	9.74	0.94		
62	20/04/07	1:51:34.23	100.22	9.89	1.83		
63	20/04/07	12:13:55.20	98.46	8.65	-0.75		
64	20/04/07	19:44:21.91	99.32	9.08	0.79		
65	21/04/07	0:37:40.11	99.49	9.05	0.79		
66	21/04/07	6:28:45.54	98.57	8.46	-0.09		
67	21/04/07	7:22:30.87	99.94	8.42	1.00		
68	21/04/07	17:31:08.58	100.91	7.66	1.40		
69	21/04/07	21:49:47.68	102.01	11.14	3.11		

Table B2.5 Earthquakes occurred in the interval from January 14 to 4 April 2007 with Date (dd/mm/yy), Origin time (UTC), Location (latitude, longitude) and magnitude regional (mb), data from USGS, 2008.

Order	dd/mm/yy	Origin time	Longitude	Latitude	mb
1	14/01/07	22:09:40.19	97.77	1.25	4.1
2	15/01/07	6:13:38.94	92.7	12.6	4.7
3	15/01/07	12:46:43.19	97.29	0.26	4.2
4	17/01/07	03:59:32.62	92.55	8.18	4.2
5	17/01/07	05:53:43.89	94.54	5.16	4
6	17/01/07	20:05:04.34	92.15	11.41	4.8
7	18/01/07	04:26:52.08	97.06	1.12	4.2
8	18/01/07	08:04:08.38	97.22	1.01	4.7
9	20/01/07	11:45:25.64	93.09	12.87	3.7
10	20/01/07	17:23:50.14	94.98	8.32	4.1
11	20/01/07	20:54:08.62	97.39	0.35	4.7
12	22/01/07	01:47:38.64	96.54	2.94	4.8
13	22/01/07	02:56:53.80	97.07	3.26	
14	22/01/07	09:24:12.32	93.14	6.24	
15	22/01/07	16:44:33.80	95.81	2.82	5.3
16	22/01/07	18:36:22.15	97.11	1.12	3.8
17	23/01/07	00:16:34.80	96.99	0.7	4.3
18	23/01/07	03:41:08.59	95.67	2.71	4.8
19	23/01/07	12:28:22.15	97.06	1.1	
20	23/01/07	15:13:17.39	99.46	-1.73	
21	23/01/07	15:39:13.12	99.52	-1.72	
22	23/01/07	16:24:39.72	99.49	-1.67	
23	25/01/07	07:38:56.64	96.17	4.81	4.4
24	25/01/07	09:18:35.62	95.29	2.75	
25	25/01/07	14:46:23.17	92.29	8.96	4.2
26	25/01/07	15:18:36.03	97.11	1.73	5.3
27	26/01/07	08:46:03.10	96.81	0.65	3.7
28	27/01/07	23:23:05.84	97.34	0.77	
29	28/01/07	16:13:27.41	97.07	0.79	
30	28/01/07	16:52:55.97	93.34	13.08	3.8
31	29/01/07	06:03:24.02	94.4	5.39	4.6
32	29/01/07	19:48:34.44	93.6	8.36	5.4
33	31/01/07	00:06:31.33	96.4	2.88	4.1
34	31/01/07	03:50:43.87	97.21	1.11	4
35	31/01/07	15:17:30.03	98.22	0.58	4.3
36	01/02/07	02:45:27.45	101.68	-1.22	3.9
37	03/02/07	00:47:59.77	93.86	13.95	4.8
38	03/02/07	01:06:57.07	96.21	2.14	
39	03/02/07	20:31:48.08	91.6	10.22	4.7

Table B2.5: (continued)

Order	dd/mm/yy	Origin time	Longitude	Latitude	mb
40	03/02/07	23:24:43.07	97.07	1.2	
41	05/02/07	09:24:37.75	92.22	11.24	4.7
42	05/02/07	22:51:34.52	99.36	2.54	4.2
43	06/02/07	14:05:17.78	96.83	1.66	
44	07/02/07	02:41:45.91	94.99	5.76	4.4
45	07/02/07	23:56:43.51	95.45	2.52	4.2
46	08/02/07	01:41:42.22	94.64	5.21	4.5
47	08/02/07	01:54:54.50	95.65	2.7	5.1
48	09/02/07	00:16:07.88	93.43	3.2	4.5
49	09/02/07	21:00:37.34	93.27	5.58	4
50	09/02/07	22:28:52.02	97.09	1.19	4.2
51	09/02/07	22:45:39.69	94.98	1.79	
52	10/02/07	00:10:13.04	97.21	1.18	4.7
53	10/02/07	01:24:10.08	95.75	2.48	4.2
54	10/02/07	08:10:17.48	97.14	1.06	4.5
55	11/02/07	10:47:35.01	94.4	6.18	5.6
56	11/02/07	22:50:56.50	95.77	2.49	4
57	12/02/07	04:44:09.81	97.11	1.51	5
58	14/02/07	15:29:47.67	96.42	2.06	
59	14/02/07	19:49:58.70	97.31	0.43	5.7
60	14/02/07	20:11:57.53	94.26	5.21	5.3
61	14/02/07	20:46:31.93	97.23	0.64	5.6
62	15/02/07	01:34:02.47	97.3	0.53	
63	15/02/07	10:20:49.97	97.2	0.57	4.7
64	16/02/07	22:07:01.08	94.67	5.44	4.3
65	18/02/07	10:45:23.99	97.37	1.07	5.1
66	18/02/07	12:26:10.91	97.05	1.23	4.8
67	18/02/07	17:45:36.38	96.72	4.3	4
68	18/02/07	22:03:01.75	100.12	0.78	
69	20/02/07	02:45:14.94	94.65	10.69	4.4
70	20/02/07	04:20:37.71	90.67	6.51	4.7
71	20/02/07	20:00:44.99	96.25	3.3	3.9
72	21/02/07	02:06:58.77	97.59	0.17	4.2
73	21/02/07	06:35:08.37	95.04	12.38	4.6
74	21/02/07	09:23:09.91	95.12	12.51	4.8
75	21/02/07	16:59:47.94	95.64	2.79	4.4
76	22/02/07	03:52:00.31	96.23	3.89	3.7
77	22/02/07	07:40:04.55	97	4.05	4.7
78	22/02/07	11:13:40.31	95.2	4.36	4.2
79	22/02/07	14:41:34.34	92.19	10.13	4.3
80	23/02/07	22:04:01.26	97.13	1.24	

Table B2.5: (continued)

Order	dd/mm/yy	Origin time	Longitude	Latitude	mb
81	23/02/07	22:30:34.25	97.14	1.21	
82	24/02/07	02:53:34.92	97.37	1	3.8
83	24/02/07	17:07:48.66	93.14	4.07	4.2
84	26/02/07	16:55:14.10	98.92	-0.63	4.4
85	27/02/07	00:11:27.04	96.36	2.23	4.1
86	28/02/07	07:57:03.05	93.03	12.53	
87	28/02/07	13:03:04.51	95.93	2.45	4.5
88	01/03/07	02:01:07.00	96.34	3.78	5.6
89	01/03/07	05:08:20.74	93.06	10.29	5
90	03/03/07	07:39:32.03	94.66	4.4	
91	03/03/07	10:09:19.65	94.16	2.68	4.3
92	05/03/07	04:22:50.97	99	-0.46	
93	06/03/07	03:23:15.13	100.04	-0.97	4.7
94	06/03/07	03:49:38.90	100.5	-0.49	6.4
95	06/03/07	04:28:35.79	100.49	-0.74	
96	06/03/07	05:49:25.43	100.53	-0.49	6.3
97	06/03/07	06:18:09.35	100.45	-0.5	
98	06/03/07	08:13:39.51	100.78	-0.45	4.6
99	06/03/07	08:49:50.38	100.71	-0.54	4.9
100	06/03/07	09:34:03.12	97.06	1.4	4.8
101	06/03/07	10:08:53.58	100.81	-0.54	4.4
102	06/03/07	12:53:06.86	100.91	-0.4	5.1
103	06/03/07	15:22:17.67	101.01	-0.45	4.5
104	06/03/07	16:02:13.99	100.67	-0.47	4.2
105	06/03/07	16:23:52.93	100.74	-0.55	4.9
106	06/03/07	17:37:21.30	100.6	-0.58	4.3
107	06/03/07	20:14:50.33	100.66	-0.67	4.6
108	07/03/07	01:14:10.69	94.52	6.55	4.3
109	07/03/07	01:24:37.55	94.79	6.87	4.4
110	07/03/07	10:53:37.59	97.91	1.96	5.9
111	08/03/07	22:36:12.57	100	-1.11	4.6
112	08/03/07	22:39:45.02	100.51	-0.72	4.2
113	08/03/07	23:51:51.58	97.31	-2.46	
114	11/03/07	06:09:00.33	93.59	13.01	4.4
115	13/03/07	00:12:16.41	92.99	10.79	4.4
116	13/03/07	03:22:43.73	95.56	4.03	
117	13/03/07	20:42:49.41	92.18	7.17	4.2
118	14/03/07	00:54:43.16	97.02	0.09	4.3
119	14/03/07	20:52:38.31	97.06	2.17	
120	16/03/07	07:19:42.83	91.86	12.89	4.7
121	16/03/07	10:07:15.52	97.04	1.57	4.1

Table B2.5: (continued)

Order	dd/mm/yy	Origin time	Longitude	Latitude	mb
122	16/03/07	14:15:47.48	101.99	-2.13	4.1
123	21/03/07	19:16:25.12	96.32	4.48	4
124	24/03/07	02:17:13.99	94.94	4.7	4.6
125	24/03/07	06:06:32.37	95.71	3.83	
126	24/03/07	11:58:40.11	93.72	10.14	4.4
127	25/03/07	04:01:14.99	93.34	14.72	3.7
128	25/03/07	18:27:09.41	93.6	8.78	4.3
129	26/03/07	03:03:37.00	97.23	0.93	4.7
130	26/03/07	10:02:22.40	93.08	10.33	4.6
131	26/03/07	17:31:56.24	99.53	1.55	
132	27/03/07	18:33:17.69	97.24	0.91	4.5
133	28/03/07	20:39:59.20	92.47	12.91	4
134	29/03/07	01:36:05.28	96.21	2.16	4.4
135	29/03/07	23:49:49.26	92.14	10.85	4.5
136	30/03/07	17:15:13.47	97.26	1.08	3.8
137	30/03/07	19:49:02.37	96.77	2.07	4.7
138	30/03/07	22:45:48.91	94.21	7.56	4
139	30/03/07	23:00:06.24	96.47	2.78	
140	31/03/07	18:34:22.13	97.46	0.74	4.2
141	01/04/07	04:29:20.31	94.1	5.14	4.2
142	01/04/07	05:08:44.73	94.45	2.55	4.7
143	01/04/07	07:08:59.89	91.52	9.2	5.1
144	01/04/07	17:17:54.80	96.07	4.78	
145	02/04/07	21:01:29.11	97.69	1.68	4.2
146	03/04/07	08:20:57.31	95.76	2.51	4.2
147	03/04/07	22:32:35.21	96.68	2.12	4.3
148	04/04/07	14:45:10.83	95.85	2.62	4.2
149	04/04/07	16:28:16.85	95.83	2.54	
150	05/04/07	19:14:51.28	97.2	1.13	4.6
151	06/04/07	11:46:17.05	99.86	0.61	4.1
152	07/04/07	00:17:49.97	92.79	7.84	4.3
153	07/04/07	01:25:11.82	93.96	13.64	4
154	07/04/07	09:51:51.62	95.7	2.92	6.1
155	07/04/07	10:55:52.49	95.44	2.78	
156	08/04/07	03:38:03.00	93.21	5.66	4.2
157	10/04/07	04:30:20.79	93.77	7.48	
158	10/04/07	04:58:12.65	96.32	4.55	4.1
159	10/04/07	13:56:53.89	92.53	12.99	5.5
160	11/04/07	06:41:55.05	97.14	1.27	4.9
161	11/04/07	12:26:27.80	95.63	2.76	4.5
162	11/04/07	13:52:29.86	97.02	1.51	

Table B2.5: (continued)

Order	dd/mm/yy	Origin time	Longitude	Latitude	mb
163	13/04/07	12:20:53.92	97.15	1.71	4.9
164	13/04/07	12:56:43.58	93.84	5.05	
165	14/04/07	06:26:20.55	95.8	3.79	4.5
166	15/04/07	09:11:12.23	97.68	1.78	4.5
167	15/04/07	16:03:54.99	97.06	1.18	
168	18/04/07	18:16:15.28	94.82	5.27	4.3
169	20/04/07	03:13:14.57	93.54	10.12	4.2
170	20/04/07	04:44:48.97	98.78	0.23	4.2
171	20/04/07	16:41:17.69	99.12	2.35	4.2
172	21/04/07	10:12:45.85	101.19	-2.96	5
173	21/04/07	17:15:54.73	97.09	1.16	4.6
174	22/04/07	17:48:50.03	96.59	2.01	4.3
175	22/04/07	21:49:52.60	96.1	4.63	4.4
176	22/04/07	22:12:58.85	95.89	2.3	4.1
177	24/04/07	05:55:29.36	97.05	1.59	4.7
178	25/04/07	20:24:13.54	96.31	2.22	4.5
179	26/04/07	06:02:02.82	97.28	0.95	4.5
180	27/04/07	08:02:49.65	94.64	5.36	6.3
181	28/04/07	19:14:29.33	99.27	1.76	4.9
182	28/04/07	20:40:48.45	100	-1.19	4.3
183	29/04/07	17:22:53.29	95.8	2.78	4.8
184	29/04/07	18:44:10.39	97.71	1.72	4.3
185	01/05/07	06:48:04.70	92.59	12.59	
186	01/05/07	16:40:57.47	92.38	8.39	4.4
187	01/05/07	19:44:19.76	94.62	5.51	5
188	01/05/07	21:43:17.66	97.86	0.08	
189	01/05/07	23:09:04.07	94.36	5.29	4.1
190	01/05/07	23:13:03.12	93.13	5.85	4.1
191	02/05/07	01:55:40.84	97.42	0.86	4.4
192	02/05/07	09:08:33.31	93.36	13.34	4.5
193	03/05/07	14:30:56.18	94.62	5.15	3.7
194	04/05/07	01:16:01.94	97.13	1.07	4.5
195	04/05/07	06:24:47.16	95.92	3.94	4.3
196	04/05/07	12:34:00.70	94.38	3.39	4.9
197	04/05/07	19:29:15.09	99.87	-2.33	5
198	04/05/07	22:25:57.43	94.3	4.98	4.7

APPENDIX C
PUBLICATION

ความเป็นไปได้ของการเปลี่ยนแปลงความเข้มข้นแก๊สเรดอนในดิน เพื่อเตือนแผ่นดินไหวล่วงหน้า: กรณีศึกษาจากรอยเลื่อนคลองมะรุ่ย ภาคใต้ของประเทศไทย

Variation of Radon Concentration in Soil Gas:an Earthquake Precursor? A Case Study from the Khlong Marui Fault Zone, Southern Thailand

ผู้วิจัย ปัทมา พิศภักดิ์
สาขาวิชาธรณีฟิสิกส์ ภาควิชาฟิสิกส์ มหาวิทยาลัยสงขลานครินทร์
อาจารย์ที่ปรึกษาวิทยานิพนธ์ รองศาสตราจารย์ ดร.ไตรภพ ผ่องสุวรรณ
ภาควิชาฟิสิกส์ คณะวิทยาศาสตร์ มหาวิทยาลัยสงขลานครินทร์

บทคัดย่อ

งานวิจัยนี้มีวัตถุประสงค์ หลักเพื่อศึกษาความเป็นไปได้ในการประยุกต์ใช้ การเปลี่ยนแปลงความเข้มข้นของแก๊สเรดอนในดินเป็นตัวเตือนล่วงหน้าก่อนเกิดเหตุการณ์ แผ่นดินไหวท้องถิ่นและในภูมิภาคโดยได้ทำการศึกษาในบริเวณรอยเลื่อนคลองมะรุ่ย ทางภาคใต้ของประเทศไทย ซึ่งอยู่ห่างจากแนวรอยมุดตัวซุนดาในทะเลอันดามัน ประมาณ 500 กม.

ในการศึกษาครั้งนี้ได้ติดตั้งระบบการวัดแก๊สเรดอนในดินและเครื่องวัดแผ่นดินไหวชนิดคาบสั้น ที่ อ.ทับปุด จ.พังงา บริเวณแนวรอยเลื่อนคลองมะรุ่ย ในระหว่างวันที่ 14 มกราคม ถึง 29 เมษายน 2550 โดยใช้เครื่องวัดRPM-256 ตรวจวัดความเข้มข้นของแก๊สเรดอนในดินเป็นเวลานาน 10 นาที ทุกๆ 3 ชั่วโมง และใช้หัววัดแผ่นดินไหวชนิดคาบสั้น Mark L4-3D ตรวจวัดสัญญาณแผ่นดินไหวท้องถิ่นและสัญญาณแผ่นดินไหวในภูมิภาคผลจากการศึกษาพบว่าความเข้มข้นของแก๊สเรดอนในดินมีข้อมูลระหว่างวันที่ 12 กุมภาพันธ์ ถึง 29 เมษายน 2550 และตรวจพบค่าสูงผิดปกติ 2 ครั้งคือ ในวันที่ 18 กุมภาพันธ์ 2550 เวลา 15:48:53 (UTC Time) ด้วย ความเข้มข้น 54 จำนวนนับ และในวันที่ 1 มีนาคม 2550 เวลา 14:34:35 (UTC Time) ด้วยความเข้มข้น 91 จำนวน นับ โดยค่าภูมิหลังของความเข้มข้นของแก๊สเรดอนในช่วงเวลาดังกล่าวมีค่าเฉลี่ยและค่าเบี่ยงเบนมาตรฐานเท่ากับ 20 จำนวนนับ และ 7.43 จำนวนนับตามลำดับ

ในการวิเคราะห์ข้อมูลเบื้องต้นพบว่าเหตุการณ์แผ่นดินไหวท้องถิ่นและในภู มิภาคมีจำนวนเพิ่มขึ้นภายหลังการตรวจพบความเข้มข้นผิดปกติของแก๊สเรดอนในดินเป็นเวลาหลายวัน ดังนั้นจึงมี ความเป็นไปได้ว่าในอนาคตเราสามารถใช้ข้อมูลแก๊สเรดอนเป็นตัวเตือนล่วงหน้าก่อนการเกิดเหตุการณ์แผ่นดินไหวในพื้นที่ศึกษา

คำสำคัญ : แก๊สเรดอนในดิน, การเตือนล่วงหน้าก่อนเกิดเหตุการณ์แผ่นดินไหว, รอยเลื่อนคลองมะรุ่ย

Abstract

The main objective of this study was to observe a possible variation of radon concentration in soil gas as an earthquake precursor. The Khlong Marui Fault Zone in Southern Thailand with the 500 km distant Sunda Subduction Zone to the west in the Andaman Sea was chosen as the study area.

A measurement system for soil gas radon and a short-period seismometer were installed in Thap Put District, Phang Nga Province along the Khlong Marui Fault Zone in Southern Thailand during 14 January and 29 April 2007. Radon concentrations in soil gas were automatically measured with the RPM-256 detector for 10 minutes every 3 hours. The local and regional earthquakes were monitored with the Mark L4-3D short-period seismometer.

Radon in soil gas data were available between 12 February and 29 April 2007. There were two clear radon anomalies observed during the period of measurement, the first on 18 February 2007 at 15:48:53 (Universal Time Coordinates, UTC +7 hrs = Thai Time) with 54 counts. The second anomaly occurred on 1 March 2007 at 14:34:35 UTC with 91 counts. The average background value for the radon emission for this period is 20 counts, with one standard deviation of 7.43 counts.

The preliminary analysis of the earthquake and radon data shows an increase of earthquake activities several days after each radon anomaly. With more data and understanding it might be possible in the future to use radon gas variations as a possible method for earthquake warning in the study area.

Key Words: Radon in Soil Gas, Earthquake Precursor, Khlong Marui Fault Zone

1. Introduction

The devastating Mw 9.3 Sumatra-Andaman Earthquake occurred on the 26 December 2004 at 00:58:53 UTC (07:58:53 Thai time), off the west coast of Northern Sumatra, Indonesia, at the Sunda Subduction Zone (USGS, 2005). Because of the subsequent uplift of parts of the ocean bottom, a tsunami with devastating effects to Indian Ocean's coastlines was triggered, including Thailand's west coast, with huge losses of life and destruction of near-shore structures (USGS, 2005). The crustal movements related to the 26 December 2004 Earthquake resulted in an increased number of reported sinkholes in Southern Thailand (DMR, 2005; Duerrast et al., 2007).

Changes of the radon concentration in air, groundwater and soil can be seen as a possible precursor of large tectonic earthquakes (e.g. Ulomov and Mavashev, 1967; Chyi et al., 2001). However, no radon monitoring station was installed in Southern Thailand before the 26 December 2004 Earthquake.

Although the past research has shown that the use of soil gas variation as an earthquake precursor is not always effective, it still can be used as a useful tool (e.g. Einarsson et al., 2008). Over the years, the techniques of radon gas sampling and detection have been improved and still are undergoing further development (e.g. Chyi et al., 2001). Further, the signal to background ratio was improved by placing the detector within a fracture zone of an active fault with upwelling gases. The environmental factors affecting radon variation have been reduced by housing the detector. The radon data recording was done continuously and retrievable at a remote site, as well as additional meteorological parameters, such as rainfall, moisture, temperature, and atmospheric pressure were measured (e.g. Chyi et al., 2002).

The variations of soil gas radon with meteorological parameters have been studied by many authors, such as Stranden et al. (1984); Wattananikorn et al. (1998); Ghosh et al. (2006). Wattananikorn et al. (1998) reviewed that the radon measurement at 100 cm depth are less effected by meteorological parameter. Therefore, before using radon measurements as an earthquake precursor, the meteorological effects should be removed.

Shortly after the devastating earthquake, the Geophysics Group in the Department of Physics at the Faculty of Science, Prince of Songkla University established in collaboration with the Department of Mineral Resources a seismic network in Southern Thailand in order to monitor possible local earthquakes along the Ranong and Khlong Marui Fault Zone (Dangmuan, 2008). The results of this study show that faults zones are reactivated and presently active, but with low magnitude seismicity.

However, there are still concerns among people and governmental agencies for larger earthquakes along the fault zones in Southern Thailand, like the Ml=2.7 earthquake on 4 May 2008 at the Khlong Marui Fault Zone (8.6388 N, 98.736 E). This study is based on field measurements of radon emission and local earthquake and shows that the correlation of radon anomalies with earthquakes can provide an important insight in an active fault zone.

Thailand is part of a geological entity extending from the Chinese province of Yunnan and Shan of Myanmar to the Malay Peninsular in the south. There are two major fault zones in the South of Thailand, both aligned NE-SW, the Ranong and Klong Marui Fault Zone (e.g. Bunopas, 1981). Both presumably converge into the

Gulf of Thailand and into the Andaman Sea, as seen in petroleum seismic sections, but later covered under a thick load of late Tertiary sediments (Garson and Mitchell, 1970). The Ranong Fault Zone is a strike-slip fault, constituted by a series of faults parallel along NE-SW from the Andaman Sea to the Northeastern part of the Gulf of Thailand in Prachuap Khiri Khan and Chumphon provinces. Onshore, the fault lies in the channel of the Kra-Buri River, with about 270 km in length. The Carboniferous-Permain rocks in the area (Kang-Kra-Chan Group) have been affected by these faults (Garson and Mitchell, 1970). The Klong Marui fault is strike-slip nature, aligned parallel to Ranong Fault Zone. It initially moved 150 km sinistral, and then moved right lateral at the transition of Jurassic and Cretaceous. In the middle of the Tertiary, the fault is similar to the Ranong Fault Zone (Tapponnier et al., 1986).

2. Objectives

1. The main objective was to observe a possible variation of radon concentration in soil gas as an earthquake precursor. The Khlong Marui Fault Zone in Southern Thailand and the 500 km distant Sunda Subduction Zone in the Andaman Sea area were chosen as the case study areas, as regional earthquakes are frequent along the subduction zone and local earthquakes were observed at the Khlong Marui Fault Zone during an earlier study.

2. The further objective is whether the radon gas variations can then be used as a possible method for earthquake warning in the study area.

3. Methodology

The location of the radon and earthquake monitoring site was situated within the Khlong Marui Fault Zone at 8°33'N and 98°39'E, in Thap Put District, about 20 km ESE from the Phang Nga Municipality, in the South of Thailand.

The radon concentrations in soil gas were automatically measured with the RPM-256 detector every 3 hours for 10 minutes. The detector is connected to a 1.5 m long and 2 inch in diameter PVC tube, which was put 1 m inside the ground. The tube is opened at its bottom end and airtight at the surface (Figure 2).These tube is covered with thin polyethylene film to filter ^{220}Rn (thoron) emission and humidity at the bottom.

The seismic recording system consists of Mark L-4-3D seismometers with a 1 Hz central frequency, and containing three geophones in three perpendicular directions, N-S, E-W, and Z components. The Seismometer connected via a data cable to the Orion short period seismograph, manufactured by Nanometrics, Canada. Inside the Orion is a data cartridge with a recording hard disk of 1.99 GB memory space. Therefore, during this study the Orion data cartridges had to be transferred via an SCSI-cable to a computer every two weeks.

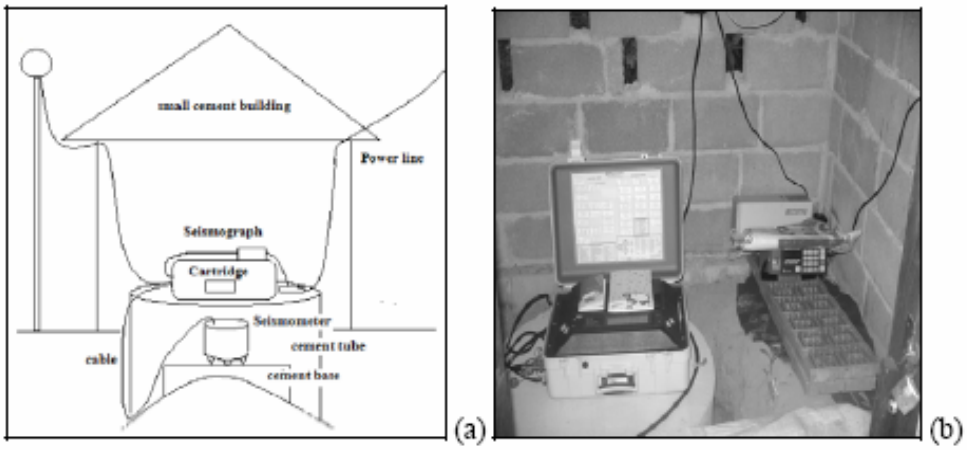

Figure 1: (a) Schematic diagram of the seismic station with the seismometer covered by a concrete tube and all inside a wooden shelter (Dangmuan, 2008). (b) Photo from the inside showing the seismograph sitting on the cover of the cement tube and continuous radon monitoring system, RPM-256, sitting inside the small house.

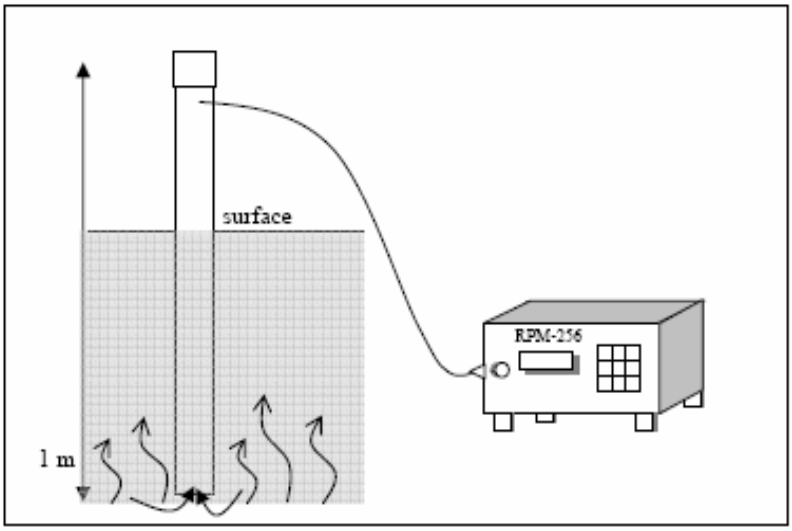

Figure 2: Schematic diagram of the radon emission and the radon detector system at the monitoring station.

After the data processing the analysis and interpretation of the seismic events was done with Seisan software (Havskov and Ottemöller, 2005). A seismogram of a regional earthquake is shown in Figure 3; one of a local earthquake is shown in Figure 4. For the first analysis of a seismic event, the primary (P-) wave arrival is marked (see Figure 3 and 4) in all three components. The first break of the P-wave was quite clearly identifiable. The later arriving secondary (S-) wave was more difficult to find. After the phase identification, the delta time between the S-wave and P-wave arrival has been determined. With this information and the traveltime tables given by Jeffreys and Bullen (1967) the distance of the earthquake from the seismic station could be determined. The distance was the criteria for the separation of the regional (> 500 km) and local (< 500 km) events. The local earthquakes then had to be separated from man-made seismic event, like in Figure 5, and seismic noise.

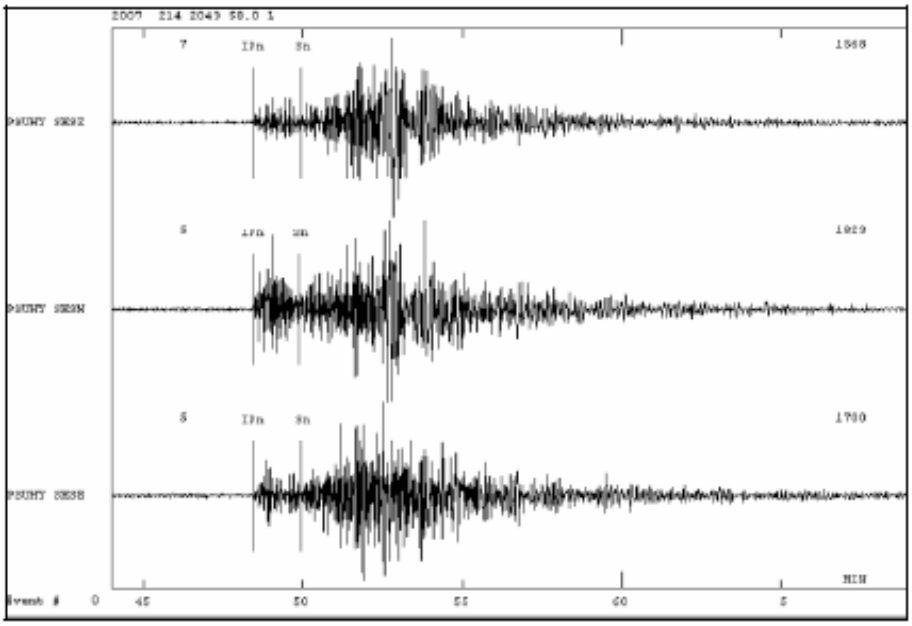

Figure 3: Seisan window showing the Z-, E-, and N-component of a regional earthquake recorded at Thap Put Station on 14 February 2007 (UTC time 20:46:29.01). The P-wave arrival (IPn) and the S-wave arrival (Sn) are marked for each component. X-axis is the time in minutes; y-axis is the amplitude in counts.

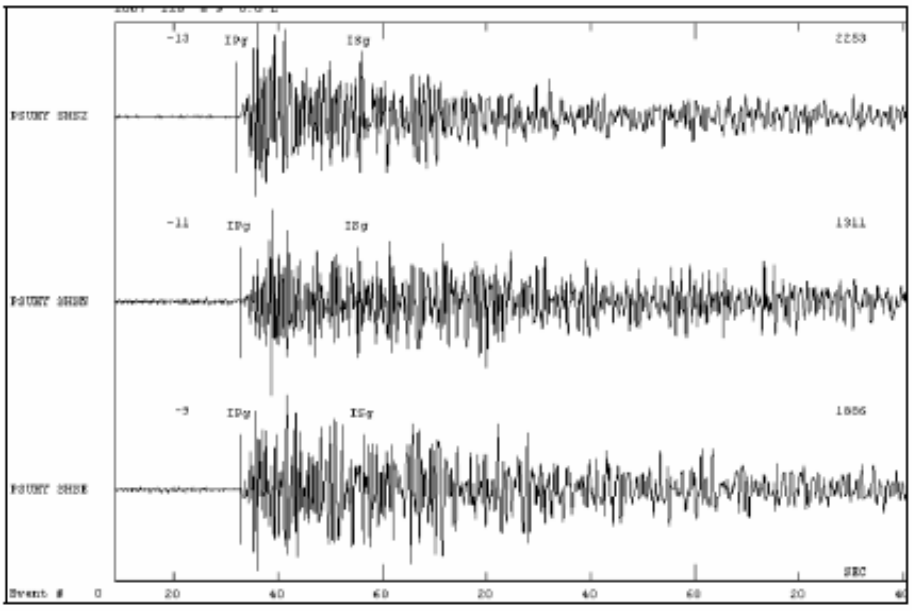

Figure 4: Seisan window showing the Z-, E-, and N-component of a local earthquake recorded at Thap Put Station on 20 February 2007 (UTC time 08:10:29.58). The P-wave arrival (IPg) and the S-wave arrival (ISg) are marked for each component. X-axis is the time in seconds; y-axis is the amplitude in counts.

For local earthquakes, the local magnitude (Ml, or Richter Scale) was determined, whereas for the regional earthquakes the body-wave magnitude (mb) was determined following Dangmuan (2008). The final location of each earthquake was

determined from the distance to the seismic station and the back azimuth, based on the first P-wave arrival in all three components. The depth for the local earthquakes was set at zero km, whereas for the regional earthquakes the depth was set at 30 km. For more details of the earthquake analysis procedure, see Dangmuan (2008).

3.1 Earthquakes

From 14 January to 21 April 2007, the short period seismic station in Thap Put could detect 224 seismic events. They occurred in areas between -4.21°N and 14.38°N and 87.39°E to 111.08°E. Among all events are 58 regional earthquakes with a magnitude range from 3.2 to 6.5 moment magnitude (mb). Further, there are 135 local earthquakes, with a magnitude range from -1.6 to 3.1 local magnitude (Ml). Additionally, 31 man made events were determined, probably blasting from quarries (see Dangmuan, 2008). Figure 6 shows the distribution of the local earthquakes in relation to the magnitude.

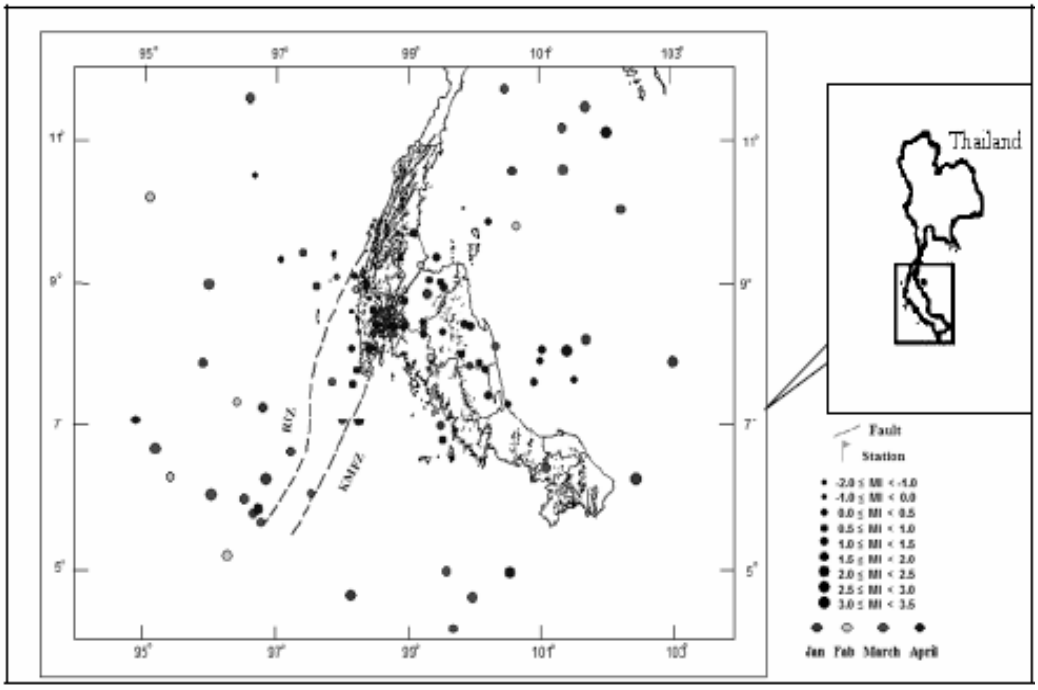

Figure 6: Locations of the local earthquakes in Southern Thailand in relation to their magnitudes, based on data from 14 January to 21 April 2007.

For the correlation between radon emission and earthquake activities the regional earthquake data were taken from the United States Geologial Survey (USGS) database (USGS, 2008). In the period between 14 January 2007 (39096 Julian Calendar day) and 4 May 2007 (39206 Julian Calendar day) altogether 198 regional earthquakes occurred in the area between 3° S-12° N and 90° E and 105° E (see Figure 7). These earthquakes are either related to the Sunda Subduction Zone (SSZ) or the adjacent fracture zones (FracZ).

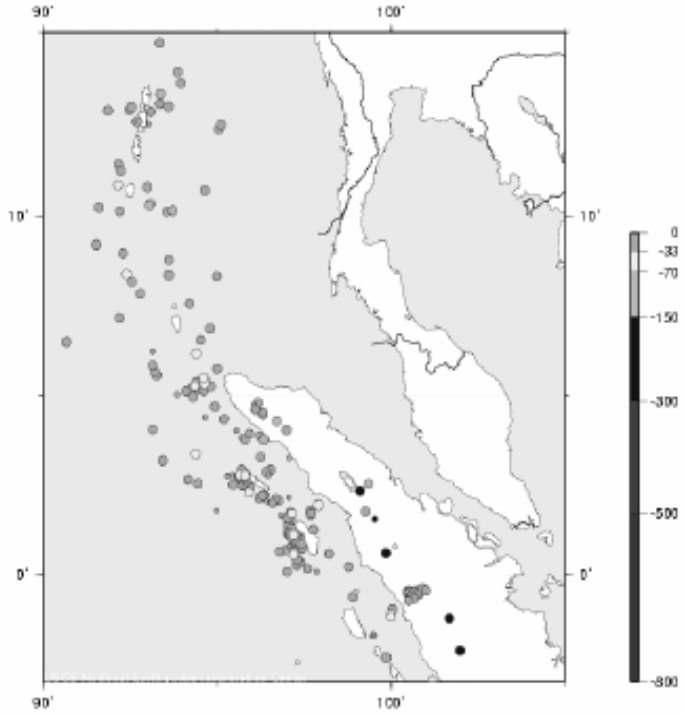

Figure 7: Locations of the regional earthquakes in relation to their depth, based on data from 14 January to 4 May 2007, from USGS (2008).

3.2 Radon and meteorological measurements

Soil gas radon was determined by measuring the α-decays of radon and its progeny with the RPM-256 Radon Progeny Monitor (UGF, Chezh Republic). The α-decays were reported in counts as shown in Figure 8, for a period between 7 February (39120 Julian Calendar date) and 18 May 2007 (39220 Julian Calendar date). However, due to data loss there is no continuous record available, as shown in Figure 8.

Further, we measured the meteorological parameters P (barometric pressure) and T (temperature) and investigated their effect on the temporal radon variations by statistic tests. First, the measured values of P and T from 7 February to 5 May 2007, and the radon measured from February 12 to 29 April 2007 were correlated as shown in Figure 8. To identify radon anomalies we used the daily average and chose an increase from the mean value by 0.5σ in the interval from February 12 to 23 March 2007 (39125-39164), by 1σ in the interval from 3 April to 12 April 2007 (39164-39184), and by $0.5\ \sigma$ in the interval from 25 April to 29 April 2007 (39197-39201). From the comparison of the anomalies with the P and T data, it can be seen that the meteorological parameters have less effect on the peaks of the soil gas radon concentration, probably because the measurements were taken at 1 m depth as suggested by Wattananikorn et al. (1998). Therefore, it is very likely that the radon anomalies are related to earthquake activities (see Figure 9).

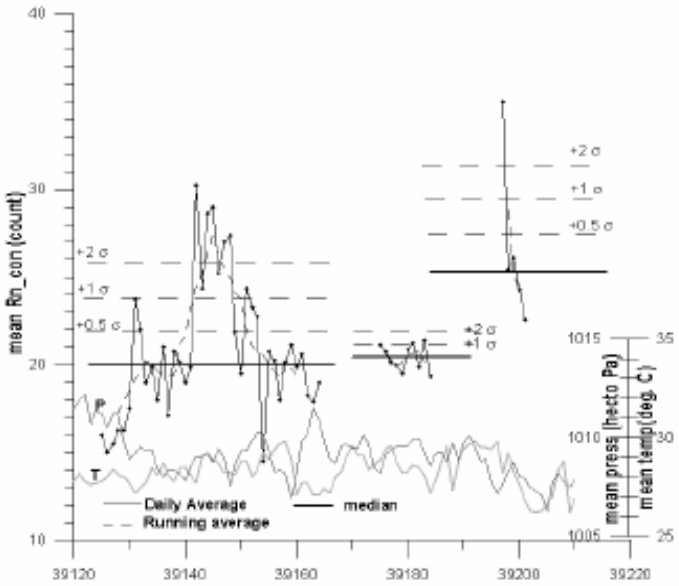

Figure 8: Radon concentration in soil gas (in counts, daily average) affected by the meteorological parameters P (barometric pressure) and T (temperature) at 1 m depth for the period between 7 February (39120 Julian Calendar, Thai date) and 18 May 2007 (39220 Julian Calendar, Thai date).

4. Results and Discussion

The radon emission data over the period between 12 February (39125 Julian Calendar, UTC date) and 29 April 2007 (39201 Julian Calendar, UTC date) together with the occurrence time and magnitude of the local and regional earthquakes are shown in Figure 9. There are two clear radon anomalies, the first on 18 February 2007 at 15:48:53 (Universal Coordinate Time, UTC +7 hrs = Thai Time) with 54 counts. The second anomaly occurred on 1 March 2007 at 14:34:35 UTC with 91 counts. The average radon value for this period is 20 counts, with one standard deviation of 7.43 counts.

After the first radon anomaly until the second one the number of local earthquakes went down, only four (see Figure 9). There were 23 regional earthquakes between the two anomalies, but the magnitudes of these earthquakes dropped significantly after the 18 February radon anomaly. However, just before the second radon anomaly there were two earthquakes with higher magnitude (mb $\geq$ 5) again.

After the second and higher radon anomaly, there was a smaller increase in the number of local earthquakes. About 5.5 days after the anomaly, a local earthquake with a higher magnitude, Ml 2.7, occurred (local earthquake No. 6 in Figure 10, see Table 1). Following that was a period with more local earthquakes, between 7.5 and 9.3 days after the anomaly. Then, after a 1.4-day gap, two earthquakes with Ml 2.2 occurred (No. 13 and 14). For the regional earthquakes there only three earthquakes until the 6 March, and then on the 6 March there were 15 earthquakes, with the highest magnitude on 6 March 03:49 UTC with mb 6.4 (regional earthquake No 5 in Figure 10, see Table 1). Figure 10 shows the locations of the local and regional earthquakes from 1 March (shortly before the radon anomaly) and 16 March 2007. After this day, there was a gap of five days without any regional earthquake. Many of the local earthquakes that occurred after the second radon anomaly are located along

the Khlong Marui Fault Zone on the land; however, others were located in the Andaman Sea and Gulf of Thailand.

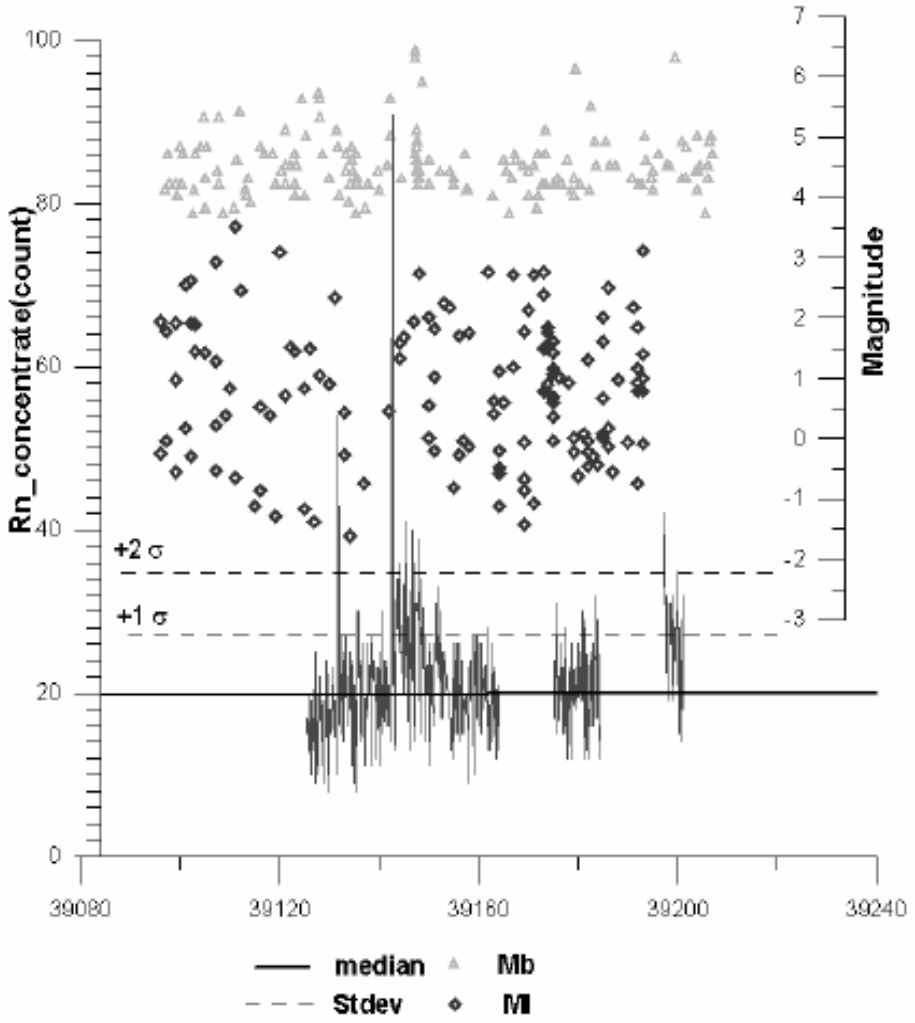

Figure 9: Radon concentration in soil gas (in counts, every 3 hrs) between 12 February (39125 Julian Calendar, UTC date) and 29 April 2007 (39201 Julian Calendar, UTC date) with median and standard deviations. Triangles are occurrence time (in UTC) and magnitude (Ml) of local earthquakes; diamonds are occurrence time (in UTC) and magnitude (mb) of regional earthquakes (from USGS, 2008).

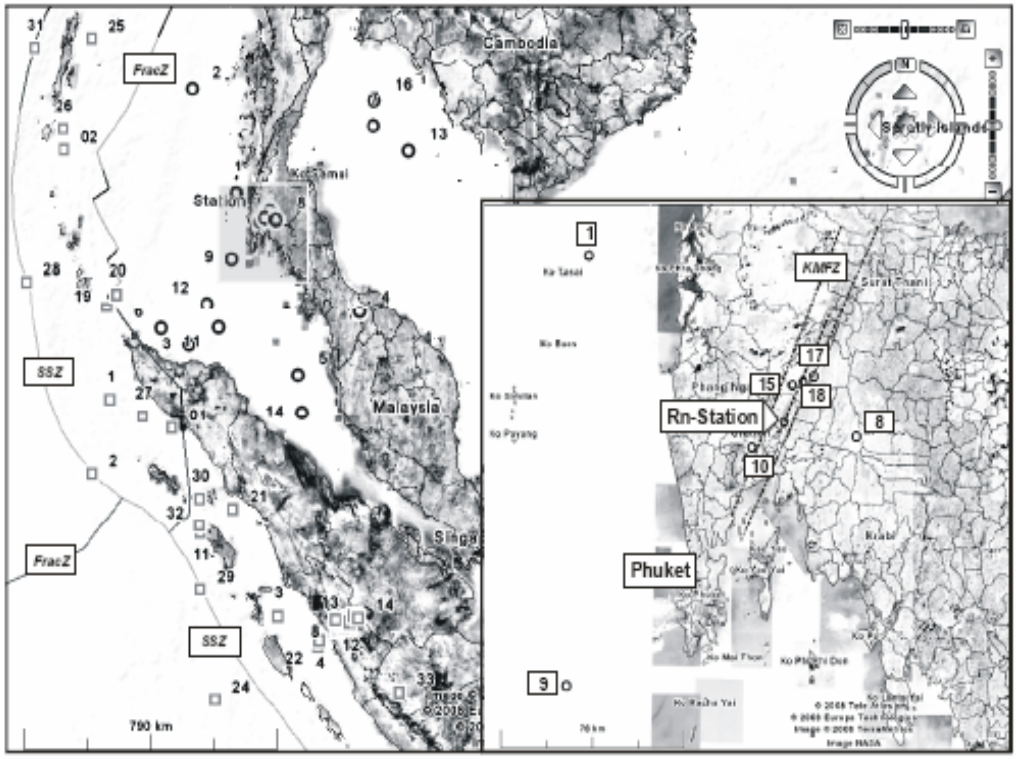

Figure 10: Locations of local and regional earthquakes shortly before and after the second radon anomaly on 1 March 2007, 21:34 UTC. Squares indicate regional events with 01 and 02 before, and 1 to 33 after the radon anomaly. Circles are local events with 1-18 after the radon anomaly. Further event details are given in Table 1. Rn-Station - radon measurement station, SSZ - Sunda Subduction Zone, FracZ - Fracture Zone, KMFZ - Khlong Marui Fault Zone. The right lower box is a magnification of the area around the measurement station. Map based on and copyright by Google™ Earth 2008.

5. Conclusions and Suggestions

1. This study presented the first soil gas radon measurements in the active fault zones of Southern Thailand, here the Khlong Marui Fault Zone.
2. The meteorological effect to soil gas radon anomalies is negligible, because the radon emission was measured at 1m depth.
3. The two radon anomalies that could be identified can be seen as a precursor for earthquake activities. Two days after the first anomaly, there was a slight increase in the number of regional earthquakes, which lasted for three days. The number of local earthquakes on the other side dropped. However, further correlation here is difficult as the second and higher radon anomaly occurred 10 days after the first one.

Table 1: Details of the earthquake activities after the second radon anomaly on 1 March 2007 21:34 UTC. See also map in Figure 10 for the locations.

Date of occurrence of radon anomaly	Earthquake occurrence				Magnitude		Epicenter distance from radon station (km)		Radon anomaly	Radon anomaly from avg. value	Delta time between Rn anomaly and EQ (Precursor time, days)	
	Local EQ (Ml)	Map O	Regional EQ (mb)	Map □	(Ml)	(mb)	(Ml)	(mb)	(Counts)	σ	(Ml)	(mb)
1/3/2007			01/03/07 02:01:07.00	01		5.6		590	91	$> 2\sigma$		-12.56 hrs
14:34:35.00	01/03/07 15:20:05.00	1	01/03/07 05:08:20.74	02	0.5	5	104	651			0.76 hr	-9.44 hrs
39142.61	03/03/07 00:07:31.50	2	03/03/07 07:39:32.03	1	1.6	-	410	640			1.40	1.71
in Julian	03/03/07 22:05:26.57	3	03/03/07 10:09:19.65	2	1.3	4.3	382	822			2.31	1.82
Calendar	04/03/07 21:26:05.59	4	05/03/07 04:22:50.97	3	1.7		358	1002			3.29	3.58
UTC date	06/03/07 18:21:06.10	5	06/03/07 03:23:15.13	4	1.9	4.7	408	1069			5.16	4.53
	07/03/07 01:24:46.75	6	06/03/07 03:49:38.90	5	2.7	6.4	403	1025			5.45	4.55
	09/03/07 03:29:30.70	7	06/03/07 04:28:35.79	6	2.0	-	377	1052			7.54	4.58
	09/03/07 07:55:46.58	8	06/03/07 05:49:25.43	7	0.0	6.3	31	1026			7.72	4.64
	09/03/07 17:48:43.81	9	06/03/07 06:18:09.35	8	0.5	-	135	1025			8.13	4.66
	10/03/07 09:57:54.70	10	06/03/07 08:13:39.51	9	-0.2	4.6	17	1027			8.81	4.74
	10/03/07 17:15:05.08	11	06/03/07 08:49:50.38	10	1.0	4.9	303	1035			9.11	4.76
	10/03/07 21:23:12.98	12	06/03/07 09:34:03.12	11	1.8	4.8	265	814			9.28	4.79
	12/03/07 06:15:07.67	13	06/03/07 10:08:53.58	12	2.2	4.4	430	1038			10.65	4.82
	13/03/07 03:22:53.42	14	06/03/07 12:53:06.86	13	2.2	5.1	498	1025			11.53	4.93
	14/03/07 10:40:30.00	15	06/03/07 15:22:17.67	14	-0.8	4.5	15	1033			12.84	5.03
	15/03/07 06:13:31.00	16	06/03/07 16:02:13.99	15	1.7	4.2	419	1027			13.65	5.06
	15/03/07 10:38:10.00	17	06/03/07 16:23:52.93	16	-0.3	4.9	21	1037			13.84	5.08
	16/03/07 10:09:30.00	18	06/03/07 17:37:21.30	17	0.0	4.3	17	1037			14.82	5.13
			06/03/07 20:14:50.33	18		4.6		1048				5.24
			07/03/07 01:14:10.69	19		4.3		511				5.44
			07/03/07 01:24:37.55	20		4.4		469				5.45
			07/03/07 10:53:37.59	21		5.9		737				5.85
			08/03/07 22:36:12.57	22		4.6		1083				7.33
			08/03/07 22:39:45.02	23		4.2		1050				7.34

Table 1 (cont.): Details of the earthquake activities after the second radon anomaly on 1 March 2007 21:34 UTC. See also map in Figure 10 for the locations.

Date of occurrence of radon anomaly	Earthquake occurrence				Magnitude		Epicenter distance from radon station (km)		Radon anomaly	Radon anomaly from avg. value	Delta time between Rn anomaly and EQ (Precursor time, days)	
	Local EQ (Ml)	Map O	Regional EQ (mb)	Map □	(Ml)	(mb)	(Ml)	(mb)	(Counts)	σ	(Ml)	(mb)
1/3/2007 14:34:35.00 39142.61 in 1/3/2007			08/03/07 23:51:51.58	24		-		1232				7.39
			11/03/07 06:09:00.33	25		4.4		749				9.65
			13/03/07 00:12:16.41	26		4.4		676	91	$> 2\sigma$		11.40
			13/03/07 03:22:43.73	27		-		609				11.53
			13/03/07 20:42:49.41	28		4.2		736				12.26
			14/03/07 00:54:43.16	29		4.3		957				12.43
			14/03/07 20:52:38.31	30		-		731				13.26
			16/03/07 07:19:42.83	31		4.7		895				14.70
			16/03/07 10:07:15.52	32		4.1		796				14.81
			16/03/07 14:15:47.48	33		4.1		1243				14.99

4. The second radon anomaly can be seen as precursor for the sharp increase in regional earthquake activities about 4.5 to 5.8 days later and around 11.4 to 15 days later. An increase in the local earthquake numbers is coming about 7.5 to 9.3 days after the radon anomaly (see Table 1), with an Ml 2.7 earthquake before and two Ml 2.2 earthquakes after this period.
5. The earthquake and radon data indicate that there might be a relationship between the local and regions earthquakes, suggesting a possible (stress/strain) relationship between the Sunda Subduction Zone and the fault zones in Southern Thailand.
6. Longer-term measurements of earthquake activities and radon emissions would be preferable, several years, as these Earth related processes have a longer period time scale.

Acknowledgements

The authors would like to thank the Department of Meteorology, Thailand, for providing the meteorological data, the Graduate School and the Prince of Songkla University (PSU) and Centennial Education Fund, Shell Company, Thailand, for research grants, the Department of Physics, and all the people of the Geophysics Group who helped during the fieldwork. The equipment was support by the International Program in Physical Science (IPPS) of Uppsala University, Sweden. We are also indebted to the Buathong family for allowing us to set up a seismic and radon measurement station.

References

Bunopas, Sangad. "Paleogeographic history of western Thailand and adjacent part of Southeast Asia: A plate tectonic interpretation." Ph.D. Thesis, Victoria University of Wellington, New Zealand, 1981.

Chyi, L.L., C.Y. Chou, F.T. Yang, and C.H. Chen. "Continuous radon measurements in faults and earthquake precursor pattern recognition." Western Pacific Earth Science, no. 2(2001): 227-246.

Chyi, L.L., C.Y. Chou, F.T. Yang, and C.H. Chen. "Automated radon monitoring of seismicity in a fault zone." Geofisica Internacional, no. 4 (2002): 507-511.

Dangmuan, Sopana. "Seismic study of Southern Thailand after the 26 December 2007 Sumastra Andaman Earthquake." Master of Science Thesis in Geophysics, Prince of Songkla University, Hatyai, Thailand, 2008.

Dürrast, Helmut, Sopana Dangmuan, and Warawutti Lohawijarn. "Khlong Marui and Ranong Fult Zones in Southern Thailand Re-Activated The 26 December 2004 Mw 9.3 Sumatra- Andaman Earthquake." GEOTHAI'07 International Conference on Geology of Thailand: Towards Sustainable Development and Sufficiency Economy, (2007): 141-144.

DMR, "Sinkhole map in southern part of Thailand from June 1995 to June 2005." Department of Mineral Resource. Bangkok, Thailand. 2005.

Einarsson, Pall, Pall Theodórsson, Asta Rut. Hjartardóttir, and Guðón I Guðjónsson. "Radon Changes Associated with the Earthquake Sequence in June 2000 in the South Iceland Seismic Zone." Pure and Applied Geophysics, no.165 (2008): 63-74.

Garson, M.S., and Mitchell A.H.G. "Transform faulting in the Thai Peninsula." Nature, no. 228 (1970): 45-47.

Dipak, Ghosh, Deb Argha, Rosalima Sengupta, Kanchan Kumar Patra, and Sukumar Bera, S. "Pronounced soil – radon anomaly – Precursor of recent earthquakes in India." Radiation Measurements, no. 42, (2007): 466-471.

Havskov, J., and Ottemöller, L. "SEISAN: The Earthquake Seismology." Modern Approaches in Geophysics 358. The Netherlands: Springer, 2005.

Jeffreys, H., and Bullen, K.E. "Seismological tables." In: Smith & Ritch LTD, London, 1967.

Planinic, J., Radolic, V., and Culo, D., 2004. "Radon as earthquake precursor." Nuclear Instruments and Methods in Physic Research A, 530, 568-574.

Stranden, E., Kolstad, A.K., Bjorn, L., 1984. "Radon exhalation: Moisture and temperature dependence." Health Phys, 47, 480-484.

Tapponnier, P., Pelzer, G., Armijo., P. "On the mechanics of collision between India and Asia" In: Coward, M., Ries, A., (Eds.), 115-157. Collision Tectonic. Geol. Soc. London: Spec. Publ., 1986.

Ulamov, V.I. and Mavashev, B.Z. "On fore – runners of a strong tectonic earthquakes." Dokl. Acad. Sci. USSR., 176 (1967): 319-322.

USGS, 2005. Summary of Magnitude 9.0 Sumatra-Andaman Islands Earthquake & Tsunami Sunday, December 26, 2004 at 00:58:53 UTC [online]. Available from:http://neic.usgs.gov/neis/bulletin/neic_slav_ts.html [1 September 2007]

USGS 2008. Earthquake Search. United States Geological Survey [online]. Available from: http://neic.usgs.gov/neis/epic/epic.html. [15 April 2008].

Wattananikorn, Kittichai, M., Kanaree, and Sodchuen Wiboolsake. "Soil gas radon as an earthquake precursor: some considerations on data improvement." Radiation Measurements, no. 29 (1998): 593-598.

VITAE

Name Miss Pattama Pisapak

Student ID 4822044

Educational Attainment

Degree	Name of Institution	Year of Graduation
B.Edu. (Physics)	Phuket Rajabhat University	2003

Scholarship Awards during Enrolment

Centennial Education Fund, Shell Company, Thailand, 2006

List of Publication and Proceedings

Pisapak, P., Bhongsuwan, T., Lohawijarn, W., and Duerrast, H. 2008. Variation of radon concentration in soil gas: an earthquake precursor? A case study from the Khlong Marui Fault Zone, Southern Thailand. Proceeding of the Conference on "the 2nd Graduate Research Conference for developing the New Knowledges". Princess Maha Chakri Sirindhorn Anthropology Centre, Silpakorn University. September 19, 2008. pp.358-372.